CANADIAN THESES

THÈSES CANADIENNES

NOTICE

The quality of this microfiche is heavily dependent upon the quality of the original thesis submitted for microfilming. Every effort has been made to ensure the highest quality of reproduction possible.

If pages are missing, contact the university which granted the degree.

Some pages may have indistinct print especially if the original pages were typed with a poor typewriter ribbon or if the university sent us an inferior photocopy.

Previously copyrighted materials (journal articles, published tests, etc.) are not filmed.

Reproduction in full or in part of this film is governed by the Canadian Copyright Act, R.S.C. 1970, c. C-30.

AVIS

La qualité de cette microfiche dépend grandement de la qualité de la thèse soumise au microfilmage. Nous avons tout fait pour assurer une qualité supérieure de reproduction.

S'il manque des pages, veuillez communiquer avec l'université qui a conféré le grade.

La qualité d'impression de certaines pages peut laisser à désirer, surtout si les pages originales ont été dactylographiées à l'aide d'un ruban usé ou si l'université nous a fait parvenir une photocopie de qualité inférieure.

Les documents qui font déjà l'objet d'un droit d'auteur (articles de revue, examens publiés, etc.) ne sont pas microfilmés.

La reproduction, même partielle, de ce microfilm est soumise à la Loi canadienne sur le droit d'auteur, SRC 1970, c. C-30.

THIS DISSERTATION
HAS BEEN MICROFILMED
EXACTLY AS RECEIVED

LA THÈSE A ÉTÉ
MICROFILMÉE TELLE QUE
NOUS L'AVONS REÇUE

LOAD DISTRIBUTION IN TEST LOADED INSTRUMENTED STEEL PILES

NIZAMUDEEN KHAN, B. Eng.

A Thesis
Submitted under the supervision of
Dr. Bengt H. Fellenius
Professor

in partial fullfillment
of the requirements of the degree of
Master of Applied Science

Department of Civil Engineering
Faculty of Engineering
University of Ottawa
Ottawa, Canada

March 13, 1987

ISBN 0-315-36513-7

UNIVERSITÉ D'OTTAWA
UNIVERSITY OF OTTAWA

ACKNOWLEDGEMENTS

This study has received partial financial support by the Natural Sciences and Engineering Research Council. The Fredericton Pile Testing Programme was financed by the New Brunswick Department of Transportation. The field test data were provided by the National Research Council.

The Author expresses his appreciation for the initiation of the study and help in the assimilation of the field data to Dr. M. Bozozuk, of the National Research Council. Sincere thanks are also expressed to the support staff of the Department of Civil Engineering, University of Ottawa for their help and assistance during the course of the study. The author is also indebted to his colleagues for their support, criticism, and advice given.

SUMMARY

A static testing programme of four steel piles, two H-piles and two pipe piles, was conducted to aid the analysis and design of piles driven through 11 metre of loose embankment fill and a 25 metre thick layer of compressible clayey silt. Two piles, one of each type, were driven to depths of 39 metre into dense sand and gravel, the remaining two piles were driven to depths of 32 metre, developing shaft resistance primarily.

Static loading tests were performed thirteen months after the piles were driven. The raw field data were first reduced to tabular form for analysis and further processing. The reduced data were analysed with the aim of developing a methodology to evaluate the residual loads in the piles and to study the effects of downdrag and residual stresses on the distribution of load in the piles.

The applied test loads were analysed to determine the load level closest to the failure load of each pile. The measured compression at these load levels for each section of the piles was converted to corresponding strain.

Previous investigators (Hunter and Davisson, 1969, Hanna and Tan, 1973, and Fellenius and Samson, 1972) showed that downdrag and residual stresses influence the distribution of shaft resistance at the pile-soil interface during a static loading test. Consequently, the distribution of load in the piles is affected, the extent of which is unknown and unquantified.

The reduced data were also analysed to determine the initial residual compression and strain in the piles before push and pull testing. Three cases of residual loads before push testing were considered: The case of zero residual strain, the case of half the algebraic sum of the increased locked-in strain induced in push and the increased locked-in strain induced in pull (Case 1), and the full sum of the same value of Case 1 (Case 2).

In both Cases 1 and 2, the residual strain was found to increase linearly to a peak value in the lower half of the pile, thereafter it decreased or remained constant.

The residual strain and the measured strain were subsequently converted to corresponding loads using the linear elastic stress-strain relation for the materials.

The distribution of initial residual load increased linearly to a peak value in the lower half of the pile, followed by a decrease with increasing depth. Peak residual load ranging from 528 KN to 660 KN (60 tons to 75 tons) were obtained at depths of approximately 26 metre (85 feet) for Case 1 and twice this value for Case 2. A major portion of the residual load originated in the clayey silt formation.

The loads computed from the strains measured in push testing were added to the residual load to determine the adjusted load mobilized in push testing. The residual loads before pull testing consist of the initial residual load plus the load locked-in as a result of the push test. These new residual loads were subtracted from the loads computed from the measured strains in pull to determine the adjusted loads mobilized in pull testing. The loads from measured strain and the adjusted loads mobilized in push and pull were plotted with respect to depth to determine the load distribution curve for each pile.

The adjusted load distributions in push testing show a linear increase of load with depth, while the unadjusted distributions show an approximately constant load. The corresponding toe and shaft resistances are greater in the lower sections of the pile for the adjusted loads as opposed to the resistances for the unadjusted loads.

The mobilized unit shaft resistance was computed by differentiating the regression polynomial describing the best curve fit of the load distributions and dividing the results by the Modulus of Elasticity (E) and cross-sectional area (A) of the pile.

When the piles were loaded to failure in push, the unit shaft resistance distribution increased linearly for the adjusted loads (Case 2). This distribution is also in close agreement with the measured undrained shear strength of the soil. When the residual loads are underestimated (Case 1) or neglected, the unit shaft resistance increased linearly to a peak value then remained constant or decreased after a depth ranging from 20 to 40 times the pile diameter.

The adjusted load distribution in pull testing decreases linearly, while the distributions of the unadjusted and the adjusted Case 1 loads were approximately constant. Case 2 distributions showed considerable larger shaft resistance and little or no apparent toe resistance as opposed to large apparent toe resistance and very small shaft resistance in the unadjusted loads and the adjusted loads of Case 1. Since there cannot be toe resistance in a pull test, it is obvious therefore that the residual loads for Case 1 were underestimated. Furthermore, the shaft resistance obtained in the pull testing is erroneous if unadjusted for residual loads.

When the maximum residual load (Case 2) was considered, the distribution of the unit shaft resistance in pull is similar in geometric configuration and magnitude to the distribution obtained in push. The observation suggests that the mobilized unit shaft resistance at failure is equal in push and pull.

The results of the analysis support the findings of O'Neill et al. (1982), Hanna and Tan (1973), Hunter and Davisson (1969) and the hypothesis of Holloway et al. (1978) on the load and shaft resistance distribution in test loaded piles.

TABLE OF CONTENTS

		Page
ACKNOWLEDGEMENTS	.....	i
SUMMARY	.....	ii
TABLE OF CONTENTS	.....	v
LIST OF TABLES	.....	viii
LIST OF FIGURES	.....	ix
LIST OF APPENDICES	.....	xi
GLOSSARY AND NOTATIONS	.....	xii
CHAPTER 1. INTRODUCTION	.....	1
CHAPTER 2. THEORETICAL BACKGROUND	.....	4
CHAPTER 3. FREDERICTON PILE TESTING PROGRAMME	.....	20
CHAPTER 4. STATIC PILE TEST DATA	.....	25
CHAPTER 5. ANALYSIS AND DISCUSSION	.....	31
CHAPTER 6. CONCLUSIONS	.....	43
REFERENCES	.....	45
TABLES	.....	51
FIGURES	.....	67
APPENDICES	.....	115

CHAPTER Page

1. INTRODUCTION 1

1.1 General 1
1.2 Objectives 2
1.3 Scope 2
1.4 Outline of Report 3

2. LITERATURE REVIEW 4

2.1 General 4
2.2 Load Transfer 4

2.2.1 Transfer Function 5
2.2.1.1 Shaft and toe resistance 6
2.2.2 Elastic Theory Approach 9
2.2.3 Finite Element Analysis 11

2.3 Failure Loads 12
2.4 Residual Strains 13
2.5 Telltale-Instrumented Piles 16
2.6 Deformation Modulus 18

3. FREDERICTON PILE TESTING PROGRAMME 20

3.1 Site Plan 20
3.2 Soil Profile 20
3.3 Test Piles 21
3.4 Pile Instrumentation 22
3.5 Test Frame 23
3.6 Penetration Resistance 23
3.7 Test Procedure 24
3.8 Results of Previous Fredericton Tests 24

4. STATIC PILE TEST DATA 25

4.1 Reduced Data 25
4.2 Reliability of Data 26
4.2.1 Applied Load 26
4.2.2 Modulus of Elasticity 26
4.2.3 Constant loading 28
4.2.4 Deformations Data 28
4.2.5 Faulty telltales 29
4.2.6 Failure Loads 29

5. ANALYSIS AND DISCUSSION 31

5.1 Introduction 31
5.2 Analysis of Residual Strains 31
5.3 Analysis of Load Distribution 34
5.3.1 Push Testing 34
5.3.2 Pull Testing 36

5.4 Discussion 38

6. CONCLUSIONS 43

LIST OF TABLES

TABLE	TITLE	Page
3.1	Subsoil Profile	51
3.2	Axial Pull Load (after Bozozuk et al. 1978)	52
3.3	Axial Push Load (after Bozuzuk et al. 1978)	53
4.1	Failure Loads	54
5.1	Pile 1; H-Pile; Push Test; Residual Compression	55
5.2	Pile 3; Pipe Pile; Push Test; Residual Compression	56
5.3	Pile 4; H-Pile; Push Test; Residual Compression	57
5.4	Pile 1; H-Pile; Pull Test; Residual Compression	58
5.5	Pile 3; Pipe Pile; Pull Test; Residual Compression	59
5.6	Pile 4; H-Pile; Pull Test; Residual Compression	60
5.7	Pile 1; H-Pile; Push Test; Calculation of Loads	61
5.8	Pile 3; Pipe pile; Push Test; Calculation of Loads	62
5.9	Pile 4; H-Pile; Push Test; Calculation of Loads	63
5.10	Pile 1; H-Pile; Pull Test; Calculation of Loads	64
5.11	Pile 3; Pipe pile; Pull Test; Calculation of Loads	65
5.12	Pile 4; H-Pile; Pull Test; Calculation of Loads	66

LIST OF FIGURES

FIGURE	TITLE	Page
2.1	Model Load Transfer Function in Piles	67
2.2	Mohr Coulomb Strength Envelope at Pile Soil Interface (modified after Kezdi 1976)	68
2.3	Typical Distributions of Unit Shaft Resistance and Load Distribution Transfer Functions in a Pile (after Vesic, 1970)	69
2.4	Model Load Distribution in Adjusted for Residual Loads (after Briaud and Tucker, 1985)	70
2.5	Load Transfer Behaviour for Piles in Compression and Tension considering Residual Stresses (after Holloway et al. 1978)	71
2.6	Load Distribution Development neglecting Residual Loads (after Hanna and Tan, 1973)	72
2.7	Load Distributions Adjusted for Residual Loads (after Hanna and Tan, 1973)	73
2.8	Load Distribution in Fixed Head Piles (modified after Hanna and Tan, 1978)	74
2.9	Load Distributions in Push and Pull. (after Hunter and Davisson, 1969)	75
2.10	Load Distribution Adjusted for Residual Loads (after Hunter and Davisson, 1969)	76
3.1	Site Plan of Test Site	77
3.2	Profile of Soil Formation, Embankment Fill, and Test Piles (after Bozozuk et al. 1978)	78
3.3	Sectional Views of H-Piles showing Telltale End Locations	79
3.4	Sectional Views of Pipe Piles showing Telltale End Locations	80
3.5	Plan of Test Pile Location (after Bozozuk et al. 1978)	81
3.6	Schematic View of Test Frame	82
3.7	Residual Load Distribution Prior to First Series of Push Testing (modified after Bozozuk et al. 1978)	83

4.1	Pile 1; H-Pile; Push Test; Load Movement Data	84
4.2	Pile 2; Pipe pile; Push Test; Load Movement Data	85
4.3	Pile 3; Pipe pile; Push Test; Load Movement Data	86
4.4	Pile 4; H-Pile; Push Test; Load Movement Data	87
4.5	Pile 1; H-Pile; Pull Test; Load Movement Data	88
4.6	Pile 2; Pipe-Pile; Pull Test; Load Movement Data	89
4.7	Pile 3; Pipe pile; Pull Test; Load Movement Data	90
4.8	Pile 4; H-Pile; Pull Test; Load Movement Data	91
4.9	Pile 2; Concreted Pipe Pile; Chord Modulus Distribution	92
5.1	Typical Example of Strain Cycle for Driven Piles	93
5.2	Example of Induced Load-Strain Cycle Before Push Testing (Pile 3)	94
5.3	Pile 1; H-Pile; Residual Compression at Telltale Ends	95
5.4	Pile 3; Pipe Pile; Residual Compression at Telltale Ends	96
5.5	Pile 4; H-Pile; Residual Compression at Telltale Ends	97
5.6	Pile 1; H-Pile; Residual Strain Distribution	98
5.7	Pile 3; Pipe Pile; Residual Strain Distribution	99
5.8	Pile 4; H-Pile; Residual Strain Distribution	100
5.9	Pile 1; H-Pile; Load Distribution in Push Testing	101
5.10	Pile 3; Pipe Pile; Load Distribution in Push Testing	102
5.11	Pile 4; H-Pile; Load Distribution in Push Testing	103
5.12	Pile 1; H-Pile; Unit Shaft Resistance Distribution in Push Testing	104
5.13	Pile 3; Pipe pile; Unit Shaft Resistance Distribution in Push Testing	105
5.14	Pile 4; H-Pile; Unit Shaft Resistance Distribution in Push Testing	106
5.15	Pile 1; H-Pile; Load Distribution in Pull Testing	107
5.16	Pile 3; Pipe Pile; Load Distribution in Pull Testing	108
5.17	Pile 4; H-Pile; Load Distribution in Pull Testing	109
5.18	Pile 1; H-Pile; Unit Shaft Resistance Distribution in Pull Testing	110

5.19 Pile 3; Pipe pile; Unit Shaft Resistance Distribution in Pull Testing 111

5.20 Pile 4; H-Pile; Unit Shaft Resistance Distribution in Pull Testing 112

GLOSSARY AND NOTATIONS

A	cross sectional area of pile
A_s	shear perimeter area per unit length of pile
b	diameter of pile
C'	ratio of the measured compresssion of pile to the calculated compression of the pile considered as a free standing column.
C	ratio of the calculated compression of pile due to a load supported entirely by shaft resistance to the calculated compression of the pile considered as a free standing column
c_u	mean undrained shear strength
D	pile embedment depth
D_c	critical depth of pile
E	modulus of elasticity of pile
E_s	modulus of elasticity of soil
K_s	ratio of the horizontal effective stress to the vertical effective stress at the pile shaft
K	pile-soil stiffness factor
L	length of pile
M	wall friction ratio, $\tan\delta/\tan\varphi'$
N	standard penetration index (blows/0.3 metre)
N_q	bearing capacity coefficient for shallow foundations
N_t	bearing capacity coefficient at pile toe
σ'_z	effective overburden pressure

Q	load applied to pile head
ΔQ	incremental load
Q_u	ultimate load
R	total static resistance
R_s	shaft resistance
R_t	toe resistance
r_s	unit shaft resistance along pile shaft
α	ratio of toe load to applied load at head of pile
β	shaft resistance coefficient
λ	empirical coefficient
δ'	wall friction angle, effective
φ'	soil internal angle of friction, effective
ν_p	Poisson's ratio of pile
ν_s	Poisson's ratio of soil
Δ_o	movement of pile head
Δ_z	deformation of pile at depth z
Δ_m	measured deformation of pile
Δ_c	pile compression as a free standing column.
Δ_s	measured elastic compression of pile due to equivalent shaft load
Δ_{sm}	elastic compression of pile as a free standing column due to equivalent shaft load
Δ_t	measured compression of pile due to equivalent toe load

CHAPTER 1

INTRODUCTION

1.1 GENERAL

A static loading test is the most common method of determining pile capacity and consists of applying an external load to the head of a pile and measuring the corresponding displacement of the pile. The load is usually applied to the head of the pile by means of a hydraulic jack and is measured by the jack pressure manometer or, more accurately, by a load cell. The hydraulic jack reacts against a reaction frame positioned over the test pile. When load is applied, the pile will deform and displace. The displacement at the pile head is measured using dial gauges acting against reference beams. The data measured are presented in a load-displacement curve. Ordinarily, the test will only establish the ultimate resistance (failure load) of the pile without separation of shaft and toe resistance.

To measure separately the deformation and the displacement of the pile under the applied load, use is made of telltales. Telltales can be rod or wire extensometers, connected to certain locations in the test pile but standing free from the pile. The telltales will thus tell the deformation between the pile head and the telltale end. With the use of several telltales placed at various depths in the pile, the toe and shaft load components of the soil resistance can be evaluated. Telltale instrumented pile tests are usually included only for special tests for large and difficult piling projects.

In 1977, the New Brunswick Department of Transportation and Communications in co-operation with the National Research Council of Canada, Division of Building Research, undertook a full-scale pile test-loading programme on the banks of the Saint John's River at Fredericton. The test programme was part of a study to obtain design parameters for the design and analysis of the foundation of a proposed 772 metre long bridge across the river. The

bridge foundation consisted of concrete piers, supported on piles driven through a 25 metre thick layer of highly compressible silty clay to toe bearing in a dense gravel formation. Large volumes of fill were required for the bridge approaches. The fill was expected to cause considerable settlement in the clay and subsequent negative skin friction in the compressible silty clay. The pile testing programme consisted of static loading in tension and compression of four single telltale instrumented steel piles and a group of three piles subjected to drowndrag.

A first series of static testing of the four single piles was conducted in October 1977, three months after the piles were driven, and the results were presented by Bozozuk et al. (1978). The deformation of a pile group under downdrag conditions was also monitored over a ten-month period and the results were presented by Bozozuk and Keenan (1985). A second series of static testing on the four single piles was performed in August 1978, and the results are presented in this thesis.

1.2 OBJECTIVES

The objectives of the study reported in this Thesis are:

(a) to determine the load distribution of the piles under compression (push) and tension (pull) test loading to failure

(b) to quantify the magnitude of the residual loads in the piles

1.3 SCOPE

The investigation included the analysis of four instrumented steel piles: two H-piles and two pipe piles driven through an embankment fill and a layer of compressible silt and into a competent dense sand and gravel formation.

The analysis of the test data was performed in four steps.

(1) reduction and compilation of field data to working data in a tabular form for analysis and easy access for further processing.

(2) preliminary analysis of the reliability of the data.

(3) detailed analysis of test data.

(4) correlation with similar studies performed by other investigators.

1.4 OUTLINE OF THESIS

The Thesis first presents the results of a literature review and theoretical background of the subject matter (Chapter 2). An account of field test procedures and soil data at the site is given in Chapter 3. The compiled test data and a study of their reliability are presented in Chapter 4. Chapter 5 contains an analysis and discussion of the results. Conclusions on the findings of the analysis are presented in Chapter 6.

CHAPTER 2

THEORETICAL BACKGROUND

2.1 GENERAL

Piles have been used for centuries to overcome difficulties of placing foundations on soft or weak soils. By means of piles, load from the superstructure is transferred through weaker upper layers of soil to deeper, more competent layers.

Axial static test loading of telltale instrumented piles is used to determine the load deformation behaviour of the piles. The static test is conducted for two directions of loading, push and pull. The ASTM D-1143 and D-3689 standards outline the test procedures and data acquisition system of the push and pull test, respectively, and includes recommendations for the arrangement of telltales in the test piles.

In this chapter, the theoretical concepts governing the load transfer behaviour in piles are examined. Also, the shaft and toe resistances of piles and the factors affecting the same are briefly discussed. In addition, the residual strain in driven piles previously investigated is reported and its effect on the load distribution of statically tested piles at failure are also discussed. Finally, the techniques used to analyse the load distribution from telltale data are presented.

2.2 LOAD TRANSFER

Load transfer in a pile-soil system is a very complex phenomenon and involves a number of parameters which are difficult to analyse in numerical terms. Several attempts have been made to develope analytical methods of load transfer in piles. Most current techniques are based on one of the following three approaches.

(1) Transfer function approach
(2) Elastic theory approach
(3) Finite or boundary element analysis.

2.2.1 Transfer Function

The transfer function approach is a step integration technique developed by Coyle and Reese (1966). This technique uses the measured relationship between the pile resistance and the pile movement at various points along the pile and requires no assumption regarding the linearity of the soil behaviour. The load transfer in the pile is obtained experimentally by installing strain gauges or load cells at different depths, z, along the pile axis. A plot of the measured axial force, Q, in the pile against depth, z, is shown in Fig. 2.1(c), the function Q(z) indicates the load transfer along the pile shaft. The slope of the function Q(z) divided by the pile perimeter area, A_s, per unit length gives the distribution of the unit shaft resistance, r_s, along the pile shaft.

When the curve Q(z) is established experimentally, the vertical displacement, Δ_z, at a depth, z, below the ground surface is known, provided that the modulus of elasticity of the pile, E, the cross-sectional area of the pile section, A, and the vertical head displacement of the pile head, Δ_o are measured during the loading test. Assuming E and A constant, then from known strength of materials the following formulae can be established:

$$\Delta_z = \Delta_o - \frac{1}{AE}\int_0^z Q(z)\, dz \qquad (2.1)$$

$$r_s = \frac{1}{A_s} \cdot \frac{dQ}{dz} \qquad (2.2)$$

In theoretical analysis, the pile is divided into n number of elements which are considered as compressible short columns of length, L_i, and which are acted upon by axial force, Q_i, and shaft resistance, r_{si}.

Various empirical relations for the unit shaft and toe resistances have been established based on the above approach using measured pile load-displacement data.

2.2.1.1 Shaft and toe resistance

The static resistance, R, of a pile is the sum of the toe and shaft resistance components, R_t and R_s, as follows:

$$R = R_t + R_s \tag{2.3}$$

In a push test, both components are present, while in a pull test, only the shaft component is acting, that is, R is equal to R_s. It is important to recognize that R_s is the mobilized resistance resulting from the applied load Q and not necessesarily equal to the ultimate resistance.

The unit shaft resistance, r_s, is a function of the horizontal soil pressure against the pile shaft, which is proportional to the effective overburden stress, σ_z', as follows:

$$r_s = K_s \sigma_z' \tan\delta' \tag{2.4}$$

where K_s denotes the ratio of the effective horizontal stress to the vertical effective stress at the pile shaft and δ' is the effective wall friction angle.

The unit toe resistance, r_t, is also a function of the effective overburden stress, σ_z', at the toe, as follows:

$$r_t = \sigma_z' N_t \tag{2.5}$$

Where N_t is the bearing capacity coefficient at the toe. N_t is usually about three times the bearing capacity coefficient of shallow foundations, N_q (Canadian Foundation Engineering Manual, 1985).

Investigations of single piles indicate that there is very little increase of toe resistance or unit shaft resistance below a certain critical depth. Vesic (1969), Mohan et al. (1963), and Robinsky and Morrison (1964) suggested that during pile driving and static loading, a high zone of straining, volume change, and arching may develop in the soil around the pile above the pile toe level. Consequently, the value of toe and shaft resistance evaluated from the test loading data would cease to be proportional to the overburden stress and become constant below a certain depth. The presence of residual loads in the piles were not accounted for in the above mentioned papers.

Meyerhof (1976) stated that the relations for unit shaft and toe resistance, Eqs. 2.4 and 2.5, are not valid for piles driven in cohesionless soils beyond the critical depth, D_c. D_c is equal to an embedment depth, D, of about 10b to 20b, where b is the pile diameter. Thus, below the critical depth, modified or new relations are required to estimate the toe or unit shaft resistance.

The Mohr Coulomb shear strength envelope, Fig. 2.2, suggests that the shearing resistance engaged at the pile-soil interface is smaller than the soil shear strength. Burland (1973) accounted for this reduction of strength in clay by introducing a beta-factor which is equal to the ratio of the average shaft resistance to the effective overburden pressure. The beta-factor also includes the influence of the ratio between the horizontal and vertical overburden pressure in the soil. Bozozuk (1972) and Bozozuk et al. (1978) introduced an M-ratio to account for a reduction between the soil strength and the pile shaft resistance. M is defined as the ratio of the effective wall friction, $\tan \delta'$, and the effective soil friction, $\tan \varphi'$.

For additional details on the effective stress approach, the critical depth, and M-ratio, see the Canadian Foundation Engineering Manual (1985).

Meyerhof (1976) suggested that the unit toe and shaft resistances for long piles depend on limiting values of toe and shaft resistances. For embedment ratios, D/b, greater than 10, the unit shaft and unit toe resistances are obtained from empirical equations using the Standard Penetration Index, N, of the soil along the pile shaft.

By correlating the results of pile test loads with soil parameters, Vijayvergiya and Focht (1972) proposed an alternative method to compute the unit shaft resistance in piles driven in clayey soils. Vijayvergiya and Focht (1972) found that the average unit shaft resistance, r_s, is the sum of the mean effective overburden stress, σ_m', and twice the mean undrained shear strength, c_u, of the soil along the pile, modified by an empirical coefficient λ, as follow:

$$r_s = \lambda(\sigma_m' + 2c_u) \qquad (2.6)$$

The coefficient, λ, was found to have a close correlation with the embedment depth, D, of the pile. It was observed that λ decreased almost linearly with increasing depth, then remained constant for depth greater than 20 metre (100 feet). Consequently, Eq. 2.8 indicates smaller capacity for very long piles driven in clay and a reduction of unit shaft resistance in the lower region of piles.

Values of λ are known only for typical clay profiles, therefore, values for specific site conditions will have to be approximated from empirically known values from similar profiles. The equation requires great accuracy in the determination of effective vertical stress and the undrained shear strength of the clay profile for accurate estimation of the pile capacity.

Fig. 2.3 illustrates how the load distribution in a pile subjected to an applied load is governed by the mobilised shaft resistance. The shape of the load distribution is a straight line for a constant unit shaft resistance as shown by Example (a). Examples (b) and (c) show parabolic load distributions for linearly increasing and decreasing unit shaft resistances. Examples (d) and (e) are illustrations of unit shaft

resistance and corresponding load distributions as presented and discussed by Vesic (1970, 1977a) and Kezdi (1976).

The transfer function approach assumes that the displacement along any element of the pile is not effected by the shaft load transferred by other elements except through the pile itself. In reality, however, the transfer of shaft load by any element to the soil affects points below and above the considered element, consequently, the concept of a unique load transfer is not true (Vesic 1970).

2.2.2 Elastic Theory Approach

The elastic theory approach assumes that the soil in which the pile is embedded is an ideal linear elastic solid defined by deformation modulus and Poisson's ratio of the soil. The approach considers the effect of the transfer of shaft load to the soil above and below the section of the pile analysed. Several investigators have developed various analytical solutions based on the elastic theory. D'Appolonia and Romualdi (1963) presented an analysis based on the elastic theory to analyse the mobilised shaft resistance in toe bearing H-piles driven to bedrock through 40 feet of sand and gravel and subjected to a static loading test. The measured shaft resistance approximated a constant distribution and agreed reasonably with the computed shaft resistance. However, the static test was not taken to bearing failure and residual strain was not considered in the analysis.

Poulos and Davis (1968) and Poulos (1968) presented a theoretical approach to the analysis of a single axially loaded incompressible pile in a linear elastic soil by considering the pile as a number of uniformly loaded cylindrical elements. The L/b ratio and the compressibility characteristics of the pile were considered. The results of the analysis was stated to show reasonable agreement between the predicted and experimental results. However, the assumption of incompressibility of the pile material and the neglect of residual strain reduces the applicability of the analysis.

Mattes and Poulos (1969) analysed the settlement of compressible piles embedded in a linear elastic soil and subject to loads well below the

failure load. The influence of the compressibility on the shaft resistance and the pile settlement distribution was examined and compared to the behaviour of incompressible piles. The results indicate that as the piles become more compressible, the shaft resistance near the head of the pile increases and the transfer of load to the toe decreases. Also, for a given load and pile geometry, the settlement of the pile head increases and the toe settlement decreases as the pile compressibility decreases. Residual strain was not considered.

Also Butterfield and Bannerjee (1971) have presented an analysis in calculation of the settlement of single axially loaded piles in homogeneous and linearly elastic soil. The effect of both radial and vertical displacement of pile and soil was also considered. Again, the pile load was assumed smaller than the bearing capacity and the residual load was not included.

Poulos (1977) suggested that effect on analysis of settlement of piles of negative skin friction (which is the cause of residual strain) may be analysed by incorporating an external soil movement in the basic analytical equations. However, the paper does not state how this would be done.

Randolph and Wroth (1978) analysed the settlement of piles by modifying the equations developed by Poulos and Davis (1968) and Poulos (1968) for considering inhomogenity or non-linearity of the soil surrounding the piles. The analysis also considered the effect of a weak stratum of soil in the lower portion of the pile. The final analytical equations presented an approximative closed-form solution for a single cylindrical pile embedded in a non-homogeneous, non-linear soil. Reasonable agreement was obtained when the results were compared to the results of similar numerical techniques. Residual strain was not included in the analysis.

All the above mentioned references concentrates on the settlement of a pile or pile group loaded to a level well below the bearing capacity. Furthermore, the analytical techniques do not consider residual strain in the piles. Therefore, the references do not provide any information applicable to the objectives of this thesis.

2.2.3 Finite Element Analysis

Attempts have been made to use finite element and boundary element analyses to predict the pile settlement behaviour. These methods allow the introduction of the stress history of the pile-soil system along with non-linear and stress-dependent response of the soil.

Balaam et al. (1975) used finite element analysis to study the load settlement behaviour of a single axially loaded pile. The pile and soil were analysed as separate bodies and equilibrium and compatibility of the pile and soil at the pile-soil interface were imposed to obtain a solution of the pile settlement. The effects of pile installation process on the pile settlement behaviour was also considered by introducing a disturbed zone around the pile having a different strength and deformation properties than the undisturbed zone. The possibility of slip at the pile-soil interface was allowed for by specifying a limiting shaft resistance. The results of the analysis showed that the settlement behaviour of the pile is influenced by the load on the pile, the strength properties, and the extent of the disturbed soil zone. Reasonable agreement was observed between the predicted solution and measured distributions of soil settlement around piles in London Clay. Residual strain was not considered.

Banerjee and Davis (1977) used the boundary element method to analyse the settlement and load distribution of single piles in a non-homogeneous soil whose modulus of elasticity increased linearly with depth. The results of the analysis were stated to be consistent with experimental results and to indicate more realistic prediction of single piles and pile group behaviour when compared to techniques by Poulos (1968) and Butterfield and Banerjee (1971). The results also indicated that the assumption of non-homogenity of the soil reduces the shaft resistance between piles in a group. Bannerjee and Davis (1978) improved on the above technique to allow for greater computational effeciency and easier selection of soil moduli in the analysis. Residual strain was not considered in the analyses.

The referenced analysis techniques deal with pile settlement and load distribution for loads smaller than the pile capacity. Furthermore, the solutions do not account for the presence of residual strain in the piles, and, therefore are of little relevance to the objectives of this thesis.

2.3 FAILURE LOADS

Methods to analyse pile failure loads have been reviewed and discussed by Fellenius (1980). The failure criteria suggested for use by the Canadian Foundation Engineering Manual (1985) are the Davisson Offset Limit Load, the Brinch-Hansen 80% method, and the Chin-Kondner method.

Davisson (1972 and 1975) assumed that a limit load of the pile is reached when the head displacement of the pile is equal to the sum of elastic compression of the pile as a free standing column, elastic compression of the soil at the pile toe, and plastic compression of the soil at the pile toe.

Brinch Hansen (1963), suggested that the failure load of a pile load, Q_u, and the displacement, Δ_u, of the pile occurs when the co-ordinates of the point, 0.80 Q_u and 0.25 Δ_u, also lie on the pile load-displacement curve.

Chin (1971), postulated that the load displacement curve was approximately hyperbolic, therefore, the ratio of the pile displacement to the head load plotted versus the pile displacement will develop a straight line having a slope equal to the inverse of the ultimate load.

2.4 RESIDUAL STRAIN

Strain that remains in impact driven piles after driving or develops before static testing is referred to by the term residual strain. Such strain is the result of the mobilization of shear stresses along the pile. The corresponding locked-in loads in the pile are in static equlibrium.

Fellenius and Samson (1976), Cooke (1978), and others indicated that neglecting residual strains when evaluating loads in test loaded piles leads to erroneous conclusions of load distribution in the pile by overestimating the shaft resistance at the expense of the toe resistance.

Locked-in loads in driven piles can be caused by driving. Holloway et al. (1978) and Briaud and Tucker (1985) rationalized that for each hammer blow during driving, a pile first moves downward, then rebounds and oscillates around a final position. The rebound is due to the unloading of the upward acting shaft and toe resistances and simultaneous elastic lengthening of the pile due to the unloading. The upward movement is sufficient to reverse the direction of the shaft shearing resistance in the upper portion of the pile from positive to negative.

Static equilibrium for zero head load is attained when the negative skin friction in the upper portion of the pile equals the positive shaft and toe resistances in the lower portion of the pile. The residual load distribution at the end of driving, and the measured load distribution adjusted for residual load in compression and tensions are shown in Fig. 2.4.

Holloway et al., (1978) discussed the effect of residual stresses on load transfer behaviour in piles, as is indicated in Figs. 2.5a and 2.5b. When an applied load, Q, mobilizes a linearly increasing unit shaft resistance distribution Curve 1 in an initially unstressed pile, a corresponding load distribution, Curve 1, results. If the pile is subjected to residual strain corresponding to unit shaft resistance according to Curve 2, the resulting residual load distribution is Curve 2. If this strain is deducted from Curve 1, the resulting apparent load distribution is represented by Curve 3, corresponding to an apparent Curve 3 unit shaft resistance. Fig. 2.5b illustrates the corresponding behaviour of a pull tested pile.

Robinsky and Morrison (1964) investigated steel piles driven in sand formation and suggested that driving and reconsolidation of the surrounding soil induced residual strain in the piles. Fellenius and Broms (1969) investigated concrete piles driven into a soil profile of clay, silt, and

sand, and showed that the reconsolidation of the remoulded clay resisted by shaft resistance in the underlying silt and sand layer.

Hanna and Tan (1973) subjected model piles, 15.9 mm to 38.1 mm in diameter and up to 1.8 metre in length to push testing. In a first test series, dry sand was placed around a set of piles which were permitted to settle during placement of the sand. A second set of piles was fixed at the head during placement of the sand.

In the free head condition, and no external compressive load, the placement of sand induced negative skin friction between the sand and the pile in the upper portion of the pile. In the lower portion, positive shaft resistance was induced. The negative and positive shear above and below the neutral plane combined into a residual load distribution.

In the fixed head condition of the second test series, the settling sand induced negative skin friction along the entire pile length which was resisted by a restraining force at the pile head.

Both test series included a static push test following the placement of sand with the load applied and removed in five equal steps. When the intial residual load distribution was neglected, considerable smaller shaft resistance was computed in the lower portions of the pile as shown in Fig. 2.6. However when the initial residual load was accounted for, the load distribution during application of an external push load was as shown in Fig. 2.7. At an applied load 0.11 KN, most of the load was resisted in the upper portion of the pile. At 0.19 KN, the initial residual load in the upper portion of the pile was fully overcome, and only a minor portion of the applied load reached the pile toe.

When the restraining force in the fixed- head pile was released, the negative shaft resistance reduced. The load distributions in loading and unloading in the fixed head piles are shown in Fig. 2.8.

The study by Hanna and Tan (1973) demonstrated the occurrence of the reversal of shear stresses along the pile shaft during load application.

Fellenius and Samson (1976), discussed locked-in compression in a shaft bearing pile in clay which was tested forty-three days after the pile was driven. The authors showed that more realistic load distribution and greater accuracy of the toe resistance approximation were achieved when the locked-in compression (residual strain) was considered in the analysis.

Hunter and Davisson (1969) evaluated the results from full-scale loading tests in push followed by pull testing on six piles each instrumented with a telltale at the toe. Large apparent tension loads occurred at the pile toe in the pull tests. Since it was not possible for tension loads to exist at the pile toe in a pull test, the authors concluded that residual loads were present at the start of the push test. The true load distribution in push, Curve 6, Fig. 2.9, was obtained by adding the residual load at the end of a pull test (Curve 4) to the compression load (Curve 1) minus the residual load of a compression test (Curve 2).

Similarly, the residual load at the end of the pull test, Curve 4 of Fig. 2.9, was subtracted from the pull test load (Curve 3) to give the real load distribution, Curve 5 in the pull test. The final distributions adjusted for residual loads are shown in Fig. 2.10.

The shaft resistance according to the adjusted load distributions was approximately 30% higher in push than the shaft resistance in pull.

Cooke (1978), recorded residual loads when tubular steel piles were jacked into clay. The residual load first increased linearly with depth to a peak value in the lower quarter of the pile, then remained constant to the pile toe.

Cooke (1978), discussed that driving piles in clayey soil caused extensive displacement and remoulding of the surrounding soil, resulting in a change in soil stress and pore water pressure. The change of stress in the soil is accompanied by the development of related forces in the pile itself. Equilibrium between the soil and pile forces for no external load, results in a residual force system locked in the pile, which must be considered in the analysis of a loading test.

O'Neill et al. (1982) found that for piles driven in overconsolidated clay, the true shaft load transfer in a push test is the difference of the applied load in push and the sum of the apparent toe load in pull and the toe load in push. The true shaft load transfer was approximately equal to the pile capacity in pull, suggesting that the peak shaft load transfer was independent of the direction of loading.

2.5 TELLTALE-INSTRUMENTED PILES

Telltales are deformation gauges that measure the axial compression between the head of the pile and the base of the telltale. For several telltales distributed evenly over the length of the pile, the compressions for a section of the pile is obtained from the difference between two telltale measurements.

Telltales have been used in static loading tests to study the stress-strain behaviour of piles and to determine the load distribution of piles. The average load Q_{ave} acting in a pile or a section of a pile is:

$$Q_{ave} = AE \frac{\Delta L}{L} \qquad (2.7)$$

where

A = average cross sectional area of pile or section considered
E = modulus of elasticity of pile
ΔL = length of pile or section considered
L = elastic shortening or lenghtening of pile or section considered

The parameters A, E and L are usually known at the start of a loading test and ΔL is measured during the test.

The average load acting in each section of a telltale instrumented pile is determined from Eq. 2.7 and is assumed to act at the mid-point between the

two telltales. The load distribution of the pile is obtained by plotting the average loads acting along the pile with respect to depth.

Leonards and Lovell (1978) analysed the load distribution of driven piles using the deformation of the pile recorded by a toe telltale. Leonards and Lovell (1978) proposed that, for a load, Q, applied at the head of a pile, the measured elastic compression of the pile is:

$$\Delta_m = C' \frac{QL}{AE} \tag{2.8}$$

C' denotes the ratio of the measured compression (or extension) of a pile to the elastic compression of the pile considered as a free standing column.

Similarly, the contribution of the pile compression due to the portion resisted along the pile shaft is:

$$\Delta_s = C \frac{QL}{AE} \tag{2.9}$$

where C denotes the ratio of the calculated compression of the pile due to a load Q supported entirely by shaft resistance to the calculated compression of the pile considered as a free standing column.

Leonards and Lovell established the relation:

$$\alpha = \frac{C' - C}{1 - C} \tag{2.10}$$

where α is the ratio of the toe resistance to the total mobilized resistance ($R_t = \alpha R$).

The ratio C' is known from measured data and C is determined from an assumed distribution of unit shaft resistance.

A plot of C' versus the inverse of the head load Q is a straight line when the change of compression ΔL, for a change of load dQ is constant, then,

$$n = \frac{AE}{L} \cdot \frac{\Delta L}{dQ} \qquad (2.11)$$

where n is a constant and when

n > 1, the pile is yielding or buckling

n < 1, the shaft resistance is not fully mobilized.

n = 1, the shaft resistance is fully mobilized.

A detailed outline of the development of the above theory is given in Appendix A.

Fellenius (1980), discussed the application of Leonards and Lovell theory to engineering practice. Lee (1986), developed a computer program for the method to determine the shaft and toe loads in a pile. The program incorporates the effects of residual stresses in the pile and uses the deformation measurement recorded by three telltales.

2.6 DEFORMATION MODULUS

Structural steel is a homogeneous material with approximately linear stress-strain behaviour in an unconfined stress state. Under bi-axial stresses, the deformation modulus of a homogeneous material changes when the confining pressure is equal and greater than the axial stress. However, as the axial stress becomes exceedingly greater than the confining pressure, the effect of confinement on the deformation modulus becomes negligible and the modulus can be approximated from an unconfined test.

For composite columns, such as a pipe pile filled with concrete, the behaviour differs from the above. Neogi et al. (1969) discussed the structural action of composite steel concrete columns under applied loads. Because the Poisson's ratio of concrete is smaller than that of the steel,

at a small applied load, the steel will have a limited load transfer effect on the concrete core. With increasing longitudinal strain, the lateral expansion of the concrete becomes greater than that of the steel. Radial pressure will develop at the concrete to steel interface setting up circumferential stresses in the steel tube. Load transfer from the steel tube to the concrete core occurs, as the steel tube cannot sustain the stress longitudinally in the presence of a circumferential tension stress. The load transfer results in a variable combined modulus of elasticity and a considerably greater structural strength than the sum of the individual compressive strength of the steel and the concrete. Therefore, the use of Kirchoff's Law to determine a constant modulus of elasticity of a compound column of steel and concrete is approximative, only.

CHAPTER 3

FREDERICTON PILE TESTING PROGRAMME

3.1 SITE PLAN

The test area was located in a newly constructed embankment fill on the South bank of the Saint John River in Fredericton. The embankment fill served as part of the redevelopment of the bank area for the approach and abutment of the bridge. Fig. 3.1 includes a plan over the area and the location of the test site.

3.2 SOIL PROFILE

The soil deposits at the site were investigated by 41 borings and the results have been presented by Bozozuk et al., (1978). A complete section through the fill embankment, dregded fill, and soil and bedrock profile along the bridge centre line is indicated in Fig. 3.2 and given in detail in Table 3.1.

During the Winter of 1977, an 11 metre high embankment was constructed on the South shore of the river in line with the proposed bridge location. The test fill was constructed in two stages. The first stage was constructed in water to Elevation +3.0 m, which served as the working base for the installation of the field instrumention. The second stage was constructed to Elevation +9.0 m, the average in-situ density of the fill was 1825 kg/m^3.

During the Summer of 1977, after construction of the main test area, dredged granular fill was placed around the main test area. The average density was 1800 kg/m^3. The upper 4 metre layer of the subsoil on which the dregded fill was placed was a deposit of organic silts, sand, pebbles,

gravel, and wood. The consistency of the material was low to medium plasticity, the angle of internal friction was 31°, and the assumed density was 1680 kg/m^3. Below this layer, a formation of gray layered clayey silt extended from Elevation - 6.0 m to -12.5 m. The average water content ranged from 23 to 38 percent, the liquid limit was 29 percent, and the plastic limit was 9 percent. The average grain size distribution was 40 percent clay and 60 percent silt. The average wet density was 1840 kg/m^3 and the maximum in-situ vane shear strength ranged from 40 KPa to 50 KPa.

From Elevation -12.5 m to Elevation -18.0 m, the soil consists of a brown layered clayey silt with properties similar to those of the above layer. The water content ranged from 29 percent to 37 percent, the average liquid limit was 34 percent and the plastic limit was 12 percent. The grain size distribution was 45 percent clay and 55 percent silt. The average wet density was 1840 kg/m^3 and the in-situ vane shear strength ranged from 60 KPa to 90 KPa.

At Elevation -18.0 m, a 1 metre thick layer of varved brown clay and silt was found. At Elevation -19.0 m, a layered brown clayey silt formation was encountered. The formation extended to Elevation -26.0 m. The water content ranged from 35 percent to 45 percent, the average liquid limit was 40 percent and the plastic limit was 20 percent. The average grain size distribution was 64 percent clay and 36 percent silt. The average wet density was 1840 kg/m^3 and the in-situ vane shear strength ranged from 90 KPa to 120 KPa.

At Elevation -26.0 m, a very dense gravel formation with sand and stone was encountered. Undisturbed samples for this formation was not possible. This formation extended to Elevation -41.0 m where bedrock was found.

3.3 TEST PILES

Four driven piles were tested: two steel H-piles and two closed-toe steel-pipe piles as shown in detail in Figs. 3.3 and 3.4. The H-Piles (Piles 1 and 4) were size HP 305 mm by 132 kg/m (12 HP 74), while the pipe piles

(Piles 2 and 3) were 329 mm outside diameter by 8 mm thick wall closed-toe piles, of weight 62 kg/m. Pile 2 was filled with concrete immediately after driving. The measured compressive strength of the concrete was 35 MPa at 28 days and the average slump of the concrete mix was 170 mm. The modulus of elasticity was 27 GPa.

The piles were placed along two lines 3 metre apart, as shown in Fig. 3.5. The centre-to-centre spacing between the piles was 2.27 metre (seven pile diameters) along each line. The upper 11 metre of each pile was coated with asphalt to counteract negative skin friction expected to develop in the test fill.

Pile driving diagrams of the four piles are given in Appendix B. The driving of Piles 1 and 2 was terminated at the predetermined depth of 39 metre in the very dense sand and gravel formation. Piles 3 and 4 were driven to a depth of 32 metre in a clayey silt layer, leaving the pile toes 2.5 metre above the dense sand and gravel formation.

3.4 PILE INSTRUMENTATION

Each pile was instrumented with eight telltales. The telltales consisted of a 6 mm rod concentrically placed inside a 19 mm O.D. steel tube. The inner rod is a stress-free reference for the deformation measurements, while the outer pipe acted as a guide. The outer pipe was continuously welded to the outer casing of the pipe piles or the inner web of the H-piles.

The locations of the telltales in each pile are also shown in Figs. 3.3 and 3.4 The first telltale was installed immediately below the asphalt coated length of the pile, at a depth a of 11.1 metre below the surface of the embankment fill. The remaining seven gauges were installed at depths of equal intervals over the remaining length of the pile with one telltale placed at the toe.

Dial-gauge mounts were used to support dial gauges and electric linear variable displacement transducers (LVDT) to monitor the deformation

response of each pile under applied load. This system produced continuous measurement and recording of all deformation to a precision of 0.0025 mm. Measurement of the pile head movement relative to the surrounding ground was done independently using two dial gauges installed diametrically opposite on the head of the pile, each acting against a steel reference beam. The precision was 0.025 mm. Optical survey provided a secondary set of pile head movements.

3.5 TEST FRAME

A steel reaction frame consisting of twin girders was positioned over the piles as shown in Fig. 3.6. Each steel girder was positioned directly over each row of test piles. These were supported by steel towers anchored to heavy reinforced concrete footings, which were in turn anchored to eight HP 304 mm, 80 kg/m, steel reaction piles driven to toe bearing in the dense sand and gravel formation. The twin towers were cross-braced for additional stiffness. The minimum centre to centre spacing between the reaction piles and the test piles was nine pile diameters.

Each test pile was fitted with a 75 mm thick steel bearing plate for a 5 MN calibrated load cell and a 5 MN hydraulic jack. Two 50 mm thick steel reaction plates were also welded to the top and bottom flanges of each girder directly above the test piles to distribute the applied load.

3.6 PENETRATION RESISTANCE

In July of 1977, the four test piles were driven through the embankment fill, with a B-225 Bermingham diesel hammer. The hammer ram weight was 13.69 KN and the rated energy was 40.0 KNm. The penetration resistance of the piles passing through the granular fill was 20 blows/0.3 metre. Piles 3 and 4 were terminated at a resistance of 56 blows/0.3 metre and 31 blows/0.3 metre, respectively. Piles 1 and 2 were terminated at a resistance of 143 blows/0.3 metre and 251 blows/0.3 metre, respectively. The pile driving diagrams are given in Appendix B.

3.7 TEST PROCEDURE

The test method used was in the form of a constant rate of loading with the load applied in increments of 90 KN (10 tons) every 10 minutes. The gauge readings on the pile head were taken at every 1, 3, 6 and 9 minutes from the start of applying a load increment. The compression loads were removed in 50 KN and 100 KN increments, while the tension loads were removed in three to five increments. The piles were tested in the order of Piles 3, 4, 2, and 1. Occasionally, the load was maintained constant for periods longer than 10 minutes.

3.8 RESULTS OF PREVIOUS FREDERICTON TESTS

In October of 1977, in a first series of testing, the four piles were statically test loaded to failure in push and pull. The analysis of the test data was presented by Bozozuk et al. (1978), which enabled the formulation of effective stress equations to estimate the magnitude of the shaft resistance of piles loaded rapidly to failure.

Initial field measurements of pile compression prior to static testing indicated that the friction piles, Piles 3 and 4 had peak residual loads (downdrag load) of 535 KN to 625 KN (60 to 70 tons) and the toe bearing piles, Piles 1 and 2 had residual loads of 625 KN to 690 KN (70 to 100 tons). The measured load distributions are indicated in Fig. 3.7.

The shaft resistance was estimated using Eq 2.4, using the M factor. The M factor was computed using a soil friction angle of 31° and a coefficient of wall friction of 0.445. Tables 3.2 and 3.3 show the estimated resistances in pull and push and failure loads of each pile.

CHAPTER 4

STATIC PILE TEST DATA

4.1 REDUCED DATA

A second series of static test loading was performed thirteen months after the piles were driven and the results have been analysed in this thesis. The raw test data were reduced to working data and compiled in Tables C4.1 through C4.8 of Appendix C, for Piles 1, 2, 3, and 4, respectively. The original system of imperial units of measurement has been retained.

Tables C4.1 through C4.8 show the measured compression by each telltale for incremental values of the head load to the maximum applied test load. The unloading of the applied load in regular increments until complete removal of load is also shown in the lower portion of the tables. It is noted that compressions remained in the pile after the complete removal of the applied load for both push and pull tests. The tables show the overall telltale gauge length to the base of the telltale and the cross sectional area of the pile including the telltale guide pipe at the base of each telltale. The deformation measurements are in 1/10,000 inch (0.000, 25 mm) and the load measurements are calibrated load cell values in short tons.

Measurements of applied load versus the pile movement are presented graphically in Figs 4.1 through 4.8. The head movement of each pile is presented in loading to a maximum head load and the subsequent unloading. The head movement curve represents the sum of the total pile compression and the toe movement of the pile in the soil. The difference between the compression curve of the toe telltale and the head movement curve represents the movement of the pile toe. For the purpose of clarity, the telltales measurements are presented in the loading stages only.

4.2 RELIABILITY OF DATA

Preliminary analyses of the test data were conducted to ascertain validity and reliablity of the data and to determine the various pile-soil parameters for use in the main load-distribution analysis. The accuracy of the recorded applied load, recorded deformation, and modulus of elasticity of each pile was investigated.

4.2.1. Applied Load

The hydraulic jack used for applying the load was affected by internal friction and eccentric load distribution. Consequently, the use of the load cell was important. However, on numerous occasions, the load cell used during testing leaked, creating a potential source of error of load measurement. In one instance during push testing of Pile 3, the error in the load cell was large enough to warrant unloading from approximately 70 tons and restarting the test using a replacement load cell.

Calibrated load-cell measurements were made for the push testing of Piles 1, 2, and 4, in addition to the jack measurements. However, due to leaking of the load cell, load cell measurements were unavailable for the push test of Pile No. 3 and all pull tests. For these tests, jack manometer pressure measurements were utilized, which were converted to load by means of correlation equations from linear regression analyses of calibrated load cell measurements versus hydraulic-jack manometer pressure readings for Piles 1, 2, and 4.

4.2.2 Modulus of Elasticity

The modulus of elasticity (E) for the non-concreted steel piles (Piles 1, 3, and 4) was 200 GPa (29×10^6 psi). The calculated stiffness value (AE/L) of each telltale gauge length (L) was determined using (E) and the average running cross sectional area (A) of the pile over the respective telltale gauge lengths.

The modulus of elasticity of the concreted pipe pile (Pile 2) in compression was 43.6 GPa (6.32 x 10^6 psi), as calculated from Kirchoff's law for composite materials. The modulus of elasticity of Pile 2 in tension was based singularly on the modulus of elasticity of the steel pipe, the contribution of the concrete core was neglected for tensile strength.

Preliminary analyses showed that the concreted pipe pile (Pile 2) failed structurally before the bearing failure was reached. A plot of the chord modulus (increment of load over increment of strain) versus the head load of each telltale of Pile 2 (push test) is indicated in Fig. 4.9. The curves show the unstable behaviour of the modulus of elasticity of the pile with respect to depth and applied load. At small load levels, the combined modulus of elasticity of the pile ranges from a peak range of 104 GPa to 35 GPa (15 x 10^6 psi to 5 x 10^6 psi) for Telltales 1A and 2B, respectively. For larger loads, the value is smaller than 7 GPa (1 x 10^6 psi). The fluctuating and unstable behaviour of the pile modulus in the load region of 2200 KN to 2670 KN (247 tons to 300 tons), is due to a constant maintained applied load at 2200 KN (247 tons).

Further evidence of unstable behaviour is also shown in the load compression curves in Fig. 4.2 which are nonlinear beyond an applied head load of 2446 KN (275 tons). Furthermore, a substantial compression of 16.9 mm (0.665 inch) remained in the pile after complete removal of head load, suggesting that the pile had exceeded the steel yield stress during loading. Preliminary calculations on the steel alone, indicated the stress exceeded the yield strength of 248 MPa (36 ksi) when the applied load was greater than 2060 KN (231 tons).

During test loading of Pile 2, it was observed that water was coming out of the pile, suggesting that the water-filled cracks and voids in the pile were being closed expelling the water.

The pull test of Pile 2 was conducted subsequent to the push test. The load movement curves in Fig. 4.6 displayed non-linear behaviour at very small stress levels, confirming that the pile was deformed beyond its linear

elastic limit in the push test. The Pile 2 test data were considered unreliable and no further analysis was made. However, the data are presented for inspection and continuity.

4.2.3 Constant Loading

During test loading, frequent adjustment of the jack pressure was necessary to maintain the applied loads. In few instances, the applied load was kept constant for periods ranging from 12 to 48 hours. The most noticeable of these was maintaining a constant load level of 2290 KN (257 tons) for 32 hours on Pile 1 during the push test. Also, Pile 2 was subjected to a maintained constant load of 2200 KN (247 tons) for 39 hours during the push test.

Changing the method of load application from increasing the load every 10 minutes to maintaining the load constant for a long period of time affected the shape of the load movement curve subsequent to the change as shown in Figs. 4.1 and 4.2. This behaviour was more pronounced in the head movement curves, than in the individual telltale compression curves. The head movement curves do not display asymptotic behaviour at the maximum load applied. For each push test, six increments of load deformation measurements beyond the load maintained constant during the loading test are considered to provide unrepresentative data and have not been used in the load distribution analysis.

4.2.4 Deformation Data

The pile compressions were recorded with a 6.35 mm (0.25 inch) range dial gauge and a system of machined 6.35 mm (0.25 inch) steel spacers. For a continuous and uninterrupted recording of compression, spacers were either inserted or removed between the dial gauge and the reference beam as required. It was assumed that the spacers were exact measurement of 6.35 mm and the time for spacer operation was instantaneous. However, it was apparent that both assumptions were invalid, as differences ranging from

+0.127 mm (0.005 inch) to -0.127 mm (-0.005 inch) existed in the reduced deformation readings after the spacer operation. The original measurements prior to the spacer operation were maintained assuming the differences were non existent and subsequent measurements after spacer operation were adjusted accordingly. Consequently, a slight inconsistency in deformation measurements is evident when subtracting the values of two telltales from each other.

4.2.5 Faulty Telltales

Telltale 8H at a depth of 30.8 metre in Pile 1 and Telltale 5E at depth of 28.80 metre in Pile 4 were apparently faulty because the cumulative deformations recorded for these telltales were smaller than the deformations recorded by telltales located immediately above. This is inconsistent with the system of cumulative deformation measurement by telltales. It is possible that friction had developed between the telltale rod and the guide pipe. Therefore, the results of these telltales were neglected in the analysis. Telltale deformation readings at the toe of Pile 1 could not be recorded due to damage of the toe telltale during installation.

4.2.6 Failure Loads

The failure loads for each test were determined according to the methods outlined in Section. 2.3, that is, the Davisson Offset Limit, Brinch Hansen 80% criterion, and the Chin-Kondner method. The graphical representation of the failure load analyses for each pile is shown in Appendix D. The results are compiled in Table 4.1 and are compared to the maximum applied load. The Brinch Hansen and the Chin-Kondner failure loads are significantly higher than the maximum applied load for Piles 1 and Pile 2 pull test. Both cases of failure analyses show that, the piles were not tested to load levels high enough to satisfy the postulated failure criteria. Therefore, the failure loads obtained by both methods were considered unrepresentative.

For the failure loads not indicated in Table 4.1, the measured data do not allow for the particular failure criterion to be satisfied.

The peak shaft load transfer were computed using Eq. 2.11 and are listed in Table 4.1. The peak shaft load transfer in pull equals the applied failure load in pull for static equilibrium of forces. In the push tests, if the toe resistance was fully mobilized before peak shaft load transfer, then peak shaft load transfer would coincide with the failure of the pile. Spread sheet calculations to determine values of 'n' in Eq. 2.11 and the subsequent peak shaft load transfer are shown in Appendix E.

The Davisson Offset Limit Load method represents the lower limit of failure of the conventional failure criteria used and indicate more realistic and representative values of failure loads. The Davisson failure loads and the peak shaft load transfer were considered as a guide to determine the loads closest to the failure load.

CHAPTER 5

ANALYSIS AND DISCUSSION

5.1 INTRODUCTION

The residual strain in a pile driven in clay soils is due primarily to strains induced by driving and reconsolidation of the surrounding soils before static testing. A second component is induced due to compressive stresses remaining in the pile after a complete loading and unloading cycle from a static test.

The residual load is a direct function of the residual strain. The total load acting in the pile during static testing is the sum of the residual loads and the loads mobilized during testing.

5.2 ANALYSIS OF RESIDUAL STRAINS

A typical plot of the head load on a pile versus total strain (including residual strain prior to static testing) is shown in Fig. 5.1. The strain cycle consist of a loading curve in push commencing at an origin, Point $0'$, offset from the true origin, Point 0, by the amount of initial residual strain in the pile. The curve returns to a positive increased locked-in strain, Point A', at a distance, A, from Point $0'$ on the abscissa. The strain cycle in pull commences at this point. In unloading to zero load from the maximum pull load, the curve returns to negative locked-in strain, Point B', at a distance, B, from Point A'.

The position of the true origin, Point 0, is unknown. However, Point 0 must lie between Point $0'$ and Point B'. Since the initial residual strain is a function of the position of Point 0, the magnitude of the initial residual strain may vary from minimum value of zero when Point 0 lies at Point $0'$

and a maximum value equal to the difference of A and B when Point 0 lies at Point B'.

For the purpose of this analysis, the initial residual strain is computed for three positions of the true origin, that is, when Point 0 lies at the Point 0', at the mid-point between Points 0' and B', and at Point B'. In other words, the initial residual strain is assumed to be zero, half the maximum possible residual strain, or the maximum possible residual strain, respectively.

It should be noted that the value of residual strain in a push test, Distance A, is a negative value when Point A' is located to the left of origin 0'. This would be due to a reduction of shaft resistance at the pile-soil interface caused by the loading test, and results in an elastic lengthening of the pile. When this is the case, the initial residual strain cannot be smaller than the absolute value of A.

Ordinarily in a static loading test, the initial residual strain prior to push testing is unknown and unaccounted for in the analysis of the test data. Fig. 5.2 shows an example of a strain cycle in push and pull of unknown initial residual strain as recorded by Telltale 2B of Pile 3. The strain cycle commences at the apparent origin, 0' on the apparent zero axis, that is, the recorded strain is measured relative to the apparent zero axis, as opposed to the true zero axis.

Tables 5.1 through 5.3 show the increased locked-in compressions A, the lengthening of the pile in pull, B, and two cases of computed residual compression for each telltale prior to push testing for Piles 1, 3, and 4. Case 1 of computed residual compression is half the maximum residual compression and equal to 0.5(B-A). Case 2 of the computed residual compression is the maximum residual compression and equal to (B-A). The missing values for various telltales were either not recorded or were erroneous as mentioned in Chapter 3.

Figs. 5.3 through 5.5 show the distribution of residual compression with respect to depth, the residual compressions are plotted at the location of

the telltale ends. The figures indicate that the major portion of the residual compression originated in the compressible clayey silt formation. Reasonable agreement is found in the distributions for Piles 1 and 4, for each case of residual load analysis, Pile 3 appears to be greater by 50%.

Tables 5.1 through 5.3 also show the average initial residual strains prior to push testing for each section of the piles. The residual strain is computed as the ratio of the difference of residual compression of two telltales and the length between the telltales. For the upper telltale, the strain is the ratio of the residual compression recorded by the telltale and the length of the telltale.

Figs. 5.6 through 5.8 show the distributions of residual strain, plotted as a constant over each telltale length considered. For comparison, the strains measured by Bozozuk et al. (1978) three months after the piles were installed (before first series of testing) are also shown.

The measured and computed distributions of residual strain increase linearly from the pile head to a peak value in the lower half of the pile. Below the peak value, the strain reduces with increasing depth. The residual strain distribution measured by Bozozuk et al. (1978) and half the maximum possible computed residual strain distribution (Case 1) are similar in magnitude to the measured values, the latter being slightly greater in the lower region of the piles. The distribution of the maximum possible strain (Case 2) is greater than the measured strain distribution and almost twice the value in the middle third of the pile. However, with the increase of time and further consolidation of the compressible clay formation, the residual strain must increase. It appears, therefore, that the strains computed for Case 1 underestimate the true residual strain acting in the second test series.

Since the pull tests were conducted after the push tests, the residual compression in the pile before pull testing is equal to the sum of the initial residual compression before push testing and the increased locked-in compression, A, after push testing. Similarly to the push tests, two possible cases, Case 1 and Case 2, of residual compression before pull

testing are computed. The values at the end of each telltale and the resulting residual strain between telltale ends are shown in Tables 5.4 through 5.6 for Piles 1, 3, and 4.

5.3 ANALYSIS OF LOAD DISTRIBUTION

5.3.1 Push Testing

The applied loads closest to the failure load for load distribution analyses in push were 4100 KN, 2080 KN, and 1600 KN (461 tons, 234 tons, and 180 tons) for Piles 1, 3, and 4, respectively. Preliminary analyses have shown that no considerable difference in results were obtained when an immediately higher or lower load level than the above values were choosen. Tables 5.7 through 5.9 show the measured compression at these load levels for each telltale, the change of compression between two telltales, the measured strain between two telltales, the residual strain before push testing, and the sum of the measured and residual strains (total or adjusted strain). The tables also show two cases of residual load analysis, the computed or unadjusted load (without residual load) from the measured strain, the residual load from the residual strain, and the total or adjusted load (with residual load) from the total strain. The loads were computed from Eq. 2.7, for known values of AE.

The residual load, the unadjusted load, and the adjusted loads (with residual load) were plotted at the mid-point between the telltales used as shown in Figs. 5.9 through 5.11 for Piles 1, 3, and 4. The load distribution curves were obtained using the best possible curve fit of the coordinates while neglecting highly scattered points. The resulting regression polynomials describing the curve fit are given in Appendix F.

The distributions of residual load are similar in most aspects. The peak residual loads ranged from 445 KN (50 tons) for Pile 3 to 670 KN (75 tons) for Pile 4, for Case 1 and twice the amount for Case 2. The values occurring at depths of 22.5 metre to 25.5 metre (75 feet to 85 feet). The distribution increases linearly to a peak value then remains constant or

decreases in the lower third of the piles. Similar distributions were obtained by Hanna and Tan (1793) in model test piles.

The various load distributions have a definite geometric pattern depending on the type and extent of load adjustment carried out. The unadjusted load distributions indicate a unit shaft resistance decreasing in magnitude with depth. Also the adjusted load distributions (Case 1) with half the maximum possible residual load indicate a unit shaft resistance which is approximately constant with increasing depth. The adjusted load distributions with the maximum possible residual load (Case 2) indicate a unit shaft resistance increasing in magnitude with depth.

Both the two adjusted load distributions (Cases 1 and 2) show distinct increase of load in the lower portions of the pile as opposed to the unadjusted load distribution (no residual load). Reasonable agreement exists in the upper half of the piles for both cases of adjusted load distribution, while considerable difference is observed in the lower half, which is due to the greater magnitude of residual loads computed for Case 2.

The load distributions also show that very small loads were mobilized in the upper 11.3 metre (37 feet) of the piles, suggesting that the bitumen coating in this section of the pile was partially effective in reducing residual loads and shaft resistance.

The unit shaft resistance distributions in the clayey silt layer were obtained by differentiating the regression polynomials describing the load distribution curve and dividing the results by the shaft perimeter area of the piles. The calculations to determine the unit shaft resistance are given in Appendix F. The shaft perimeter area of the H-piles is assumed to be square section equal to the flange width of the piles. The results of the above procedure, when applied to Piles 1, 3, and 4, are shown in Figs. 5.12 through 5.14, respectively. The measured shear strength distribution of the soil at the time of the first series of static testing is also indicated.

The unit shaft resistance distributions are in reasonable agreement for each case of analysis in the upper half of the pile. However, considerable difference is observed in the lower half. The unadjusted distribution is constant or decreases after a peak value at depths of approximately 40b. The Case 1 adjusted distribution lies between the unadjusted distribution and the adjusted distribution of Case 2, and is of considerable smaller value than the measured shear strength. The Case 2 adjusted distributions for Piles 3 and 4 show a linear increase of unit shaft resistance, the values are in reasonable agreement with the measured shear strength of the surrounding soil.

The unit shaft resistance distribution for Pile 1 shown in Fig. 5.12 is a product of the derivative of the linear regression curve fit of the load distributions and is constant for all three cases of analysis. The value of the unit shaft resistance decreases with increasing order of residual load adjustment. Increased residual load results in a corresponding increase of toe resistance and a decrease in shaft resistance. Consequently, the rate of change of unit shaft decreases correspondingly.

Furthermore, the distribution of unit shaft resistance in push is approximately constant in the region of the compressible clayey silt for Pile 1. It is also possible that the pile-soil shear strength of Pile 1 was not fully mobilized, because the pile was not tested to failure as supported by the failure plots of Pile 1 of Appendix D. This would contribute to a constant or decreased rate of change of unit shaft resistance.

5.3.2 Pull Testing

The applied loads closest to the failure loads in pull were 1975 KN, 1510-KN, and 1110 KN (222 tons, 170 tons, and 125 tons) for Piles 1, 3, and 4, respectively. The computed strains and loads for the pull tests were determined similarly to the above push tests. The lengthening of the pile measured by each telltale, the difference of lengthening between two telltales and the corresponding strain, the residual strain before pull,

and the difference between the measured and residual strain (total or adjusted strain) are shown in Tables 5.10 through 5.13. The residual loads from residual strain, the load computed from measured strain, and the total or adjusted load from total strain were calculated using Eq. 2.7 and are given in Tables 5.10 through 5.13.

The load distribution curves in pull were obtained similarly to the curves in the push tests and are shown in Figs. 5.15 through 5.17. Small residual loads are present in the pile before pull for Piles 3 and 4, and are almost negligible in the lower regions of the piles.

The unadjusted load distributions are parabolic having considerable apparent toe resistance and small shaft resistance. Although slightly greater in toe resistance, the distributions are in reasonable agreement with the adjusted load distributions of Case 1. The adjusted load distributions, Case 2, are linear and parabolic. As in the push tests, reasonable agreement exist in the upper half of the piles. However, a small apparent toe resistance was found in Pile 4, while no toe resistance and no negative shaft resistance were observed the lower sections of Piles 1 and 3.

Generally, when the residual loads are not included or underestimated in the analysis of the pull test, large apparent toe resistance and little or no shaft resistance are evident.

An apparent toe tension resistance is found in the piles for the pull tests of the unadjusted distributions and Case 1 of the adjusted distributions. It is obvious that the residual loads prior to pull testing for these distributions were also underestimated. Underestimation of residual load is most obvious in the lower sections of the piles where the initial residual strain was partially released during the unloading of the applied push load. That is, the increased locked-in strain value, A, was recorded as a negative value.

Case 2 produced slightly large residual loads before pull testing. The corresponding adjusted load distribution in the lower sections of Piles 1

and 3 indicate a zero or negative load transfer. Ideally, in a pull test the load distribution is a gradual decrease to zero load at the pile toe. It appears that the computed residual load before pull testing for Case 2 is slightly overestimated for these piles. The residual load before pull for Pile 4 is a close approximation of the true value, although slightly small, it results in an approximate ideal load distribution and unit shaft resistance distribution.

The unit shaft resistance in pull was determined similarly to the unit shaft resistance in push. The calculations are shown in Appendix F and the distributions in Figs. 5.18 through and 5.20 for Piles 1, 3 and 4 respectively. The unadjusted unit shaft resistance distributions in pull for Piles 1; 3, and 4 are approximately constant with slight indication of an increase with depth. As in the push tests, the unadjusted and adjusted (Case 1) distributions are in close agreement in magnitude and geometric configuration. Both distributions show linear increase of resistance with depth and lie within + 10% of each other. The adjusted distribution Case 2, is also a linear increasing distribution for Piles 1 and 4. However, the rate of increase of unit shaft resistance is almost twice as large as the Case 1 and the unadjusted values.

The distribution also correlates closely with measured shear strength. Similarly, close correlation of unit shaft resistance distribution with the measured shear strength was shown for the Case 2 of the push tests. The presence of an apparent toe resistance would probably account for the decrease of unit shaft resistance in the pull test of Pile 4.

5.4 DISCUSSION

The residual loads in the piles are due to downdrag resulting from the action of the compressible clayey silt formation under the weight of the surcharged embankment fill. Bozozuk et al. (1978) recorded initial residual loads of magnitude ranging from 445 KN to 890 KN (50 to 100 tons) in the first three months after installation of the piles. It was expected that during an additional period of ten months, the residual loads would

increase until the excess pore water pressure in the clayey silt formation has dissipated and consolidation of the formation has ended. The computed results of the analysis, Case 2, confirm this and show that for this extended period of time the maximum residual load is increased to range from 940 KN to 1245 KN (106 to 140 tons)

Case 1 produced reasonable agreement of computed residual loads with the measured values recorded by Bozozuk et al. (1978). Since it was expected that the computed residual loads would be greater than the recorded values, the computed values of Case 1 appears to underestimate the residual loads present in the piles.

The residual loads of Case 1 also resulted in apparent toe load in the adjusted load distribution of the pull tests. Since there cannot be toe loads in the pull test of a pile, the computed residual loads underestimate the true residual loads.

The unit shaft resistance in push is greater than pull by 50% to 75% for the unadjusted and Case 1 adjusted loads. However for the Case 2 adjusted load, a very close agreement is obtained, and the unit shaft resistance distribution in both push and pull correlates closely with measured shear strength. This is probable indicative of the true position of the zero axis and implies that the true residual compression lies closer to the values computed in Case 2 than those in Case 1.

Generally, a correct analysis of load distribution is only possible when the investigation considers the presence of residual loads in the piles.

The geometric configuration of the residual strain and residual load distribution before push testing is similar to those reported by Hanna and Tan (1973). In each case, the distribution increases linearly and reaches a peak value in the lower half of the pile then remains constant or decreases with depth. The findings are consistent with a neutral plane present in piles. The adjusted and unadjusted load distributions are also in reasonable agreement with corresponding distributions in model test piles investigated by Hanna and Tan (1973). Similar agreement is found with model

load distributions considering the presence of residual loads as suggested by Briaud and Tucker (1985).

Both the adjusted and unadjusted load distributions in the push and pull tests and their corresponding unit shaft resistance distributions are consistent with the load transfer behaviour of piles as hypothesised by Holloway et al. (1978). Also the equal magnitude of unit shaft resistance in push and pull tests (Case 2), closely support similar findings by O'Neill et al. (1982). This suggests that the mobilised unit shaft resistance is independent of the direction of loading.

The results of the investigation by Hunter and Davisson (1969) are outlined in Section 2.4, and are consistent with the results of Case 2 of the present analysis. However, the adjusted distribution in the pull test by Hunter and Davisson (1969) is a gradual and even distribution of load in the lower section of the pile to zero toe load. In the present analysis, that same technique results in an overestimation of the residual load leading to no load transfer in the lower sections of the Piles 1 and 3, which indicates the necessity of using several telltales in the piles.

A relative comparison of the load distributions of Mohan et al. (1963) and D'Appolonia and Romualdi (1963) is equivalent to the unadjusted load distributions of Piles 3 and 4, since the presence of residual loads were not considered by the investigators. The lack of consideration of residual loads in the piles in push testing would probably account for the constant shaft resistance, a decrease rate of increase, and a negative shaft resistance found in the lower section of the piles tested by these authors. However, both papers developed analytical techniques based on the transfer function and the elastic theory approach and obtained results that were in reasonable agreement with their experimental results. It appears that the developed analytical techniques could be adjusted to measurements without disclosing the neglect of residual loads in the piles.

The results of the present analysis indicate that when the residual loads were not considered or underestimated, the unit shaft resistance appears to be constant or decreasing at "critical depths" of 20b to 40b. When the

maximum residual load were accounted for there is no "critical depth" and the unit shaft resistance increases linearly for the entire length of the pile. Also, the unit shaft resistance correlates closely with the measured shear strength of the soil. It is proposed that the concept of critical depth may be incorrect and caused by inadequate analysis of test data.

It must be recognized that the accuracy of the load distribution and the unit shaft resistance distribution is a function of the technique used to determine the residual load in the piles. The technique is only approximate and depends on the assumption of the true zero load axis location of the load strain cycle. The results suggest that the true origin, 0, lies further left of position adopted in Case 1, especially for lower sections of the piles. Consequently, the residual loads prior to push testing and pull testing are apparently larger than Case 1 values and slightly smaller than Case 2.

The computed strain or load value is a function of two telltale measurements, while a shaft resistance value is a function of three telltale measurements. The results of strain and load in the piles were computed based on the differences of telltale measurements. Therefore, the scatter of computed strain and load is due to the imprecision of the data used and the inconsistent telltale measurement with respect to each other. The precision of the deformation measurement was measured to 1 in 10,000 inch. However, errors in measurement of 1 in 1,000 inch cannot be eliminated and would translate to a value of 9.6 KPa (0.09 tsf) of computed unit shaft resistance.

The accuracy of the unit shaft resistance is also a function of the accuracy of the regression polynomial describing the load distribution coordinates and the derivative of the polynomial. Errors in the regression polynomials are greatly amplified when the equation is differentiated and the results inverted. Although accuracy of the polynomials was indicated by a correlation coefficient of 0.97, even an extremely small change in slope of the distribution curve is translated in exaggerated values of shaft resistance as shown in the lower sections of Pile 4, push test.

The results of the analysis also indicate that the use of telltales in static tests is inadequate to evaluate the true load distribution of a pile. Evaluation of pile capacities from telltale measurements are approximate, and only holds good when the presence of residual loads development during driving in the piles are minimal or zero. In this case, the assumption of load strain origin at the start of the push test, holds good. However, when large residual loads are anticipated, provisions must be made to determine the magnitude of residual loads in the piles, otherwise the telltale measurement alone in a static test is insufficient.

The accuracy and effeciency of the system of telltale measurements in static tests are lacking. An improved system of control in static tests is required. The system must be capable of measuring loads acting in driven piles, commencing at the time of driving. A system of control using load cells incorporated or systemic with the piles before driving appears to be the ideal solution. Cooke (1978) used a similar technique in tubular jacked piles to obtain extremely accurate load distribution.

A 10% to 30% increase of pile capacity is observed when the results of the present analysis were compared to the results obtained by Bozozuk et al. (1978). Similar increase of individual shaft and toe capacity were also observed. It must be recognised that the results obtained by Bozozuk et al. (1978) were computed using soil parameters measured at the time of the first series of testing. The relations developed by Bozozuk et al. (1978) to estimate the shaft resistance would support the present computed shaft resistance of the piles providing there is an increase of soil strength and a decrease of pore water pressure during the period between the two series of static testing. Laboratory measurements of the soil shear strength along the pile shaft and the pore water pressure at the time of the second series of test loading were not available for analysis. Consequently, it was not possible to check the accuracy of Bozozuk et al. (1978) relations, and to compare the predicted and the computed shaft resistances.

CHAPTER 6

CONCLUSIONS

The analysis of load-displacement measurements of piles recorded in static push and pull tests indicates that residual loads are present prior to push and pull testing in piles driven in a compressible clayey silt formation. The residual loads are due to a negative skin friction induced by the compressible clayey silt formation and resisting positive shaft resistance in an underlying soil layer.

An improved and modified technique was used to determine the magnitude of the residual load. The results of the analysis indicate that the approximate magnitude of the residual loads can be evaluated sucessfully from a push and pull static test.

The results of the analysis confirm that the predicted residual loads in the piles over a period of thirteen months are greater than the measured values obtained in the initial three months after driving. The results also indicate the approximate range of the residual loads. The residual loads tend to increase linearly to a peak value in the lower half of the pile, then remain constant or reduce with increasing depth. The results are consistent with the presence of a neutral plane in the piles.

The results indicate that the true residual loads in the piles should be computed for the position of the load strain origin close to the end of the pull test, that is, Point B'.

The adjusted load distribution decreases linearly having greater shaft and toe resistance in the lower sections of the pile, as opposed to the unadjusted and partially adjusted load distributions.

The pile toe capacity increases in push test when the residual loads are considered while the shaft resistance decreases correspondingly. Large apparent toe resistance and little or no shaft resistance are evident in the pull test when the residual loads were not considered or underestimated.

When neglecting residual strain, the unit shaft resistance distribution increases linearly then remains constant or decreases below "critical depths" of 20b to 40b. There is no "critical depth" when the maximum residual loads are considered and the unit shaft resistance increases linearly for the entire length of the pile.

When the maximum possible residual load are considered, the unit shaft resistance is approximately equal in magnitude in the push and pull tests, supporting the findings of O'Neill et al. (1982). The unit shaft resistance also correlates closely with the measured shear strength of the soil.

The results of the analyses are consistent with the hypothesis and findings of previous investigators as outlined in Chapter 2, in particular the findings of Hanna and Tan (1973) and Hunter and Davisson (1969). The results also support the hypothesis of Holloway et al. (1978) on the load and shaft resistance distribution in driven piles.

Further analysis and the use of more accurate test data are required to substantiate the findings of the unit shaft resistance distribution in push testing. The use of load cell is recommended as a means of measuring directly the loads acting in various locations of the pile and would also alleviate the problems and errors occuring in the measurement of the load deformation data.

REFERENCES

BALAAM, N. P., POULOS, H. G., and BOOKER, J. R, 1975. Finite element analysis of the effects of installation on pile load-settlement behaviour. Geotechnical Engineering, Vol. 6, No. 1, pp. 33-48.

BANERJEE, P. K., and DAVIES, T. G., 1977. Analysis of pile foundation groups embedded in Gibson soil. Proceedings of the 9th International Conference on Soils Mechanics and Foundation Engineering, Tokyo. Vol. 1 pp. 381-386.

BANERJEE, P. K., and DAVIES, T. G., 1978. The behaviour of axially and laterally loaded single piles embedded in non-homogeneous soils. Geotechnique, Vol. 28, No. 23, pp. 309-326.

BOZOZUK, M., 1972. Downdrag measurements on a 160-ft floating pipe test pile in marine clay. Canadian Geotechnical Journal, Vol. 9, No. 3, pp. 127- 136.

BOZOZUK, M., KEENAN, G. H., and PHEENEY, P. E., 1978. Analysis of load test on instrumented steel piles in compressible silty soil. American Society of Testing and Materials, ASTM Symposium on the Behaviour of Deep Foundations, R. Lundgren, Editor, Special Techncal Publication, STP 670, 1979, pp. 153-180.

BOZOZUK, M., and KEENAN, G. H., 1985. Downdrag on a 3-pile group of piles. Proceedings of the 11th International Conference of Soil Mechanics and Foundation Engineering, San Francisco. Vol. 13, pp. 1407- 1412.

BRIAUD, J-L., and TUCKER, L., 1985. Piles in Sand: A method including residual stresses. American Society of Civil Engineers, ASCE Journal of Geotechnical Engineering, Vol. 110, No. 11, pp. 1666-1679.

BURLAND, R. B., 1973. Shaft friction on piles in clay. A simple fundamental approach. Ground Engineering, London, Foundation Publications, Ltd., Vol. 6, No. 3, pp. 30-42.

BUTTERFIELD, R., and BANERJEE, P. K., 1971. The elastic analysis of compressible piles and pile groups. Geotechnique, Vol. 21, No. 1, pp. 43- 60.

CANADIAN FOUNDATION ENGINEERING MANUAL, 1985. Second Edition, Part 1: Fundamentals; Part 2: Shallow Foundations; Part 3: Deep Foundations; Part 4: Excavations and Retaining Structures. Canadian Geotechnical Society, Technical Committee on Foundations, BiTech Publications, Vancouver, 426 p.

CHIN, F. K., 1971. Pile tests Arkansas River project, Discussion. American Society of Civil Engineers, ASCE Journal of Soil Mechanics and Foundation Engineering, Vol. 9, SM6, pp. 930-932.

COOKE, R. W, 1978, Influence on residual installation forces on the stress transfer and settlement under working loads of jacked and bored piles in cohesive soils. American Society of Testing and Materials, ASTM symposium on the Behaviour of Deep Foundations, R. Lundgren, Editor, Special Technical Publication, STP 670, pp. 231-249.

COYLE, H. M., and REESE L. C., 1966. Load transfer for axially loaded piles in clay. American Society of Civil Engineers, ASCE Journal of Soil Mechanics and Foundation Engineering, Vol. 92, No. SM2., pp. 1-26.

D'APPOLONIA, E., and ROMUALDI, J. P., 1963. Load transfer in end-bearing steel H-piles. American Society of Civil Engineers, ASCE Journal of Soil Mechanics and Foundation Division. Vol. 89, SM2, pp. 1-25.

DAVISSON, M. T., 1972. High Capacity Piles. Proceedings, Lecture Series. Innovations in Foundation Construction. American Society of Civil Engineering, Soil Mechanics and Foundation Engineering, Illinois Section, Chicago.

DAVISSON, M. T., 1975. Pile Load Capacity. Proceedings, Seminar on Design, Construction, and Performance of Deep Foundations, American Society of Civil Engineers, San Francisco, 48 p.

DESAI, C., and ABEL, J. F., 1972. Introduction to Finite Element Method. New York, Van Nostrand Reinhold Co.

DESAI, C., 1977. Numerical Methods in Geotechnical Engineering. Deep Foundations. Desai and J. T. Christian, Editors, New York, McGraw-Hill. Chapter 7, pp. 235-269.

FELLENIUS, B. H., and BROMS, B. B., 1969. Negative skin friction for long piles driven in clay. Proceedings of the 7th International Conference on Soil Mechanics and Foundation Engineering, Mexico City, Vol. 2, pp. 93-98.

FELLENIUS, B., and SAMSON, L. S., 1976. Testing of drivability of concrete piles and disturbance of sensitive clay. Canadian Geotechnical Journal, Vol. 13, No. 2, pp. 139-160.

FELLENIUS, B. H., 1980. Analysis of results from routine pile load tests. Ground Engineering, Foundation Publications Ltd., London, Vol. 13, No. 6, pp. 19-31.

HANNA, T. H. and TAN, R. H. S., 1973. The behaviour of long piles under compressive loads in sand. Canadian Geotechnical Journal, Vol. 10, No. 3, pp. 311-340.

HANSEN, J. B., 1963. Hyperbolic stress-strain response: cohesive soils, Discussion. American Society of Civil Engineers, ASCE Journal of Soil Mechanics and Foundation Division, Vol. 89 No. SM4 pp. 241-245.

HOLLOWAY, D. M., CLOUGH, G. W., and VESIC, A. S., 1978. A rational procedure for evaluating the behaviour of impact-driven piles. American Society for Testing and Material, ASTM Symposium on Behaviour of Deep Foundations, R. Lundgren, Editor, Special Technical Publication, STP 670, 1978, pp. 335-357.

HUNTER, A. H., and DAVISSON, M. T., 1969. Measurements of pile load transfer. American Society for Testing and Material, ASTM Symposium on Performance of Deep Foundations, Special Technical Publication, STP 444, 1969, pp. 106-117.

KEZDI, A., 1976. Foundation Engineering Handbook. Pile Foundations, F. Winterkorn and H-Y. Fang, Editors, Chapter 19, pp. 556-600.

LEE, Q. S., 1986. Analysis of static test data using telltales. M. Eng. Thesis, University of Ottawa, Faculty of Science and Engineering, Department of Civil Engineering. (In Preparation)

LEONARDS, G. A., and LOVELL, D., 1978. Interpretation of load test from high capacity driven piles. American Society for Testing and Material, ASTM Symposium on Behaviour of Deep Foundations, R. Lundgren, Editor, Special Technical Publication, STP 670, pp. 388-415.

MATTES, S. N., and POULOS, H. G., 1969. Settlement of single compressible piles. American Society of Civil Engineers. Journal of Soil Mechanics and Foundation Division. Vol. 95, No. SM1, pp. 189-207.

MEYERHOF, G. G., 1976. Bearing capacity and settlement of pile foundation. American Society of Civil Engineers. ASCE Journal of the Geotechnical Engineering Division, Vol. 102, No. GT3, pp. 197-228.

MOHAN, D., JAIN, G. S., and KUMAR, V., 1963. Load bearing capacity of piles. Geotechnique, Vol. 13, No. 1, pp. 76-86.

NEOGI, P. K., SEN, H. K., and CHAPMAN, J. C., 1969. Concrete filled tubular steel columns under eccentric loadings. Structural Engineer, Vol. 47, No. 5, pp. 187-190.

O'NEILL, M. W., HAWKINS, R. A., and MAHAR, L. J., 1982. Load transfer mechanisms in piles and pile groups. American Society of Civil Engineers, ASCE Journal of Geotechnical Engineering, Vol. 108, No. GT12, pp. 1605-1623.

POULOS, H. G., 1968. Analysis of the settlement of pile groups. Geotechnique, Vol. 18, pp. 449-471.

POULOS, H. G., 1977. Numerical Methods in Geotechnical Engineering. Settlement of Pile Foundations. C. Desai and J. T. Christian, Editors, New York, McGraw-Hill. Chapter 10, pp. 326-363.

POULOS, H. G., and DAVIS, E. H., 1968. The settlement behaviour of single axially-loaded incompressible piles and piers. Geotechnique, Vol. 18, pp. 351-371.

POULOS, H. G., and DAVIS, E. H., 1980. Pile Foundation Analysis and Design. Series in Geotechnical Engineering, John Wiley and Sons Inc., 397 p.

RANDOLPH, M. F., and WROTH, C. P., 1978. Analysis of deformation of vertically loaded piles. American Society of Civil Engineers. ASCE Journal of Geotechnical Engineering, Vol. 104, No. GT 12, pp. 1465-1488.

ROBINSKY, E. I., and MORRISON, C. F., 1964. Sand displacement and compaction around model friction piles. Canadian Geotechnical Journal, Vol. 1, No. 2, pp. 81-93.

STEWART, J. F., and KULHAWY, F. H., 1981. Interpretation of uplift load distribution data. Proceedings of the 10th International Conference on Soil Mechanics and Foundation Engineering. Stockhlom, Vol. 2, pp. 277-280.

VESIC, A. S., 1969. Load transfer, lateral load and group action of deep foundations. Performance of Deep Foundations, ASTM Special Technical Publication. ASTM 444 pp. 5-14.

VESIC, A. S., 1970. Load transfer in pile-soil systems. Proceedings on the Conference of Design Installation of Pile Foundation and Cell Structure. Lehigh, Pennsylvania.

VESIC, A. S., 1977a. On significance of residual loads for load response of piles. Proceedings of the 9th International Conference on Soil Mechanics and Foundation Engineering. Session 2, Behaviour of Foundations and Structures, Panel Discussion, Tokyo, Vol. 3, pp. 374-379.

VESIC, A. S., 1977b. Design of pile foundations. National Cooperative Highway Research program Synthesis of Highway Practice No. 42, United States Transportation and Research Board, National Research Council. Washington, D.C., pp. 1-68.

VIJAYVERGIYA, V. A., and FOCHT, J. A., Jr., 1972. A new way to predict capacity of piles in clays. Proceedings of the 4th Offshore Technology Conference, Houston. Vol. 2, pp. 865-864.

TABLES

TABLE 3.1

Elev. (m)	Soil Description	Density kg/m^3	In-Situ Vane Shear strength (KPa)	N	w_n (%)	LL	PL
+9.0 to -2.0	Loose sand and random dredged fill	1825					
-2.0 to -6.0	Fine sand, gravel with traces of organic silt and pebbles	1680		5			
-6.0 to -12.5	Gray clayey silt. 40% clay, 60% silt	1840	40-50		23-38	29	20
-12.5 to -18.0	Gray brown layered clayey silt		60-90	14			
-18.0 to -19.0	Varved brown clay and silt						
-19.0 to -26.0	Brown clayey silt 64% clay, 36% silt	1840	90-120	10	35-45	40	20
-26.0 to -41.0	Very dense gravel and sand			64			
-41.0	Bedrock						

N is the Standard Penetration Index (blows/0.3 metre)

TABLE 3.2 AXIAL PULL LOADS First Fredericton Test

Pile No.	Depth of Penetration	Estimated Shaft Resistance			Measured Failure Load
		Clayey Silt	Dense Gravel	Total	
	(m)	(KN)	(KN)	(KN)	(KN)
1	39.6	935	490	1425	1245
2	38.8	935	445	1380	1470
3	31.7	710	——	710	675
4	31.5	710	——	710	590

After Bozozuk et al. (1978)

TABLE 3.3 AXIAL PUSH LOADS First Fredericton Test

Pile No.	Depth of Penetration	Estimated Resistance				Measured Failure Load
		Shaft		Toe	Total	
		Clayey Silt	Dense Gravel			
	(m)	(KN)	(KN)	(KN)	(KN)	(KN)
1	39.6	1690	890	270[a]	2850	3425
		1690	890	755[b]	3335	3425
2	38.8	1690	800	1245[a]	3735	3645
3	31.7	1335	———	175	1510	1555
4	31.5	1335	———	45	1380	1379

(a) denotes estimation from Vesic (1977) using actual area of pile toe
(b) denotes estimation from Vesic (1977) using 50% of box enclosing pile toe

After Bozozuk et al. (1978)

TABLE 4.1 FAILURE LOADS (KN)

METHOD OF ANALYSIS	PILE No. 1		2		3		4	
	Push KN	Pull KN	Push KN	Pull KN	Push KN	Pull KN	Push KN	Pull KN
MAXIMUM APPLIED LOAD	4200 (472)	3090 (347)	3800 (427)	2625 (295)	2190 (246)	1620 (182)	1995 (224)	1320 (148)
Davisson Limit Load	4100 (461)	1935 (224)	3780 (425)	1185 (133)	1885 (212)	1555 (175)	1640 (184)	1105 (124)
Brinch Hansen 80% Criterion	7955 (894)	2920 (328)	3905 (439)		2145 (241)	1840 (207)	2080 (234)	1150 (129)
Chin	7223 (812)	7115 (800)	4420 (497)	3930 (442)	2400 (270)	2090 (235)		
Leonards and Lovell	2795 (314)	1680 (189)		1185 (133)	1885 (212)	1405 (158)	1395 (157)	845 (95)

All units in brackets are in tons.

Table 5.1 **Pile 1; H-Pile; Push Test** **Residual Compression**

CASE 1

Tell. No.	Length (ft)	Increased Compression (A) (inch)	Locked-in Compression (B) (inch)	Assumed Residual Compression 0.5(B-|A|) (inch)	Residual Strain Strain ($1x10^{-3}$)	Residual Strain Telltale Length
2B	37.1					
6F	50.2	0.0237	0.0803	0.0285	0.0473	Head-6F
3C	63.3	0.0177	0.1223	0.0525	0.1526	6F-3C
7G	76.4	0.0082	0.1570	0.0745	0.1399	3C-7G
4D	89.5	0.0061	0.1980	0.1021	0.1752	7G-4D
8H	102.7					
5E	115.8	0.0400				
1A	127.9					

CASE 2

Tell. No.	Length (ft)	Increased Compression (A) (inch)	Locked-in Compression (B) (inch)	Assumed Residual Compression 0.5(B-|A|) (inch)	Residual Strain Strain ($1x10^{-3}$)	Residual Strain Telltale Length
2B	37.1					
6F	50.2	0.0237	0.0803	0.0570	0.0946	Head-6F
3C	63.3	0.0177	0.1223	0.1050	0.3053	6F-3C
7G	76.4	0.0082	0.1570	0.1490	0.2798	3C-7G
4D	89.5	0.0061	0.1980	0.2040	0.3504	7G-4D
8H	102.7					
5E	115.8	0.0400				
1A	127.9					

Table 5.2 Pile 3; Pipe Pile; Push Test Residual Compression

CASE 1

Tell. No.	Length (ft)	Increased Locked-in Compression (A) (inch)	(B) (inch)	Assumed Residual Compression 0.5(B-|A|) (inch)	Residual Strain Strain ($1x10^{-3}$)	Telltale Length
2B	37.1	0.0687	0.0792	0.0053	0.0117	Head-2B
6F	46.5	0.0599	0.1072	0.0237	0.1617	2B-6F
3C	56.9	0.0455	0.1560	0.0556	0.2572	6F-3C
7G	66.2	0.0312	0.1898	0.0793	0.2110	3C-7G
4D	76.4	0.0150	0.2329	0.1089	0.2422	7G-4D
8H	86.2	-0.0023	0.2742	0.1383	0.2393	4D-8H
5E	96.1	-0.0046	0.2889	0.1468	0.0711	8H-5E
1A	104.9					

CASE 2

Tell. No.	Length (ft)	Increased Locked-in Compression (A) (inch)	(B) (inch)	Assumed Residual Compression (B-A) (inch)	Residual Strain Strain ($1x10^{-3}$)	Telltale Length
2B	37.1	0.0687	0.0792	0.0106	0.0238	Head-2B
6F	46.5	0.0599	0.1072	0.0474	0.3234	2B-6F
3C	56.9	0.0455	0.1560	0.1112	0.5144	6F-3C
7G	66.2	0.0312	0.1898	0.1586	0.4220	3C-7G
4D	76.4	0.0150	0.2329	0.2178	0.4844	7G-4D
8H	86.2	-0.0023	0.2742	0.2766	0.4786	4D-8H
5E	96.1	-0.0046	0.2889	0.2936	0.1422	8H-5E
1A	104.9					

Table 5.3 Pile 4; H-Pile; Push Test — Residual Compression

CASE 1

Tell. No.	Length (ft)	Increased Locked-in Compression (A) (inch)	Increased Locked-in Compression (B) (inch)	Assumed Residual Compression 0.5(B-|A|) (inch)	Residual Strain Strain ($1x10^{-3}$)	Residual Strain Telltale Length
2B	37.1	+0.0009	0.0082	0.0036	0.0080	Head-2B
6F	46.9	-0.0009	0.0139	0.0074	0.0361	2B-6F
3C	56.7	-0.0085	0.0293	0.0189	0.0977	6F-3C
7G	66.2					
4D	76.4	-0.0583	0.0524	0.0555	0.1557	3C-4D
8H	86.2	-0.0689	0.0635	0.0662	0.0926	4D-8H
5E	96.1					
1A	104.9	-0.0807	0.0772	0.0790	0.0568	8H-1A

CASE 2

Tell. No.	Length (ft)	Increased Locked-in Compression (A) (inch)	Increased Locked-in Compression (B) (inch)	Assumed Residual Compression (B-|A|) (inch)	Residual Strain Strain ($1x10^{-3}$)	Residual Strain Telltale Length
2B	37.1	+0.0009	0.0082	0.0072	0.0160	Head-2B
6F	46.9	-0.0009	0.0139	0.0148	0.0646	2B-6F
3C	56.7	-0.0085	0.0293	0.0378	0.1916	6F-3C
7G	66.2					
4D	76.4	-0.0583	0.0524	0.1106	0.3115	3C-4D
8H	86.2	-0.0689	0.0635	0.1324	0.1853	4D-8H
5E	96.1					
1A	104.9	-0.0807	0.0772	0.1579	0.1136	8H-1A

Table 5.4 Pile 1; H-Pile; Pull Test Residual Compression before Pull

CASE 1

Telltale No.	Length (ft)	Residual Compression before Pull (inch)	Residual Strain Before Pull: Strain ($1x10^{-3}$)	Residual Strain Before Pull: Telltale Length
2B	37.1			
6F	50.2	0.0522	0.0866	Head-6F
3C	63.3	0.0702	0.1148	6F-3C
7G	76.4	0.0827	0.0795	3C-7G
4D	89.5	0.0960	0.0846	7G-4D
8H	102.7			
5E	115.8			
1A	127.9			

CASE 2

Telltale No.	Length (ft)	Residual Compression before Pull (inch)	Residual Strain Before Pull: Strain ($1x10^{-3}$)	Residual Strain Before Pull: Telltale Length
2B	37.1			
6F	50.2	0.0807	0.1339	Head-6F
3C	63.3	0.1227	0.2671	6F-3C
7G	76.4	0.1572	0.2194	3C-7G
4D	89.5	0.2101	0.3365	7G-4D
8H	102.7			
5E	115.8			
1A	127.9			

Table 5.5 Pile 3; Pipe Pile; Pull Test Residual Compression before Pull

CASE 1

Telltale No.	Length (ft)	Residual Compression before Pull (inch)	Residual Strain Before Pull: Strain ($1x10^{-3}$)	Residual Strain Before Pull: Telltale Length
2B	37.1			
6F	46.5	0.0873	0.1564	Head-6F
3C	56.9	0.1061	0.1506	6F-3C
7G	66.2			
4D	76.4	0.1240	0.0764	3C-4D
8H	86.2			
5E	96.1	0.1422	0.0769	4D-5E
1A	104.9			

CASE 2

Telltale No.	Length (ft)	Residual Compression before Pull (inch)	Residual Strain Before Pull: Strain ($1x10^{-3}$)	Residual Strain Before Pull: Telltale Length
2B	37.1			
6F	46.5	0.1072	0.1921	Head-6F
3C	56.9	0.1560	0.3873	6F-3C
7G	66.2			
4D	76.4	0.2329	0.3286	3C-4D
8H	86.2			
5E	96.1	0.2843	0.2174	4D-5E
1A	104.9			

Table 5.6 Pile 4; H-Pile; Pull Test Residual Compression before Pull

CASE 1

Telltale No.	Length (ft)	Residual Compression before Pull (inch)	Residual Strain Before Pull Strain ($1x10^{-3}$)	Telltale Length
2B	37.1	0.0045	0.0101	Head-2B
6F	46.9			
3C	56.7	0.0104	0.0250	2B-3C
7G	66.2			
4D	76.4	0.0000	0.0000	3C-4D
8H	86.2	0.0000	0.0000	4D-8H
5E	96.1			
1A	104.9	0.0000	0.0000	8H-1A

CASE 2

Telltale No.	Length (ft)	Residual Compression before Pull (inch)	Residual Strain Before Pull Strain ($1x10^{-3}$)	Telltale Length
2B	37.1	0.0082	0.0184	Head-2B
6F	46.9			
3C	56.7	0.0293	0.0897	2B-3C
7G	66.2			
4D	76.4	0.0523	0.0972	3C-4D
8H	86.2	0.0635	0.0952	4D-8H
5E	96.1			
1A	104.9	0.0772	0.0610	8H-1A

Table 5.7 Pile 1; H-Pile; Push Test Load = 461 tons

CASE 1

Tell. No.	Length (ft)	Measured Compr. (inch)	Change in Compr. (inch)	Measured Strain $1x10^{-3}$ (-)	Residual Strain $1x10^{-3}$ (-)	Total Strain $1x10^{-3}$ (-)	AE $1x10^{-3}$ (ton)	Load from Measured Strain (ton)	Load from Residual Strain (ton)	Total Load (ton)
2B	37.1									
6F	50.2	0.6794	0.6794	1.1280	0.0473	1.1861	418	472	20	492
3C	63.3	0.8084	0.1290	0.8206	0.1526	0.9732	409	342	56	398
7G	76.4	0.9219	0.1135	0.7229	0.1397	0.8626	409	299	53	352
4D	89.5	1.0248	0.1029	0.6555	0.1752	0.8310	399	261	70	331
8H	102.8									
5E	115.8	1.2028	0.1780	0.5640	0.1420	0.7060	394	222	56	278
1A	127.9									

CASE 2

Tell. No.	Length (ft)	Measured Compr. (inch)	Change in Compr. (inch)	Measured Strain $1x10^{-3}$ (-)	Residual Strain $1x10^{-3}$ (-)	Total Strain $1x10^{-3}$ (-)	AE $1x10^{-3}$ (ton)	Load from Measured Strain (ton)	Load from Residual Strain (ton)	Total Load (ton)
2B	37.1									
6F	50.2	0.6794	0.6794	1.1280	0.0946	1.2226	418	472	40	511
3C	63.3	0.8084	0.1290	0.8206	0.3053	1.1259	409	342	112	454
7G	76.4	0.9219	0.1135	0.7229	0.2798	1.0027	409	299	111	410
4D	89.5	1.0248	0.1029	0.6555	0.3505	1.0059	399	261	140	401
8H	102.8									
5E	115.8	1.2028	0.1780	0.5640						
1A	127.9									

Table 5.8 Pile 3; Pipe Pile; Push Test load 234 tons

CASE 1

Tell. No.	Length (ft)	Measured Compr. (inch)	Change in Compr. (inch)	Measured Strain $1x10^{-3}$ (-)	Residual Strain $1x10^{-3}$ (-)	Total Strain $1x10^{-3}$ (-)	AE $1x10^{-3}$ (ton)	Load from Measured Strain (ton)	Load from Residual Strain (ton)	Total Load (ton)
2B	37.1	0.4637	0.4637	1.0410	0.0117	1.0532	215	224	3	227
6F	46.5	0.5170	00533	0.4685	0.1617	0.6302	215	101	35	136
3C	56.9	0.5481	0.0311	0.2491	0.2572	0.5063	208	52	53	105
7G	66.2	0.5677	0.0196	0.2144	0.2110	0.4600	208	45	51	96
4D	76.4	0.5792	0.0116	0.0939	0.2422	0.3361	196	18	48	66
8H	86.2	0.5842	0.0050	0.0425	0.2393	0.2818	196	8	47	55
5E	96.1	0.5993	0.0151	0.1271	0.0711	0.1982	187	24	13	37
1A	104.9									

CASE 2

Tell. No.	Length (ft)	Measured Compr. (inch)	Change in Compr. (inch)	Measured Strain $1x10^{-3}$ (-)	Residual Strain $1x10^{-3}$ (-)	Total Strain $1x10^{-3}$ (-)	AE $1x10^{-3}$ (ton)	Load from Measured Strain (ton)	Load from Residual Strain (ton)	Total Load (ton)
2B	37.1	0.4637	0.4637	1.0410	0.0238	1.0648	215	224	6	229
6F	46.5	0.5170	00533	0.4685	0.3234	0.7882	215	101	70	169
3C	56.9	0.5481	0.0311	0.2491	0.5144	0.7635	208	52	106	158
7G	66.2	0.5677	0.0196	0.2144	0.4220	0.6364	208	45	102	132
4D	76.4	0.5792	0.0116	0.0939	0.4844	0.5783	196	18	96	113
8H	86.2	0.5842	0.0050	0.0425	0.4786	0.5211	196	8	94	102
5E	96.1	0.5993	0.0151	0.1271	0.1422	0.2693	187	24	26	50
1A	104.9									

Table 5.9 **Pile 4; H-Pile; Push Test** **Load = 180 tons**

CASE 1

Tell. No.	Length (ft)	Measured Compr. (inch)	Change in Compr. (inch)	Measured Strain $1x10^{-3}$ (-)	Residual Strain $1x10^{-3}$ (-)	Total Strain $1x10^{-3}$ (-)	AE $1x10^{-3}$ (ton)	Load from Measured Strain (ton)	Load from Residual Strain (ton)	Total Load (ton)
2B	37.1	0.1806	0.1806	0.4054	0.0080	0.4134	418	169	4	173
6F	46.9	0.2061	0.0255	0.2159	0.0361	0.2500	418	90	15	105
3C	56.7	0.2271	0.0210	0.1785	0.0977	0.2762	408	73	40	113
7G	66.2									
4D	76.4	0.2438	0.0167	0.0707	0.1669	0.2376	399	28	67	95
8H	86.2	0.2489	0.0051	0.0431	0.0879	0.0130	399	2	50	52
5E	96.1									
1A	104.9	0.2519	0.0003	0.0133	0.0524	0.0657	389	1	24	25

CASE 2

Tell. No.	Length (ft)	Measured Compr. (inch)	Change in Compr. (inch)	Measured Strain $1x10^{-3}$ (-)	Residual Strain $1x10^{-3}$ (-)	Total Strain $1x10^{-3}$ (-)	AE $1x10^{-3}$ (ton)	Load from Measured Strain (ton)	Load from Residual Strain (ton)	Total Load (ton)
2B	37.1	0.1806	0.1806	0.4054	0.0160	0.4214	418	169	7	176
6F	46.9	0.2061	0.0255	0.2159	0.0646	0.2805	418	90	27	117
3C	56.7	0.2271	0.0210	0.1785	0.1916	0.3701	408	73	78	151
7G	66.2									
4D	76.4	0.2438	0.0167	0.0707	0.3115	0.3822	399	28	124	152
8H	86.2	0.2489	0.0051	0.0431	0.1853	0.2285	399	2	89	91
5E	96.1									
1A	104.9	0.2519	0.0003	0.0133	0.1136	0.1269	389	1	48	49

Table 5.10 **Pile 1; H-Pile; Pull Test** **Load = 222 tons**

CASE 1

Tell. No.	Length (ft)	Measured Compr. (inch)	Change in Compr. (inch)	Measured Strain $1x10^{-3}$ (-)	Residual Strain $1x10^{-3}$ (-)	Total Strain $1x10^{-3}$ (-)	AE $1x10^{-3}$ (ton)	Load from Measured Strain (ton)	Load from Residual Strain (ton)	Total Load (ton)
2B	37.1									
6F	50.2	0.3230	0.3230	0.5360	0.0866	0.4494	418	224	36	188
3C	63.3	0.4070	0.0840	0.5303	0.1148	0.4155	409	217	47	170
7G	76.4	0.4776	0.0706	0.4490	0.0795	0.3695	409	183	32	151
4D	89.5	0.5428	0.0652	0.4147	0.0846	0.3301	399	165	33	132
8H	102.8									
5E	115.8	0.6711	0.1283	0.4065	0.1420	0.2645	394	160	56	104
1A	127.9									

CASE 2

Tell. No.	Length (ft)	Measured Compr. (inch)	Change in Compr. (inch)	Measured Strain $1x10^{-3}$ (-)	Residual Strain $1x10^{-3}$ (-)	Total Strain $1x10^{-3}$ (-)	AE $1x10^{-3}$ (ton)	Load from Measured Strain (ton)	Load from Residual Strain (ton)	Total Load (ton)
2B	37.1									
6F	50.2	0.3230	0.3230	0.5360	0.1333	0.4027	418	224	56	168
3C	63.3	0.4070	0.0840	0.5303	0.2671	0.2632	409	217	108	108
7G	76.4	0.4776	0.0706	0.4490	0.2194	0.2296	409	183	90	94
4D	89.5	0.5428	0.0652	0.4147	0.3365	0.0782	399	165	134	31
8H	102.8									
5E	115.8	0.6711	0.1283	0.4065						
1A	127.9									

Table 5.11 Pile 3; Pipe Pile; Pull Test Load = 170 tons

CASE 1

Tell. No.	Length (ft)	Measured Compr. (inch)	Change in Compr. (inch)	Measured Strain $1x10^{-3}$ (-)	Residual Strain $1x10^{-3}$ (-)	Total Strain $1x10^{-3}$ (-)	AE $1x10^{-3}$ (ton)	Load from Measured Strain (ton)	Load from Residual Strain (ton)	Total Load (ton)
2B	37.1									
6F	46.5	0.4267	0.4267	0.7646	0.1564	0.6082	215	164	34	130
3C	56.9	0.5173	0.0906	0.7259	0.1506	0.5753	206	149	30	119
7G	66.2									
4D	76.4	0.6457	0.1284	0.5487	0.0764	0.4723	200	110	16	94
8H	86.2									
5E	96.1	0.7388	0.0931	0.3988	0.0769	0.3219	190	77	16	61
1A	104.9									

CASE 2

Tell. No.	Length (ft)	Measured Compr. (inch)	Change in Compr. (inch)	Measured Strain $1x10^{-3}$ (-)	Residual Strain $1x10^{-3}$ (-)	Total Strain $1x10^{-3}$ (-)	AE $1x10^{-3}$ (ton)	Load from Measured Strain (ton)	Load from Residual Strain (ton)	Total Load (ton)
2B	37.1									
6F	46.5	0.4267	0.4267	0.7646	0.1072	0.6574	215	164	23	141
3C	56.9	0.5173	0.0906	0.7259	0.1560	0.5699	206	149	32	117
7G	66.2									
4D	76.4	0.6457	0.1284	0.5487	0.2329	0.3160	200	110	47	63
8H	86.2									
5E	96.1	0.7388	0.0931	0.3988	0.2843	0.1145	190	77	55	22
1A	104.9									

Table 5.12 Pile 4; H-Pile; Pull Test Load = 125 tons

CASE 1

Tell. No.	Length (ft)	Measured Compr. (inch)	Change in Compr. (inch)	Measured Strain $1x10^3$ (-)	Residual Strain $1x10^3$ (-)	Total Strain $1x10^3$ (-)	AE $1x10^3$ (ton)	Load from Measured Strain (ton)	Load from Residual Strain (ton)	Total Load (ton)
2B	37.1	0.1315	0.1315	0.2953	0.0184	0.2769	418	124	8	116
6F	46.9									
3C	56.7	0.1929	0.0614	0.2605	0.0897	0.1708	414	108	37	71
7G	66.2									
4D	76.4	0.2489	0.0560	0.2368	0.0972	0.1396	407	96	39	57
8H	86.2	0.2698	0.0210	0.1769	0.0952	0.0817	404	71	38	33
5E	96.1									
1A	104.9	0.2990	0.0292	0.1300	0.0610	0.0690	399	53	25	28

CASE 2

Tell. No.	Length (ft)	Measured Compr. (inch)	Change in Compr. (inch)	Measured Strain $1x10^3$ (-)	Residual Strain $1x10^3$ (-)	Total Strain $1x10^3$ (-)	AE $1x10^3$ (ton)	Load from Measured Strain (ton)	Load from Residual Strain (ton)	Total Load (ton)
2B	37.1	0.1315	0.1315	0.2953	0.0184	0.2769	418	124	8	116
6F	46.9									
3C	56.7	0.1929	0.0614	0.2605	0.0897	0.1708	414	108	37	71
7G	66.2									
4D	76.4	0.2489	0.0560	0.2368	0.0972	0.1396	407	96	39	57
8H	86.2	0.2698	0.0210	0.1769	0.0952	0.0817	404	71	38	33
5E	96.1									
1A	104.9	0.2990	0.0292	0.1300	0.0610	0.0690	399	53	25	28

F I G U R E S

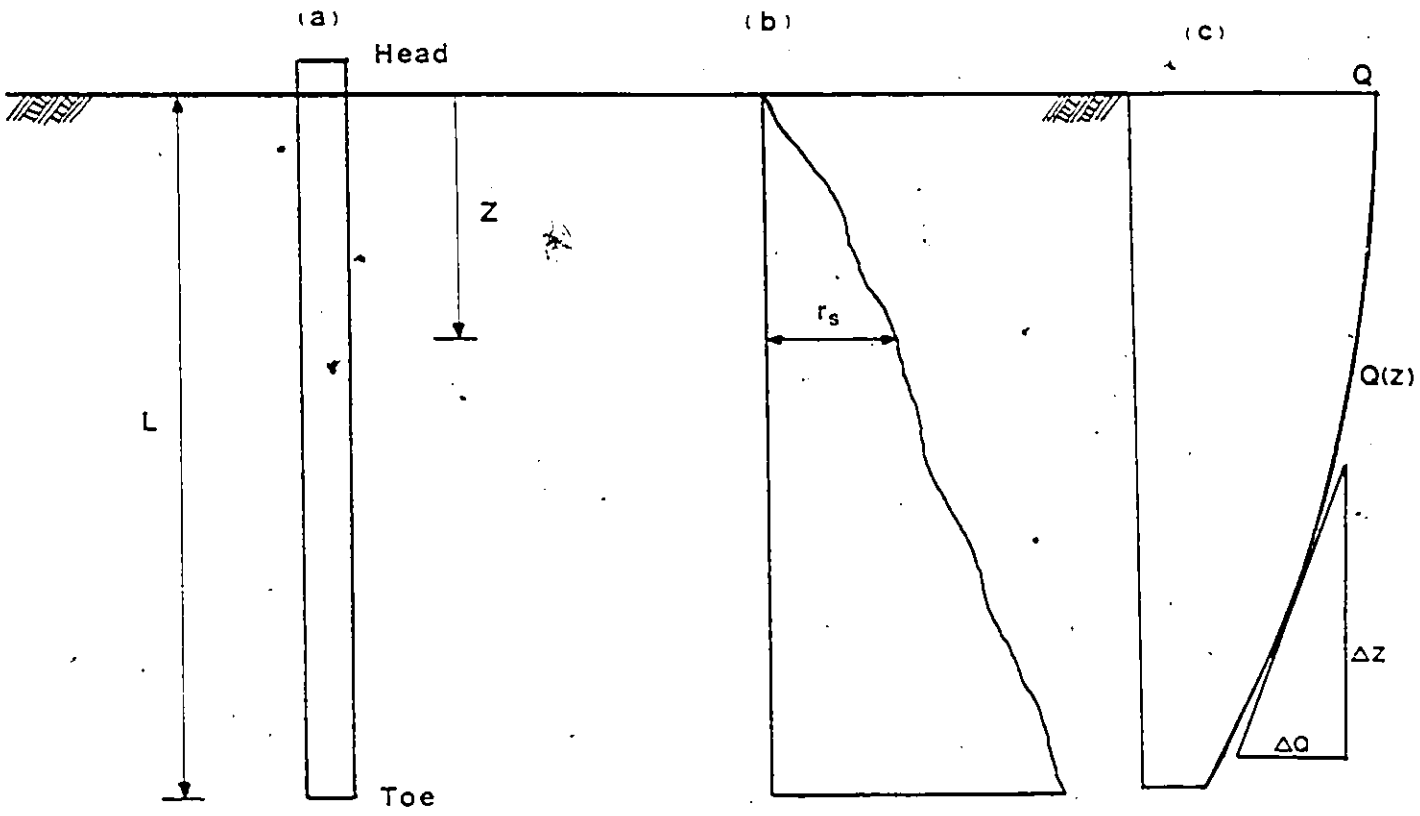

Fig. 2.1 Load transfer function in Piles.

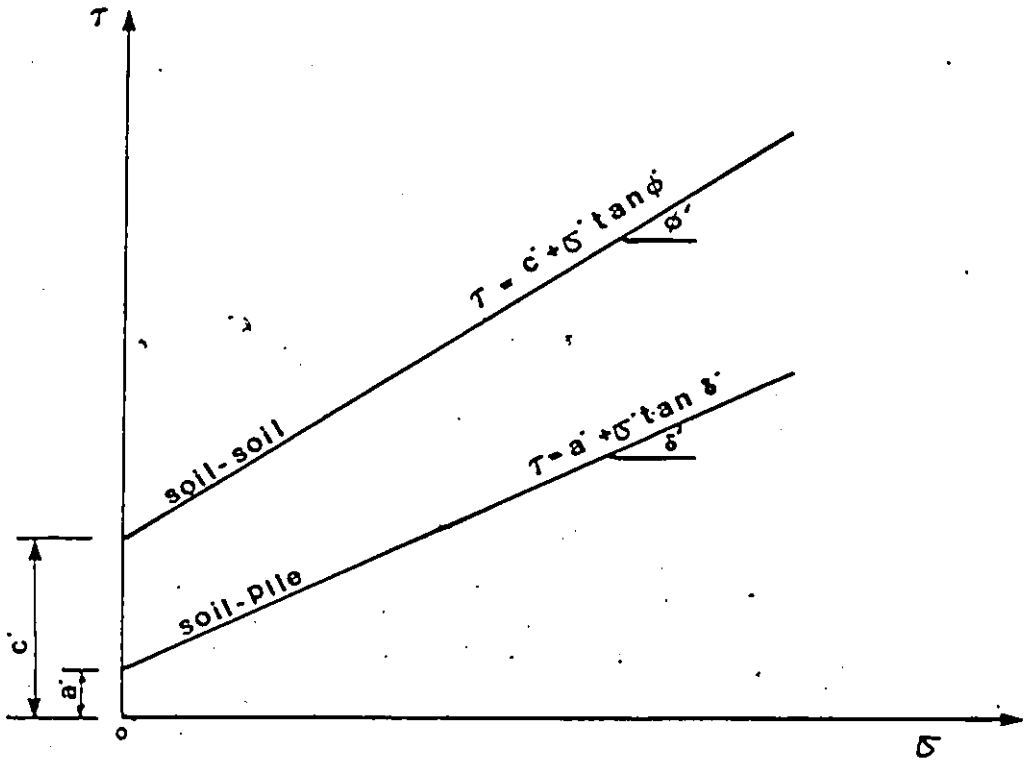

Fig. 2.2 Mohr Coulomb Strength Envelope at Pile Soil Interface (modified after Kezdi 1976)

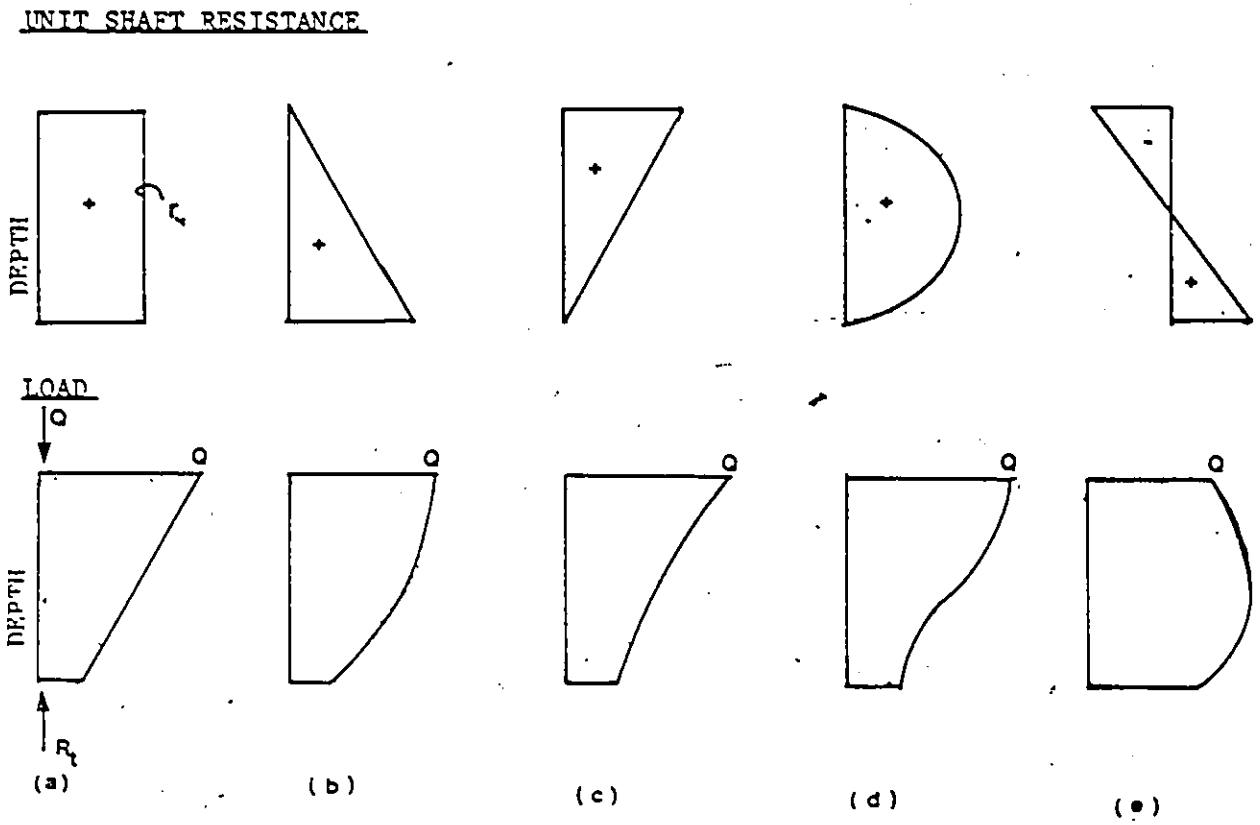

Fig. 2.3 Typical distribution of unit shaft resistance distribution and load transfer function in a pile (after Vesic 1970)

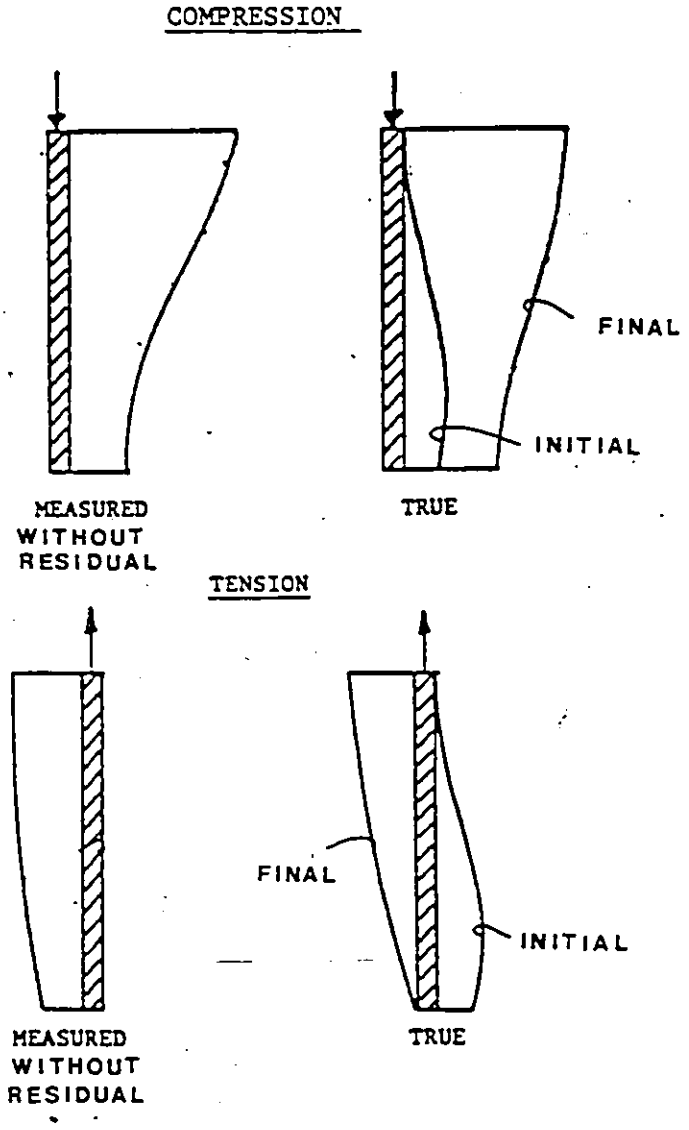

Fig. 2.4 Model load distributions adjusted for residual loads (after Briaud and Tucker 1985)

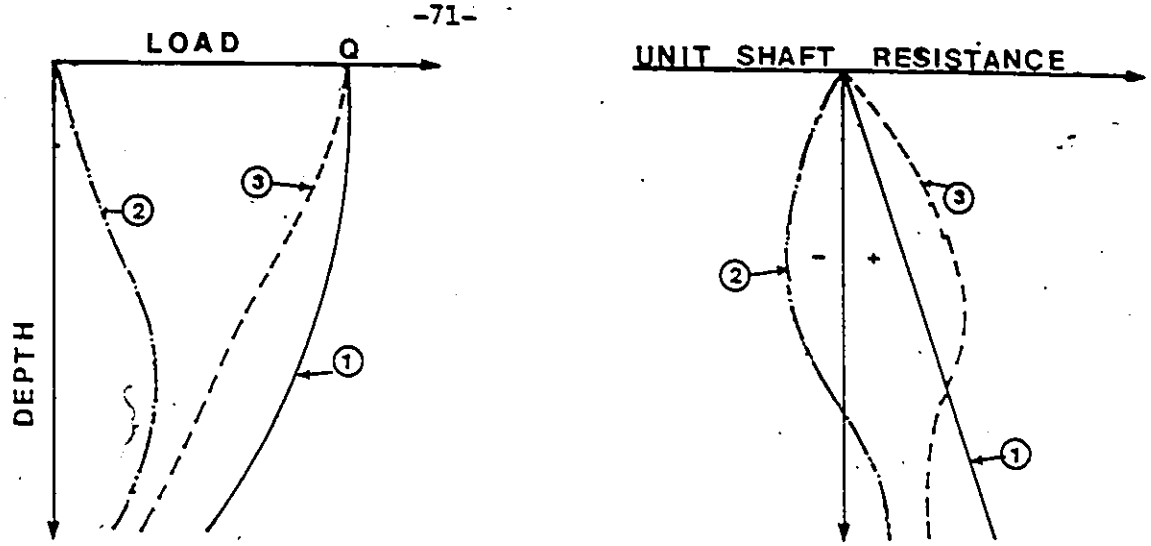

(a)
COMPRESSION TEST

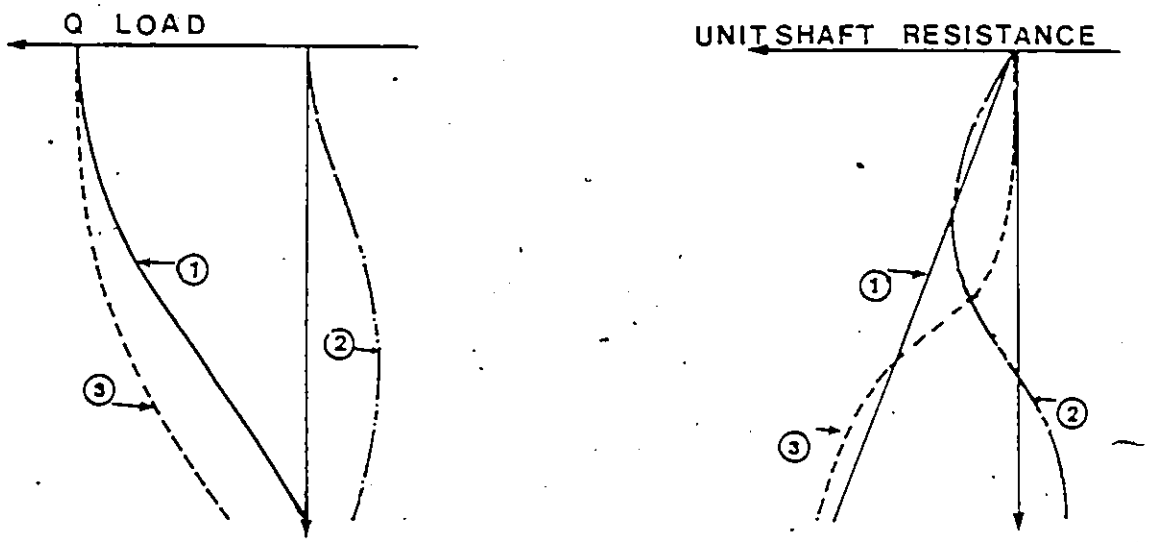

(b)
TENSION TEST

Fig. 2.5 Load transfer behaviour for piles in compression and tension considering residual stresses (after Holloway et al. 1978)

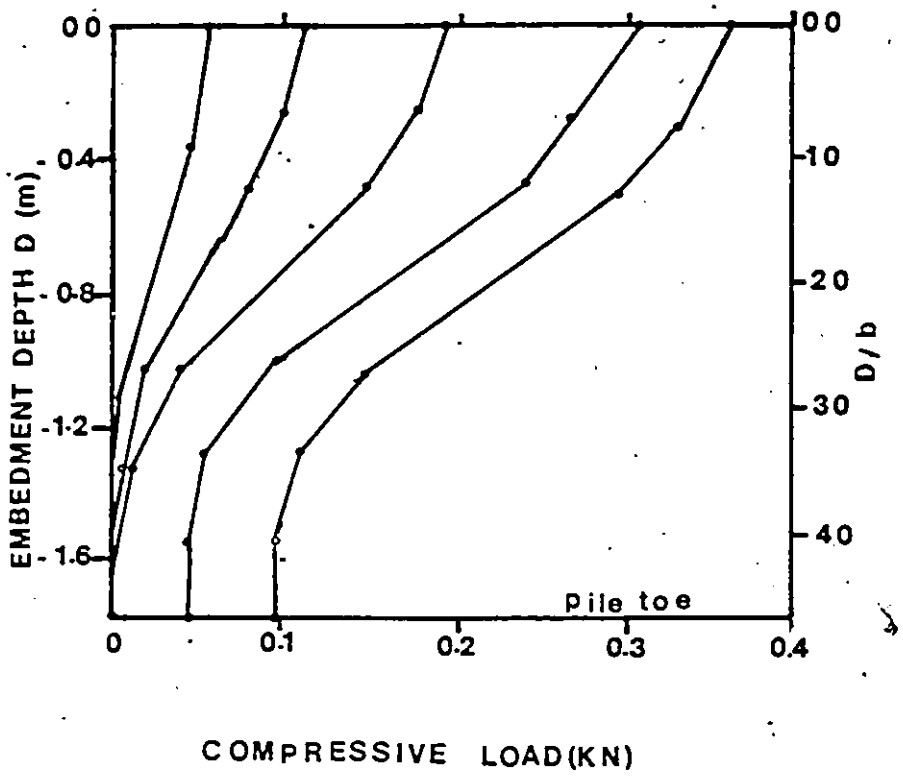

Fig. 2.6 Load distribution development neglecting residual loads (after Hanna and Tan, 1973)

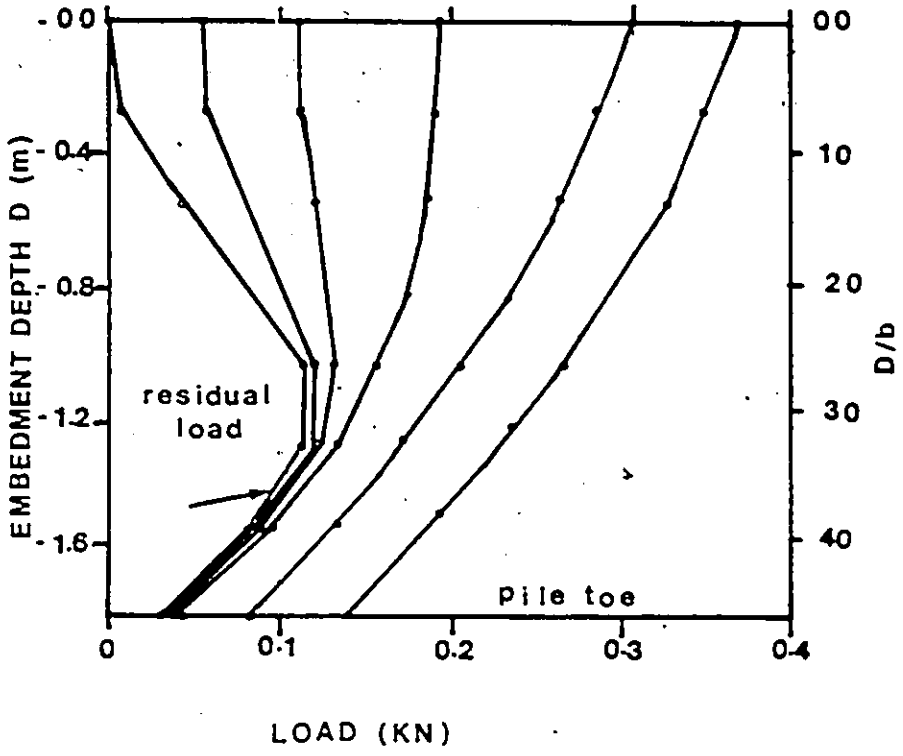

Fig. 2.7 Load distribution adjusted for residual loads (after Hanna and Tan, 1973)

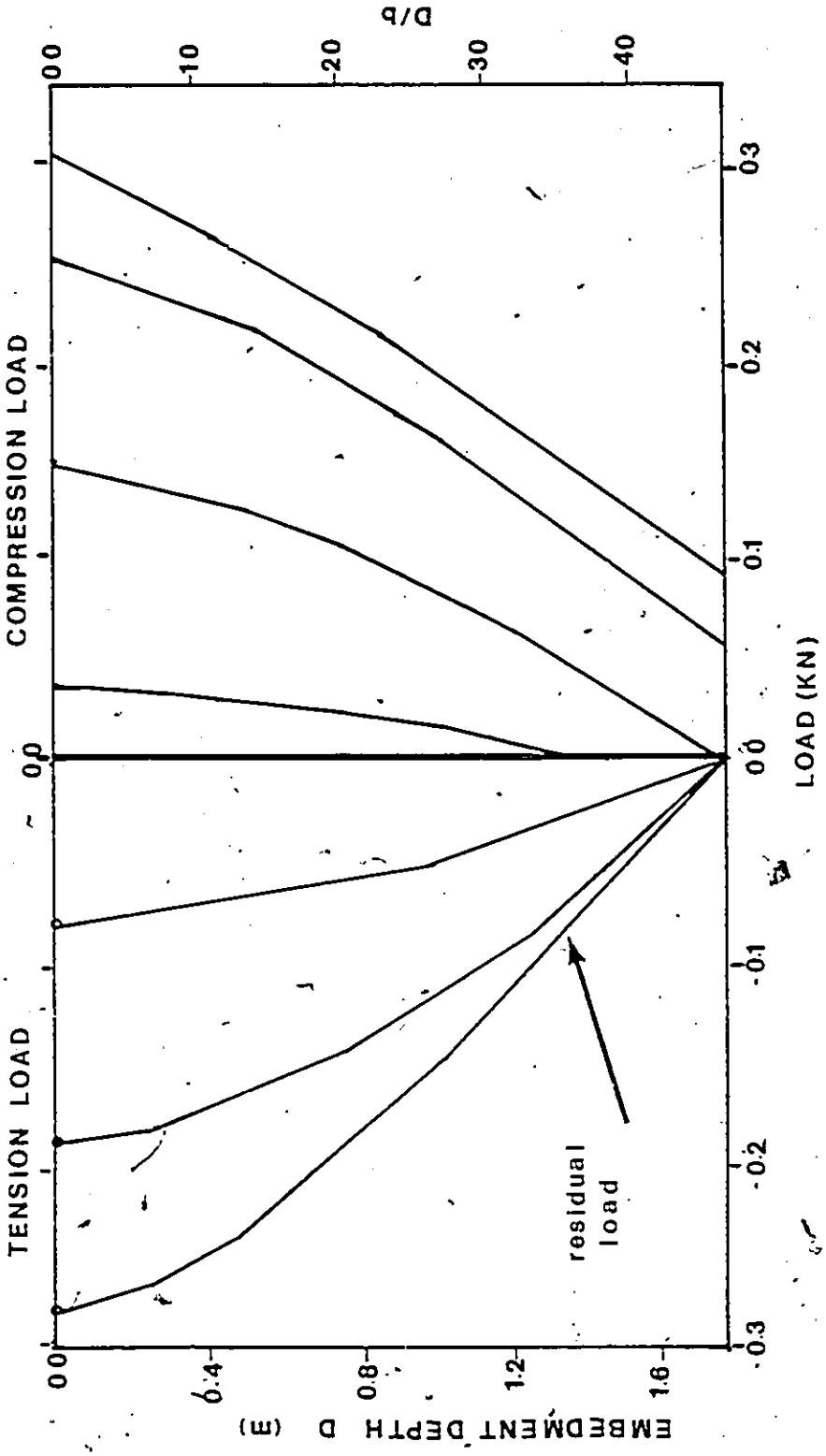

Fig. 2.8 Load distribution in fixed head piles (modfied after Hanna and Tan, 1973)

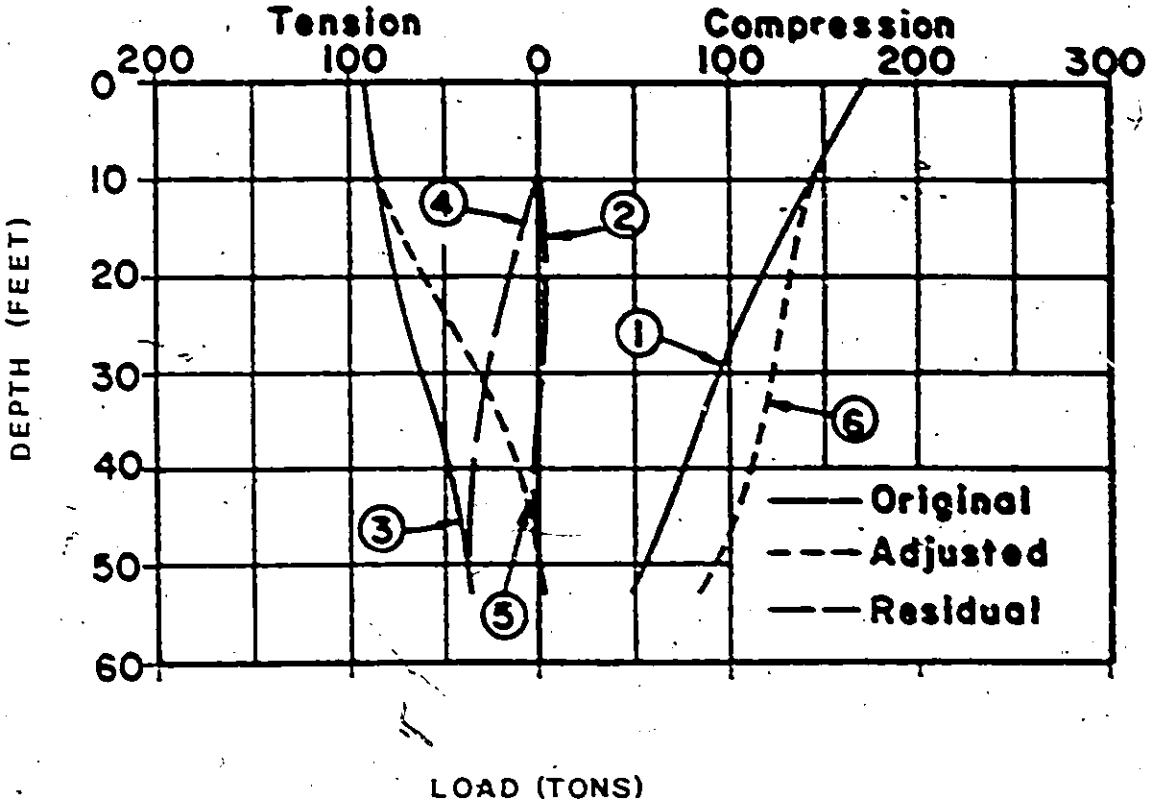

Fig. 2.9 Load distribution in push and pull.
(after Hunter and Davisson, 1969)

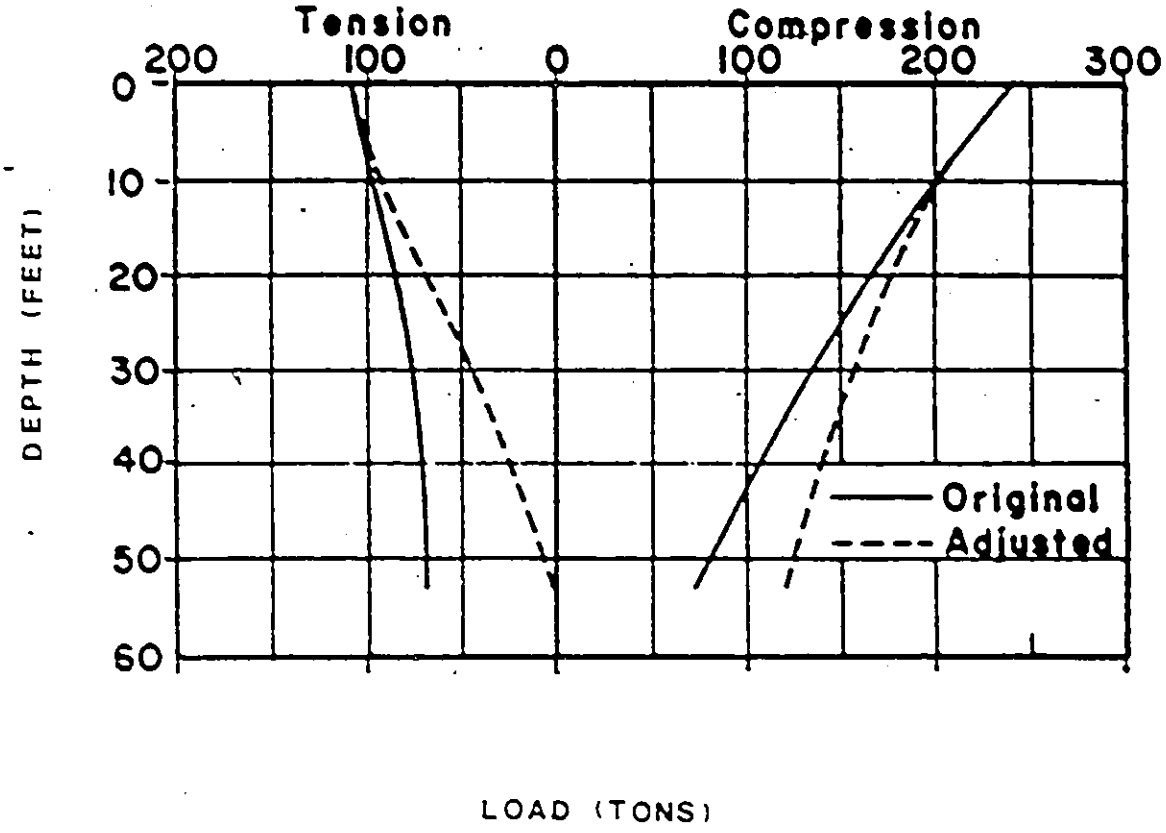

Fig. 2.10 Load distribution adjusted for residual loads. (after Hunter and Davisson, 1969)

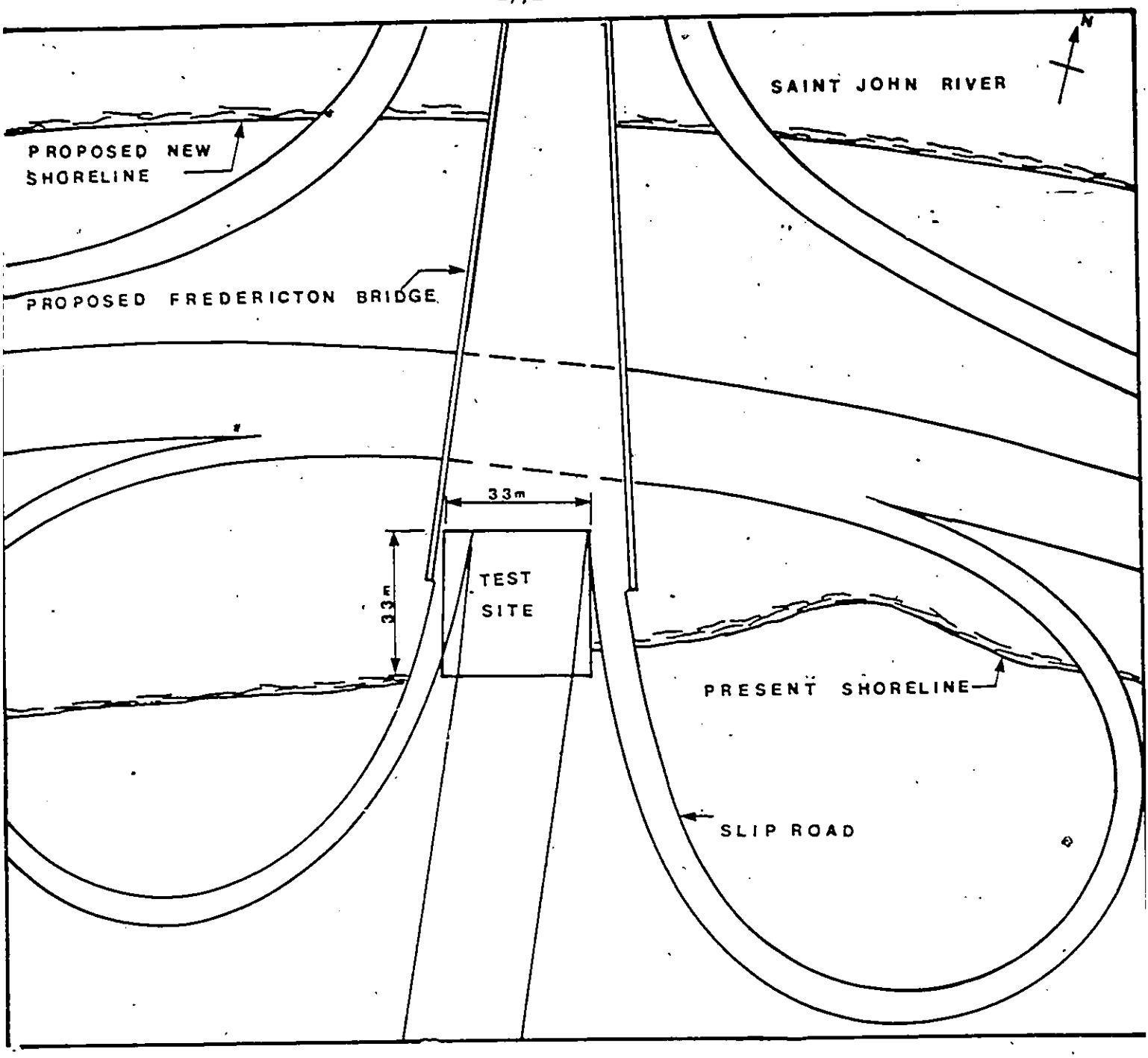

Fig. 3.1 Site Plan of test site

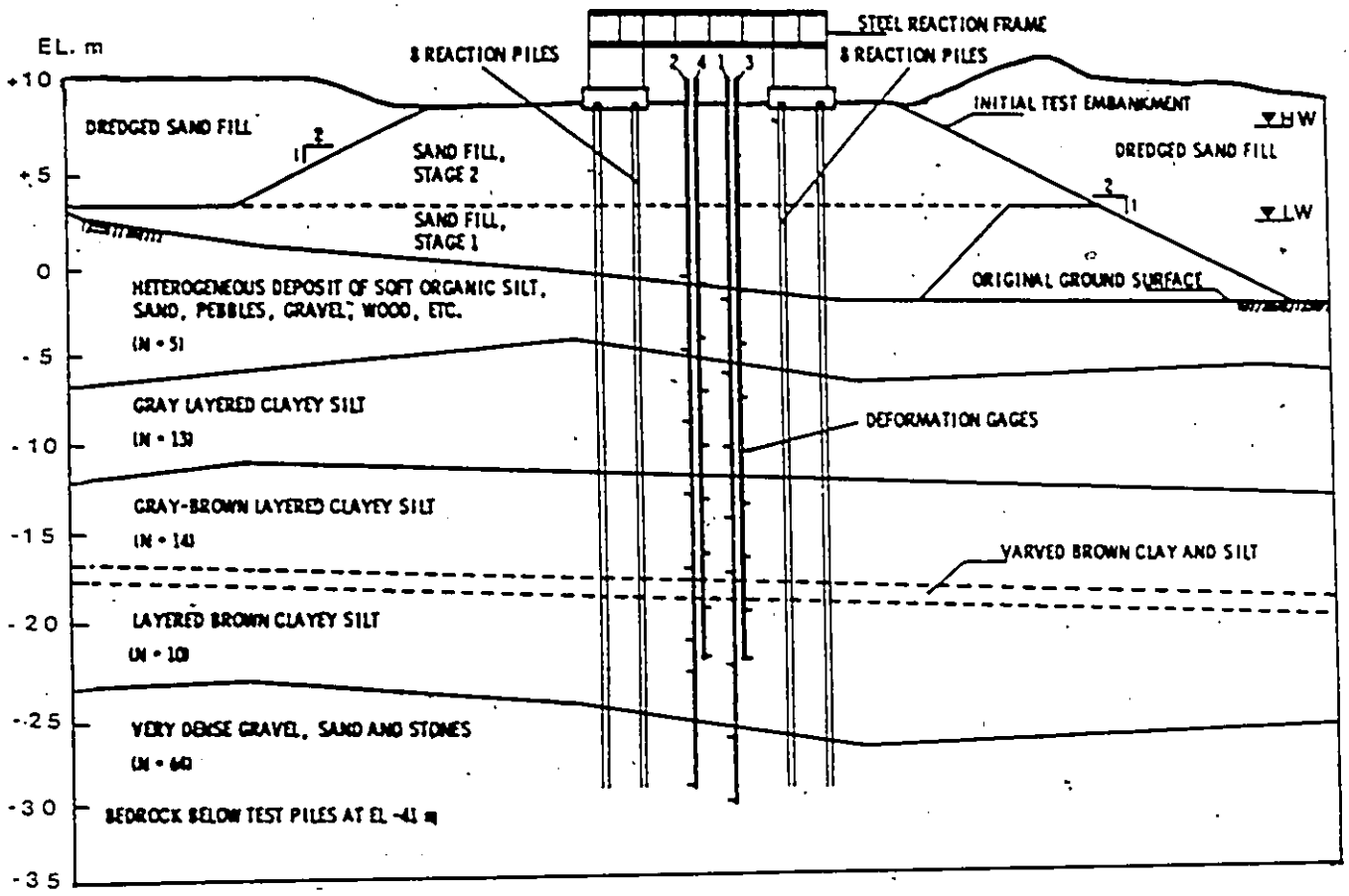

Fig. 3.2 Profile of soil formation, embankment fill and test piles (after Bozozuk et al. 1978)

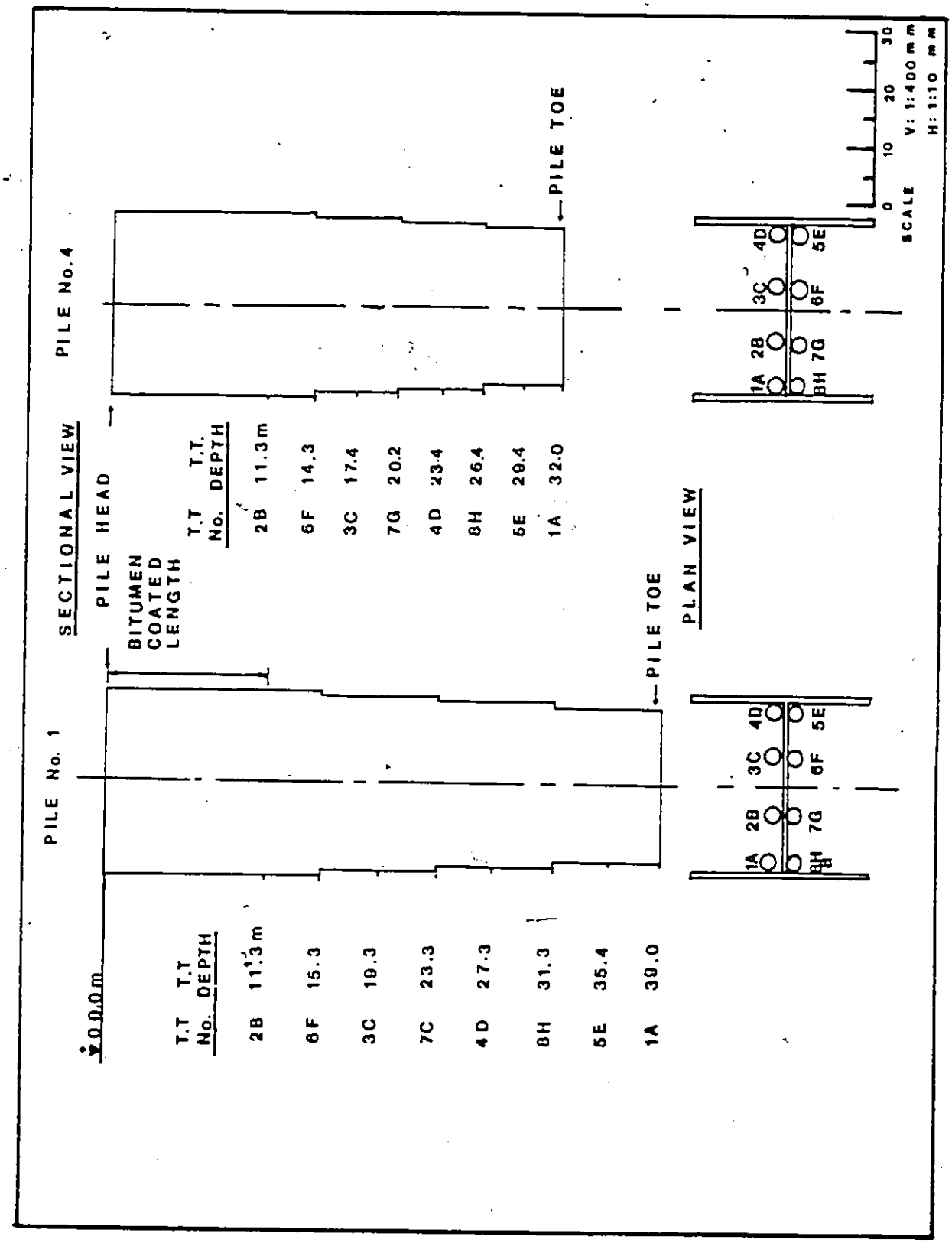

Fig. 3.3 · Sectional views of H-piles showing telltale end location.

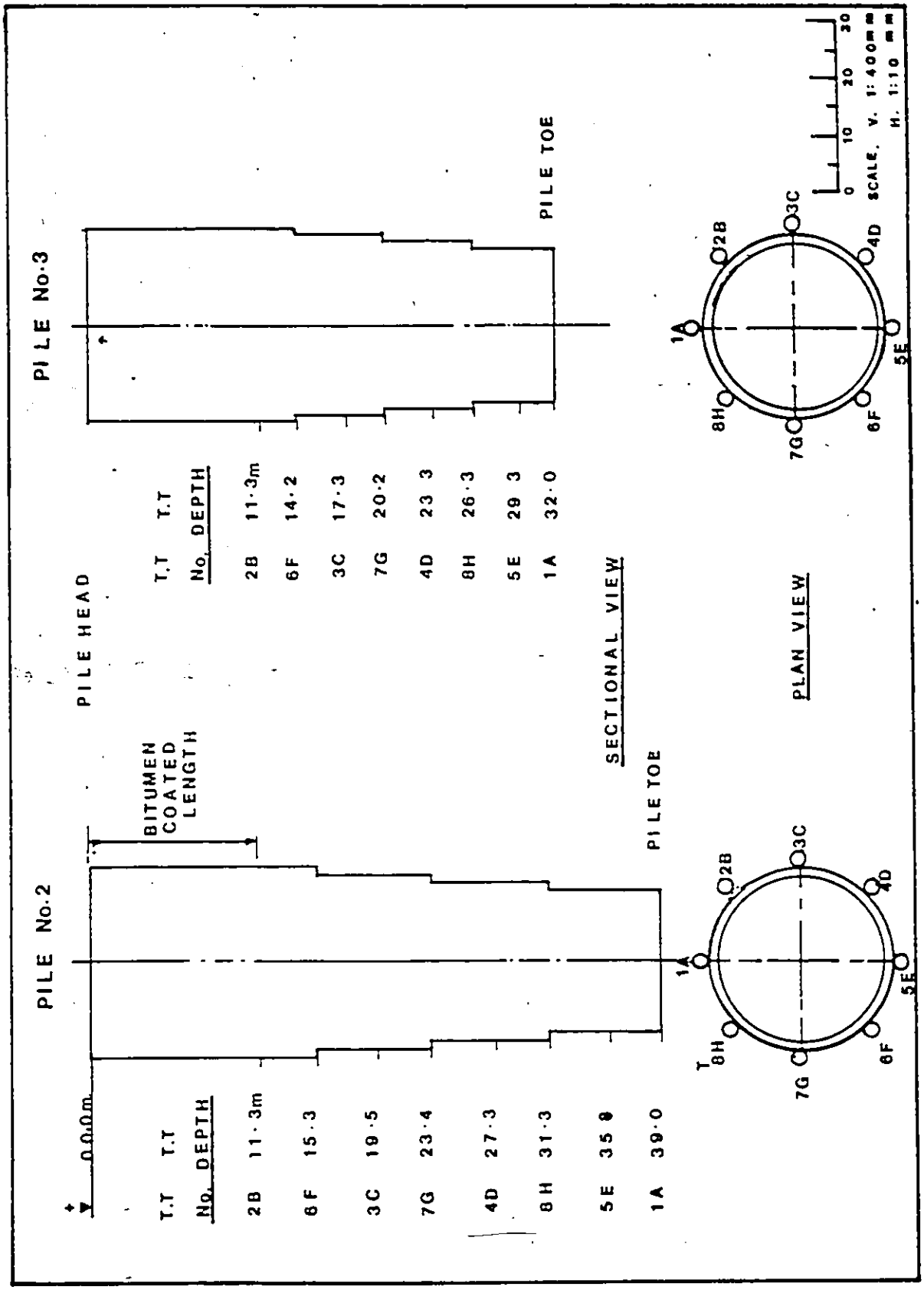

Fig. 3.4 Sectional views of pipe piles showing telltale end locations.

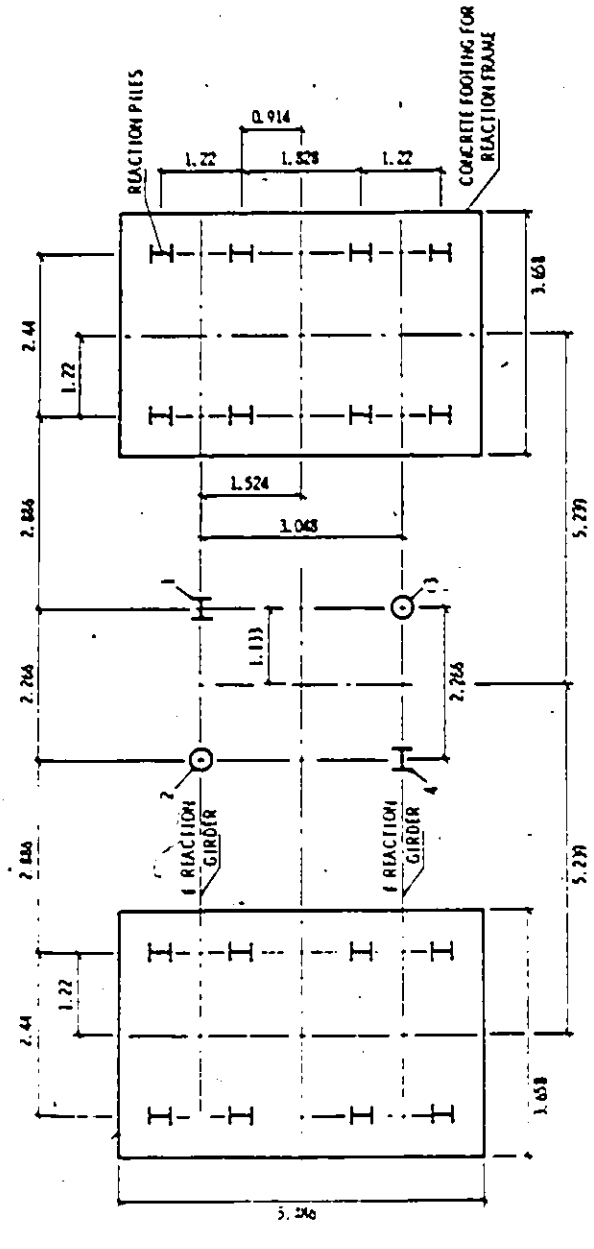

Fig. 3.5 Plan of test pile location (after Bozozuk et al., 1978)

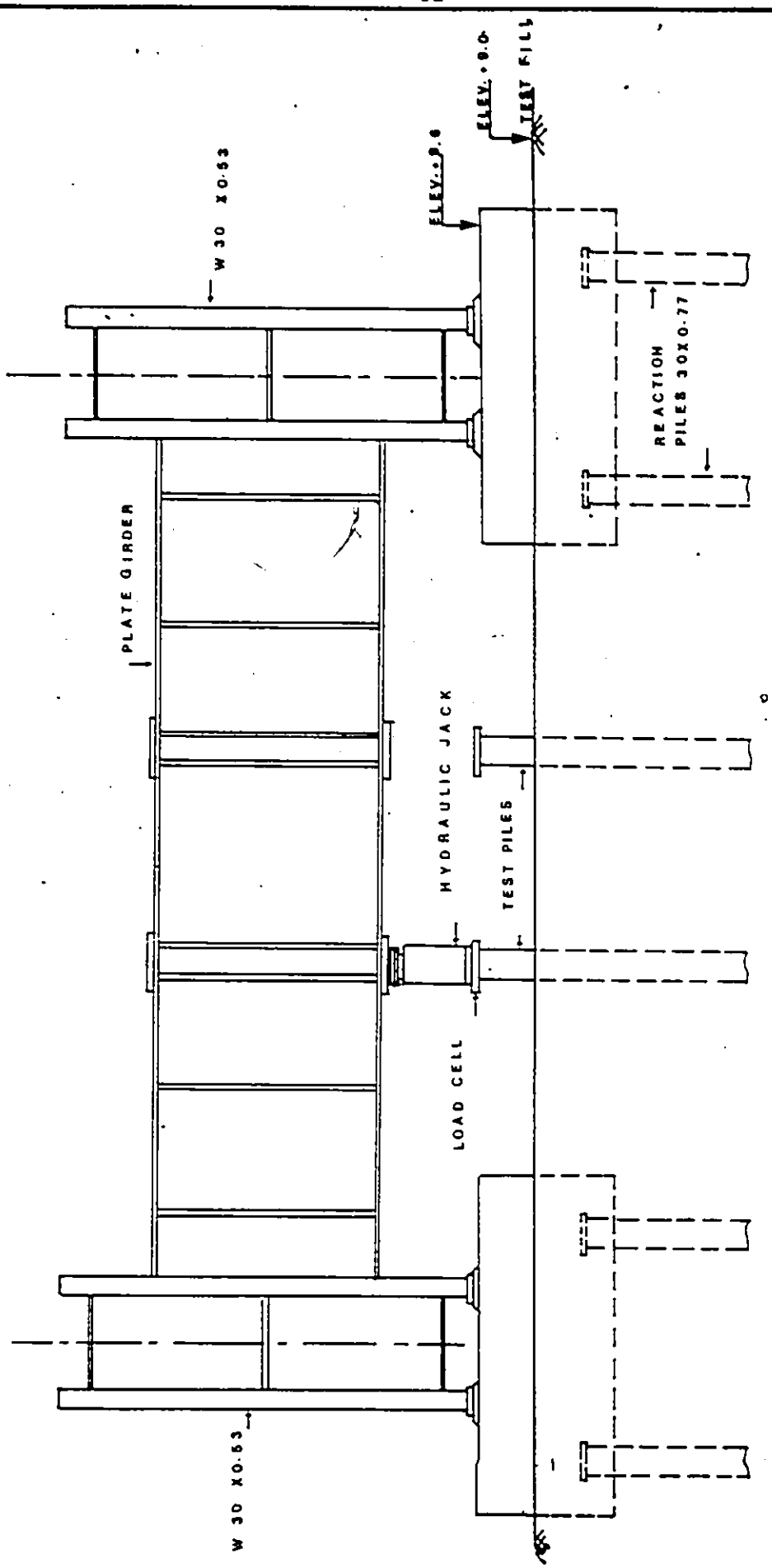

FIG. 36 SCHEMATIC VIEW OF TEST FRAME

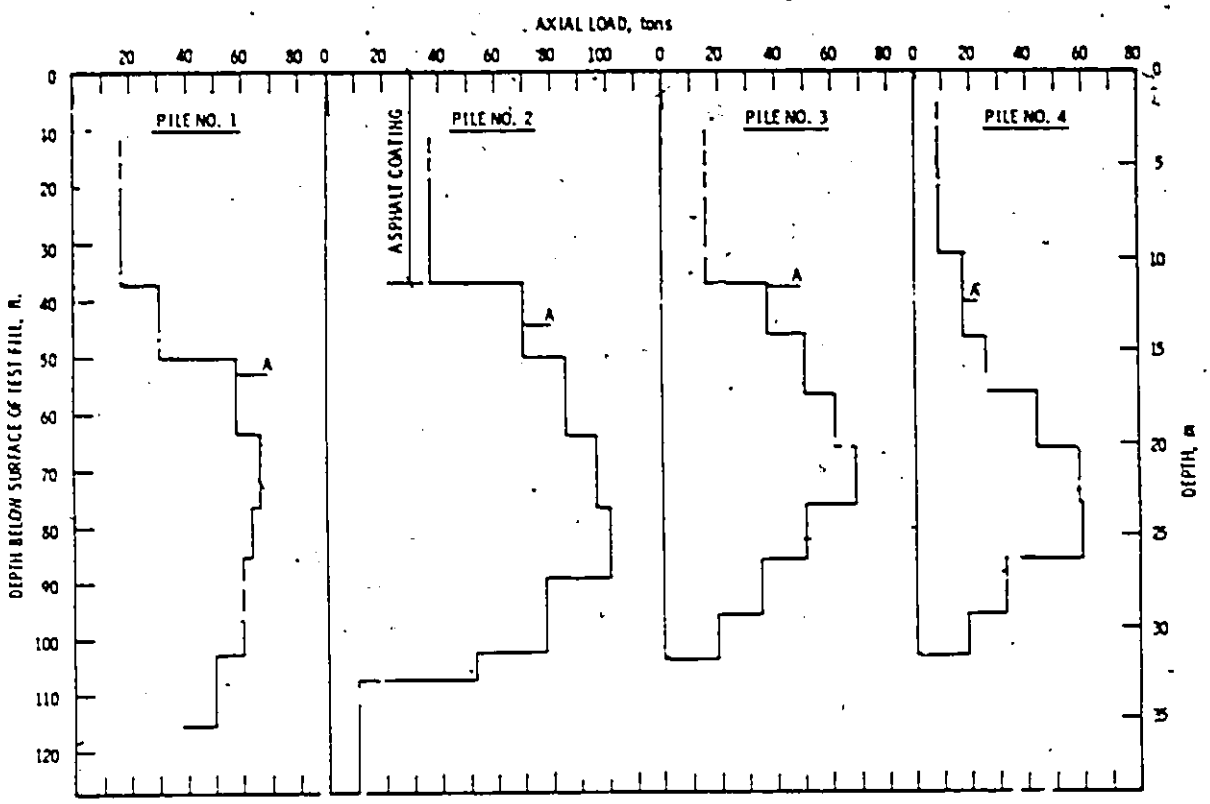

Fig. 3.7 Residual load distribution prior to first series of push testing (modified after Bozozuk et al.1978)

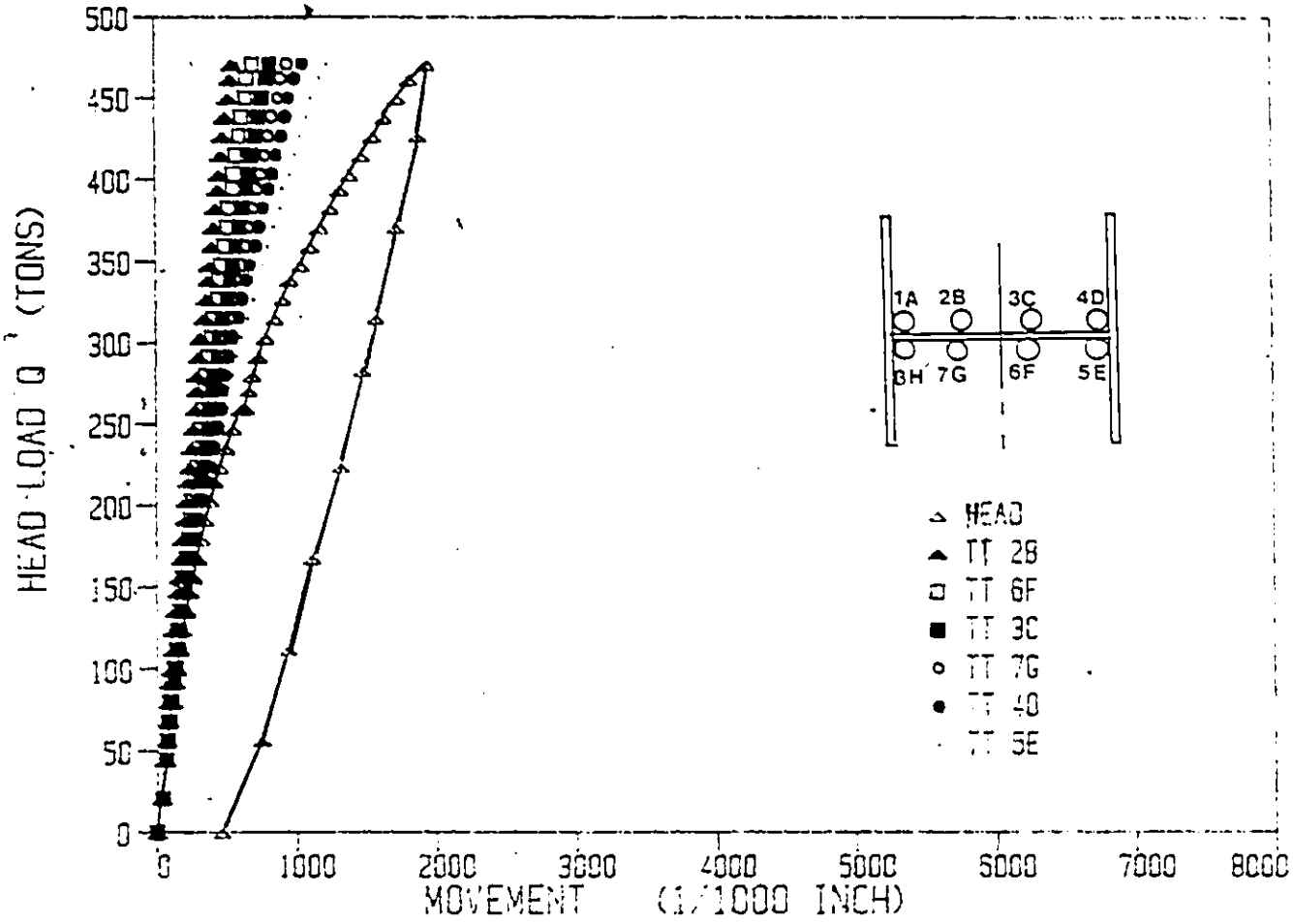

Fig. 4.1 Pile 1; H-Pile; Push Test; Load Movement data

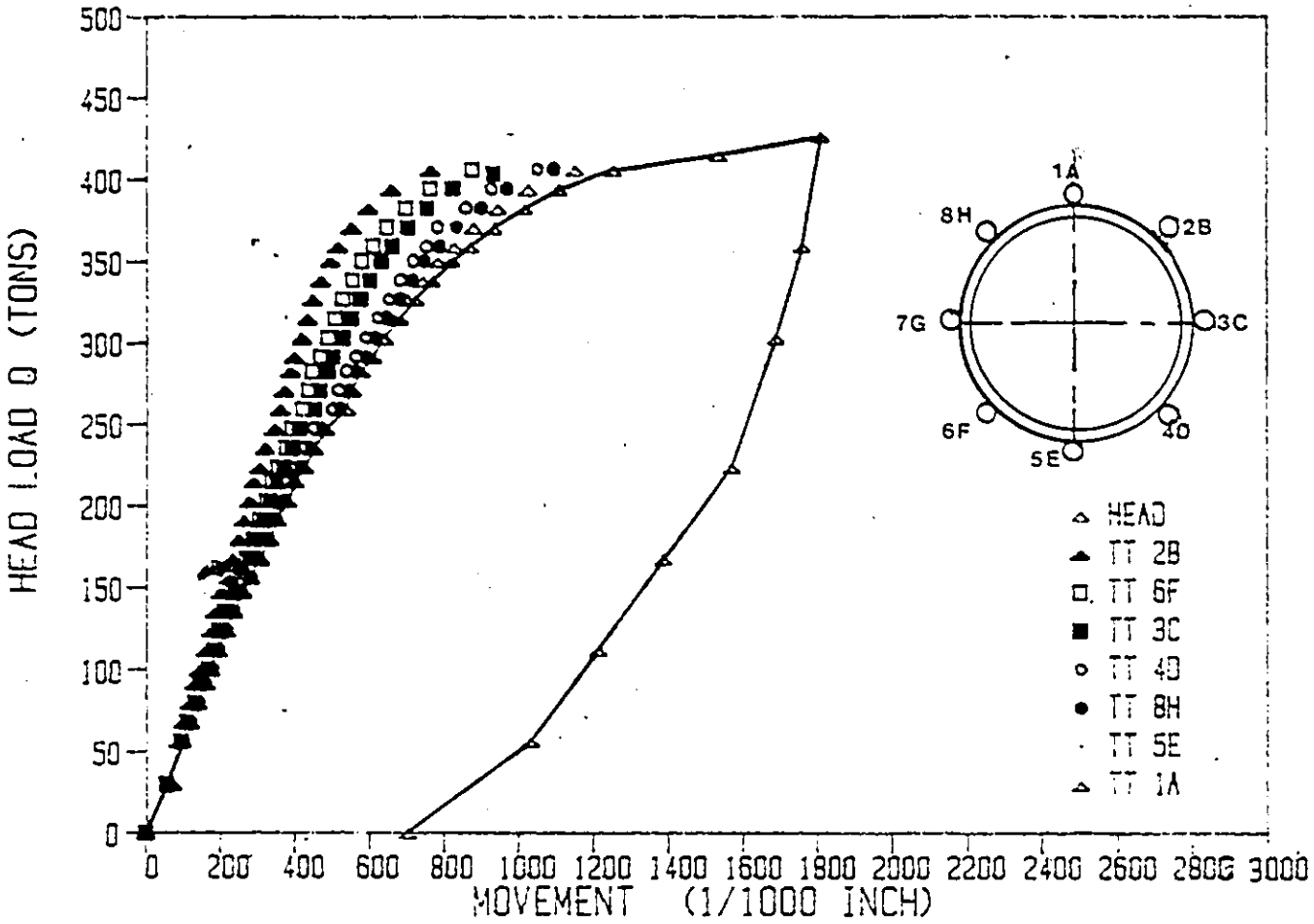

Fig. 4.2 Pile 2; Pipe pile; Push Test;-Load Movement data

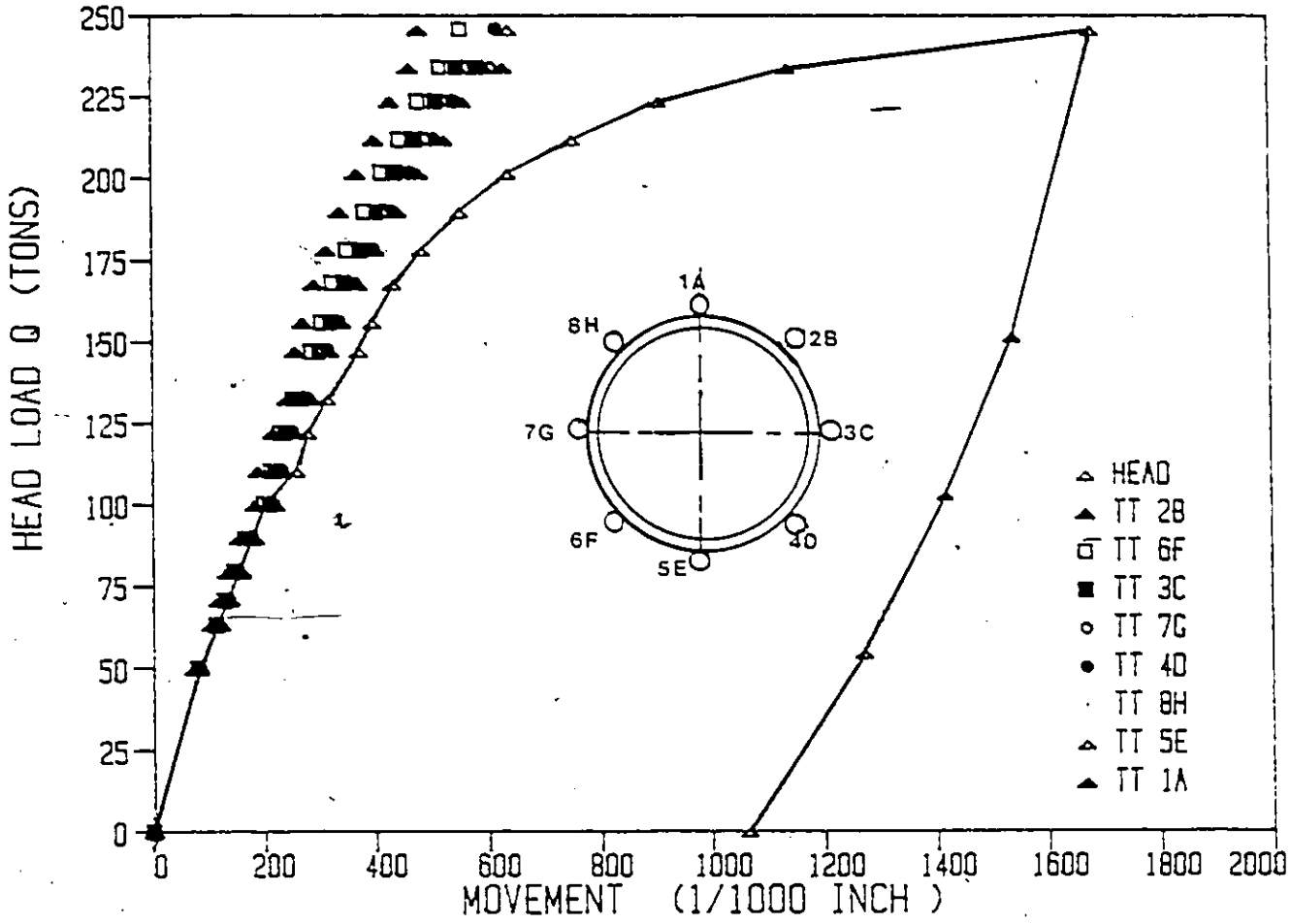

Fig. 4.3 Pile 3; Pipe pile; Push Test; Load Movement data

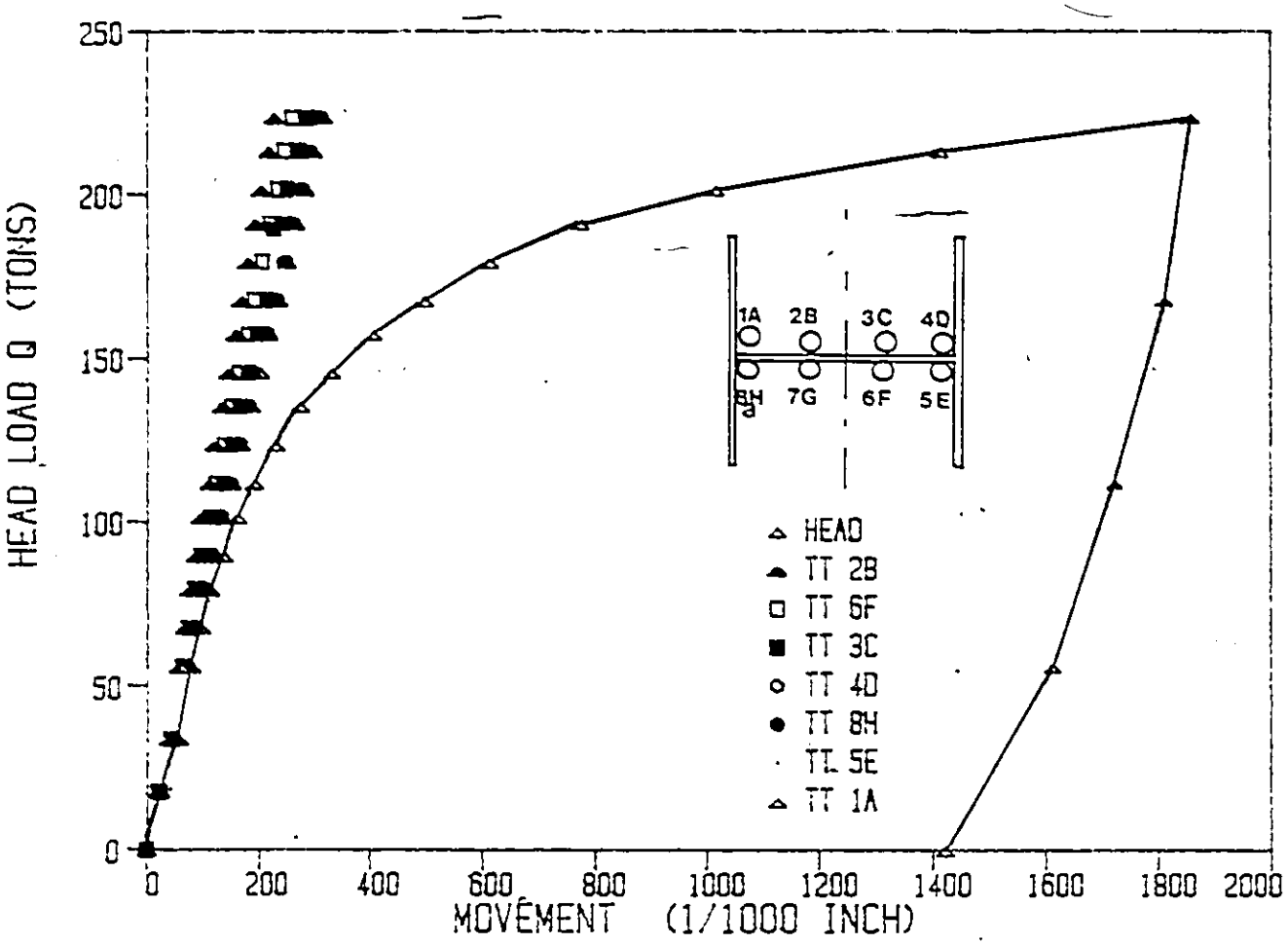

Fig. 4.4 Pile 4; H-Pile; Push Test; Load Movement data

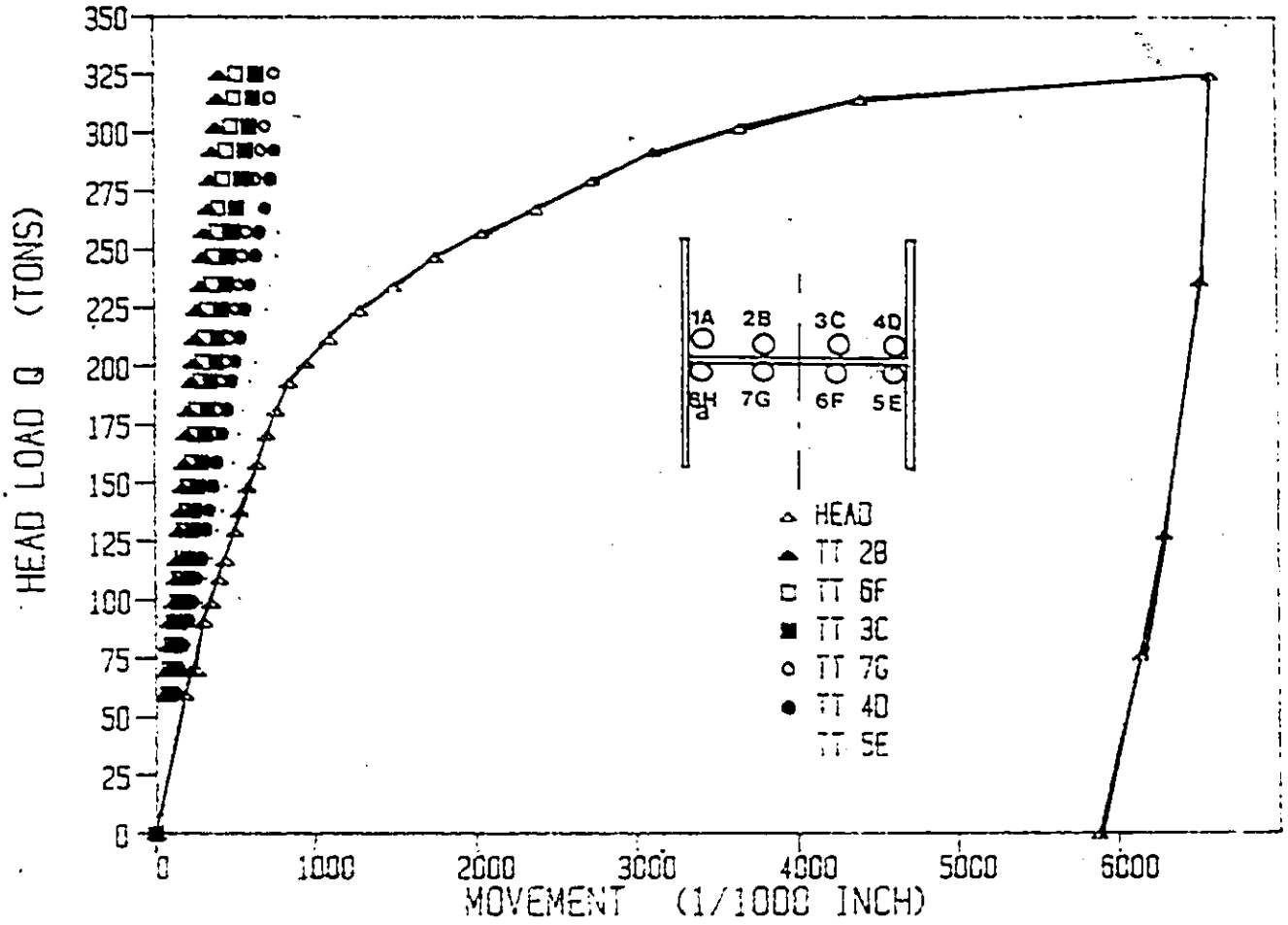

Fig. 4.5 Pile 1; H-Pile; Pull Test; Load Movement data

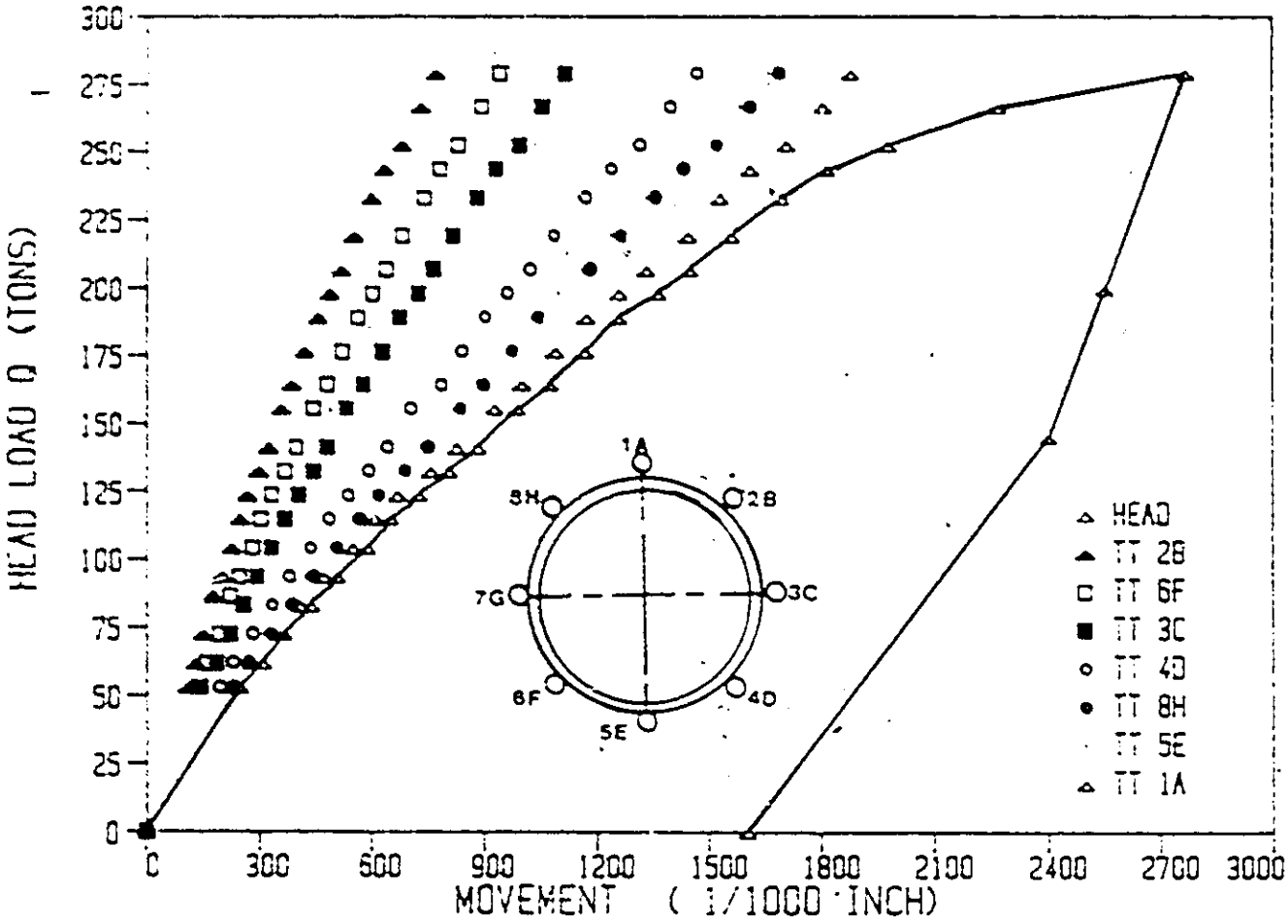

Fig. 4.6 Pile 2; Pull Test; Load Movement data

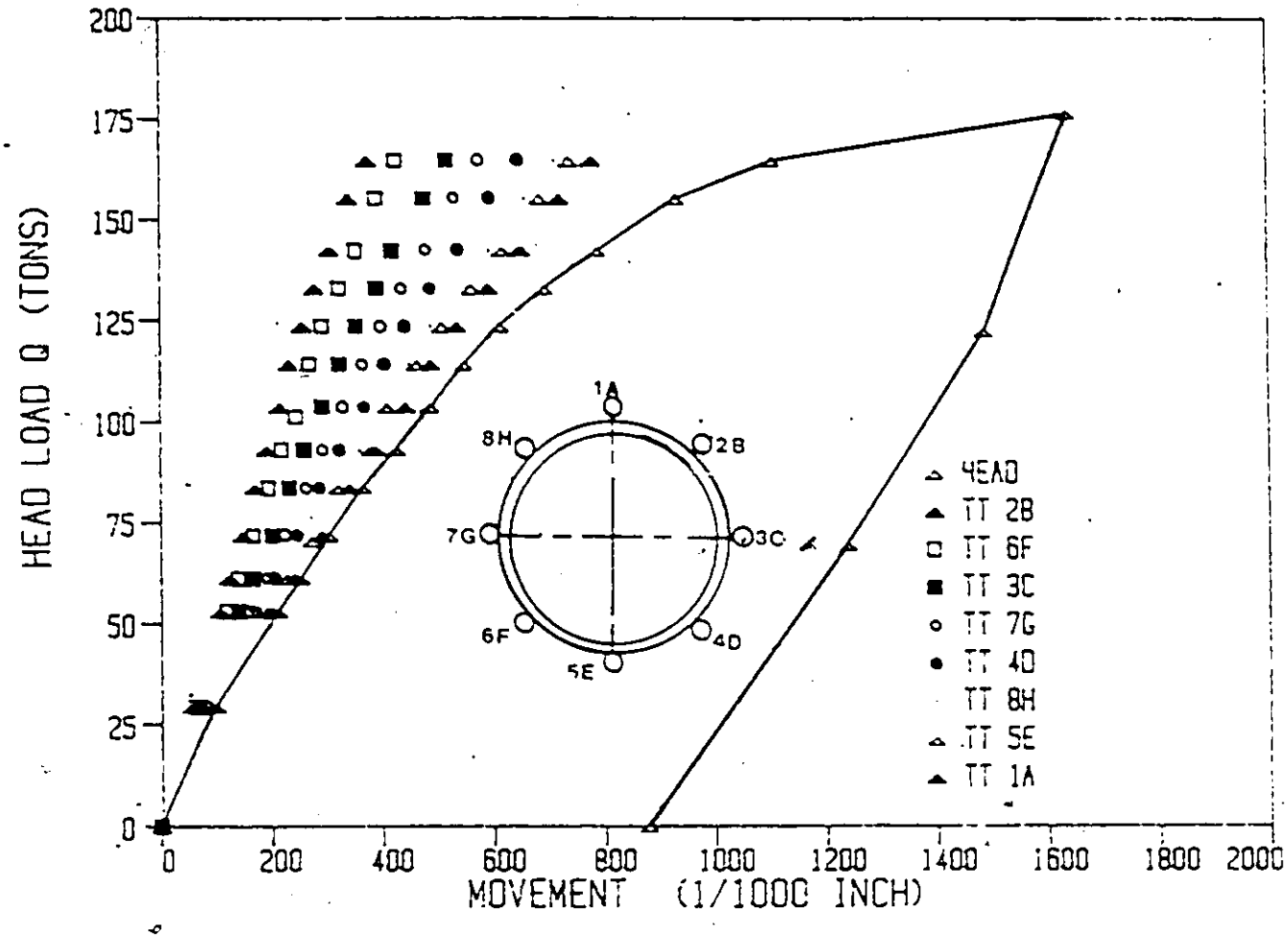

Fig. 4.7 Pile 3; Pipe pile; Pull Test; Load Movement data

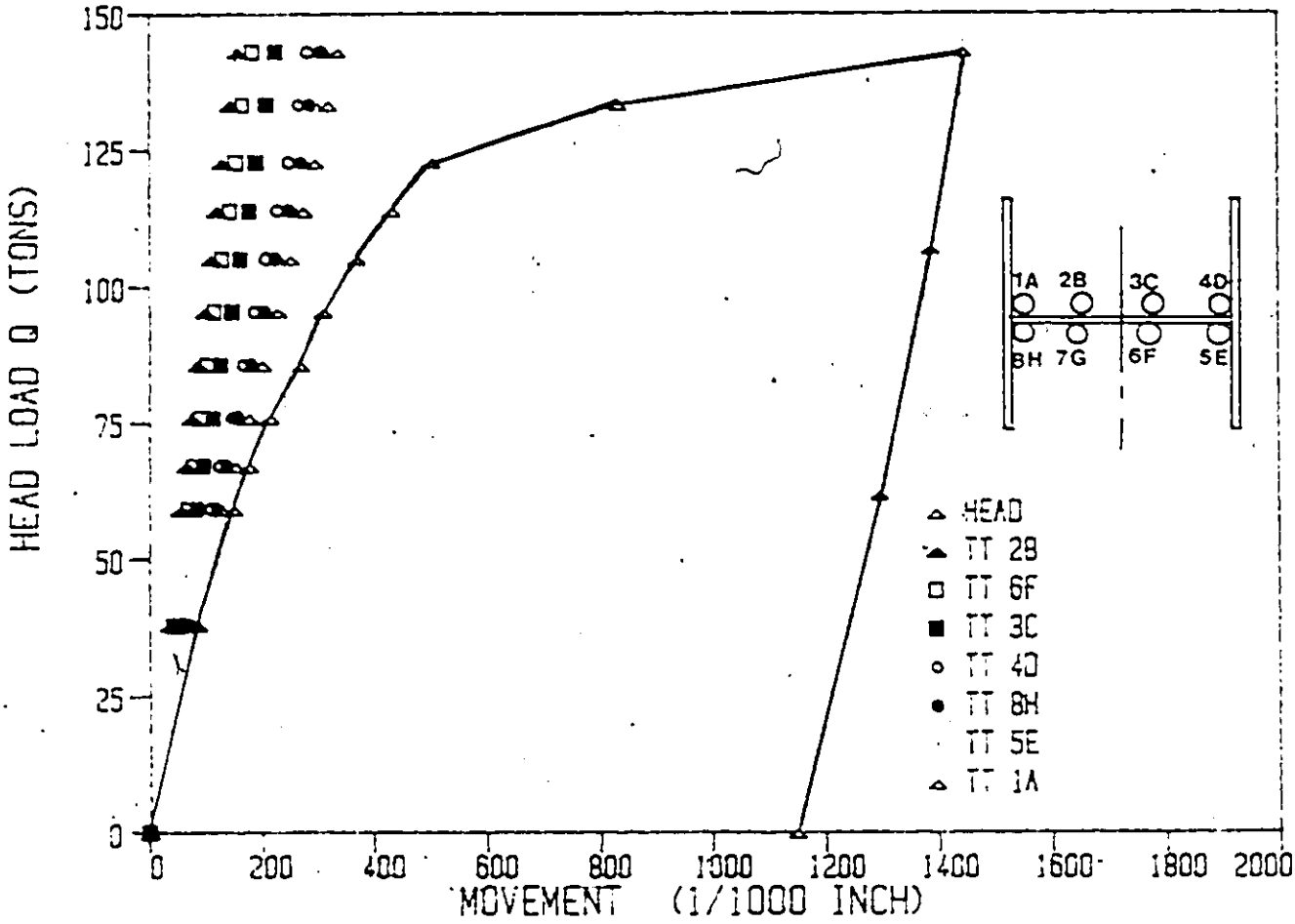

Fig. 4.8 Pile 4; H-Pile; Pull Test; Load Movement data

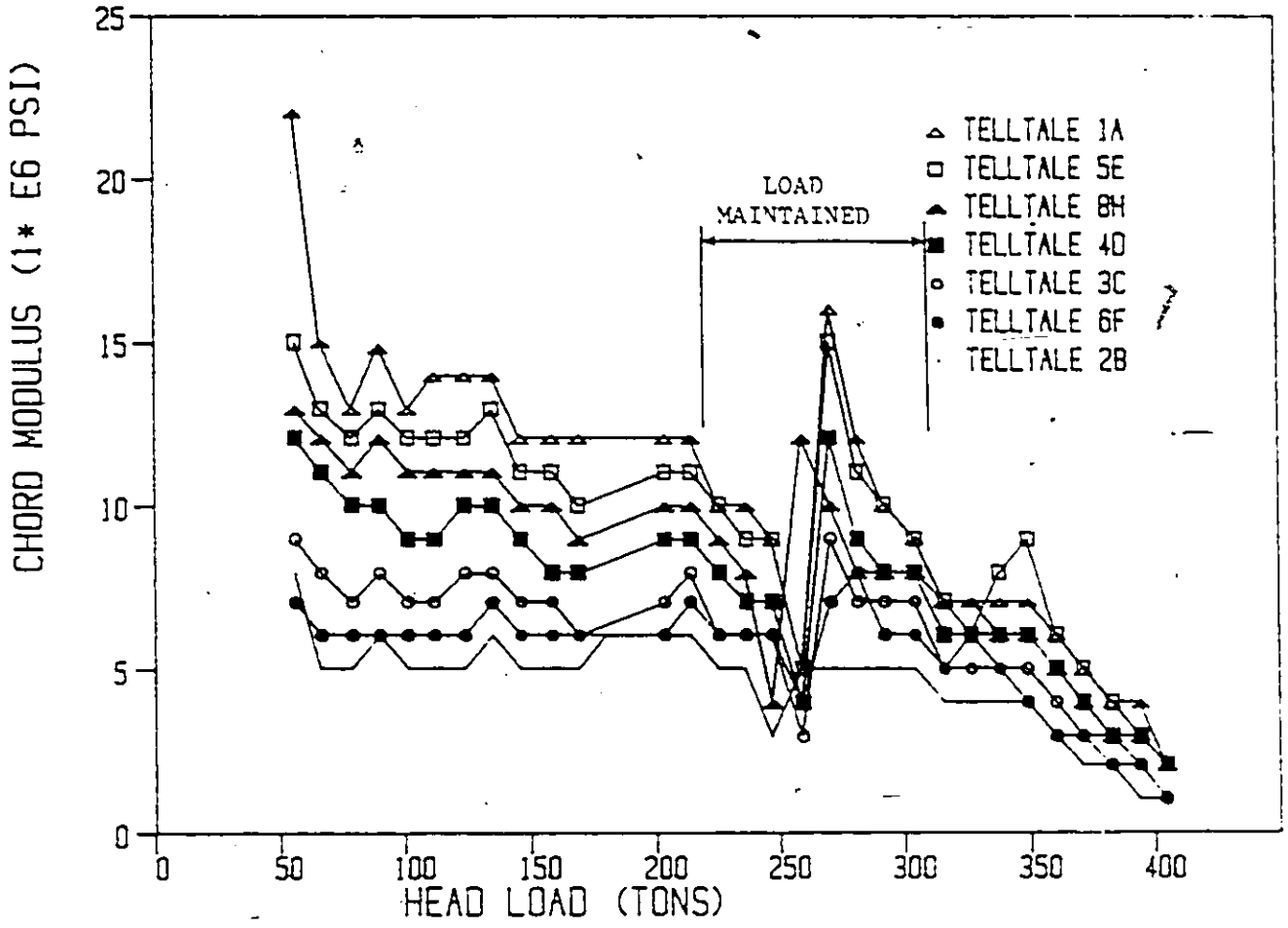

Fig. 4.9 Pile 2; Concreted Pipe pile; Chord Modulus distribution

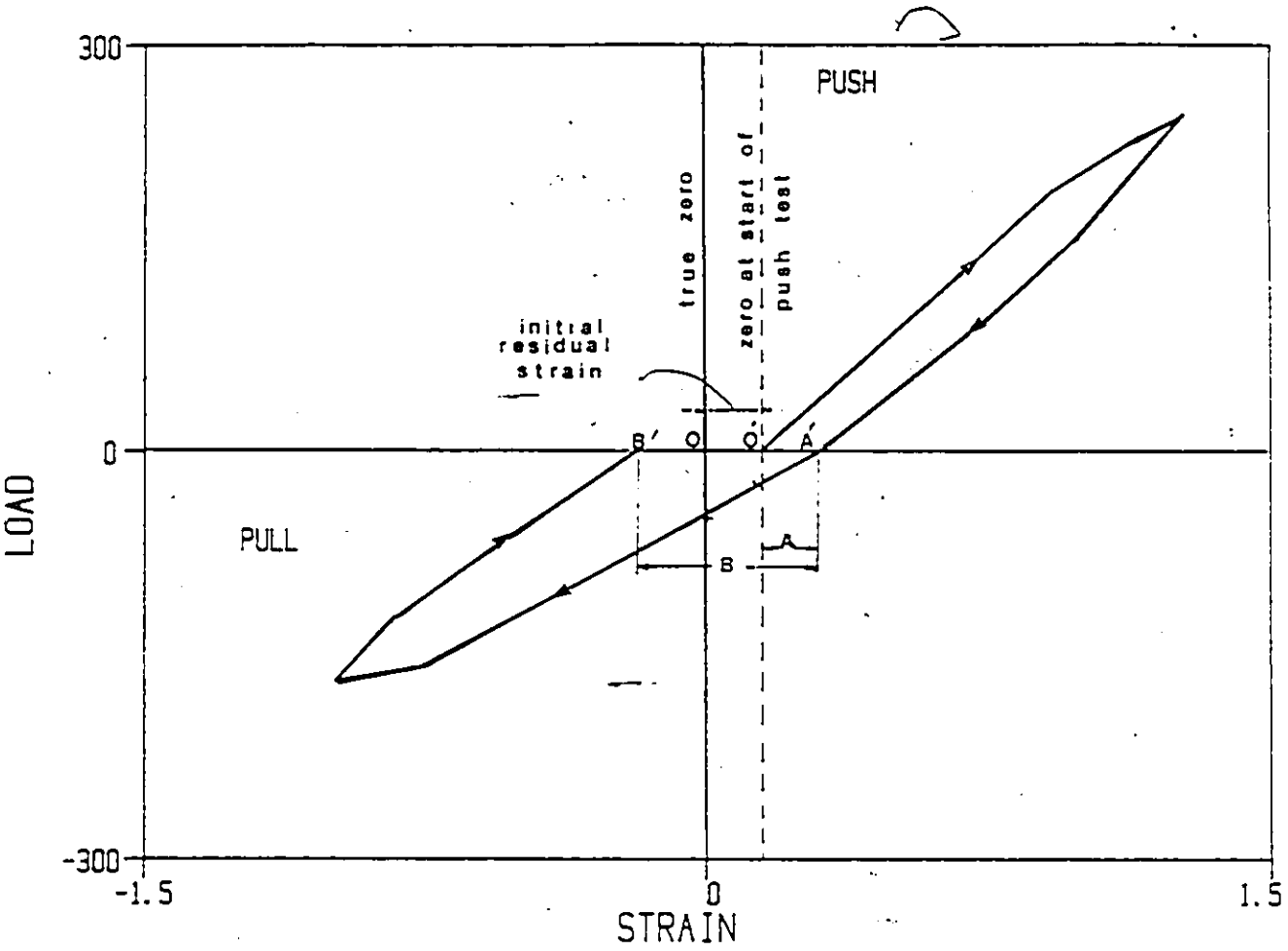

Fig. 5.1 Typical example of load strain cycle for driven piles

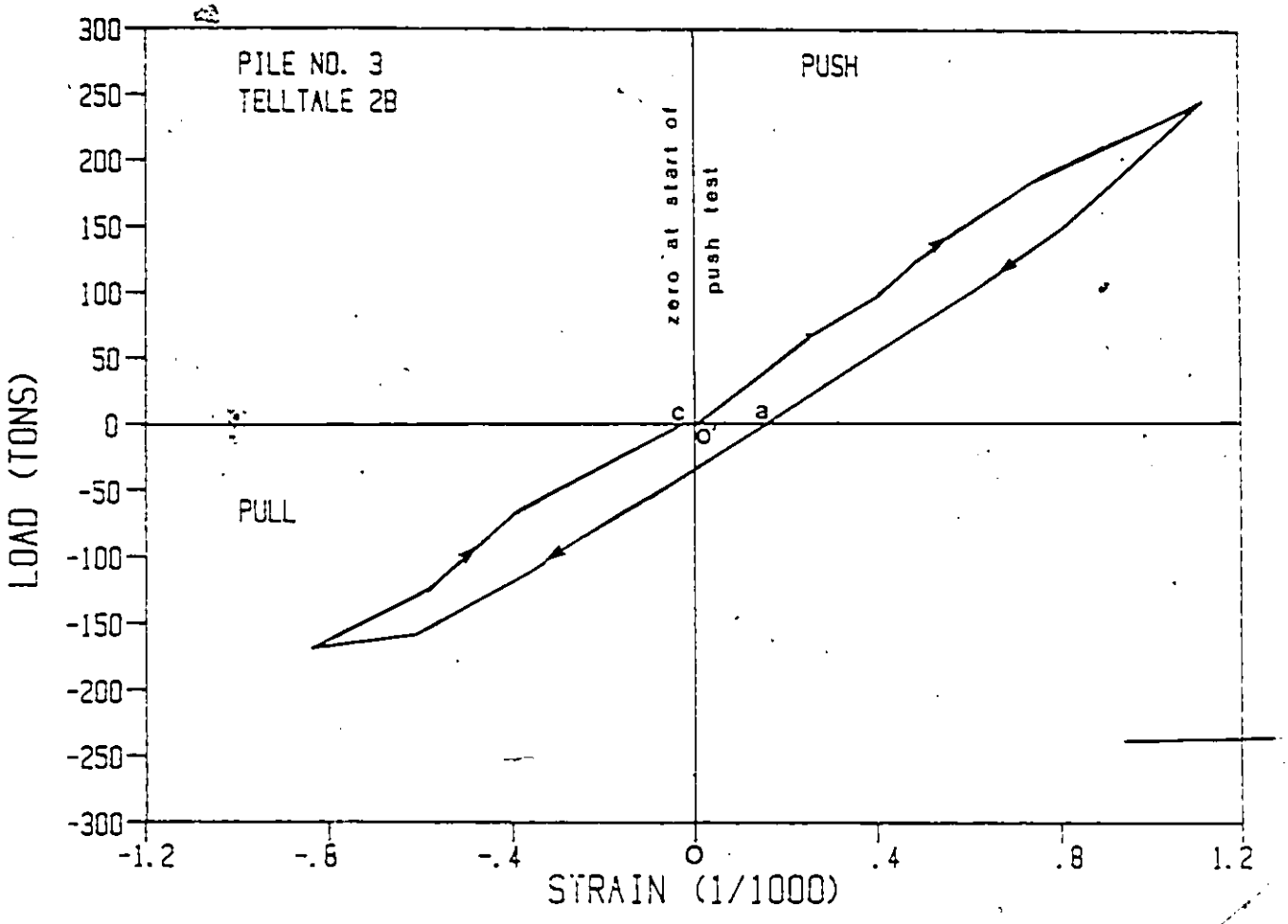

Fig. 5.2 Example of induced load strain cycle before push testing (Pile 3)

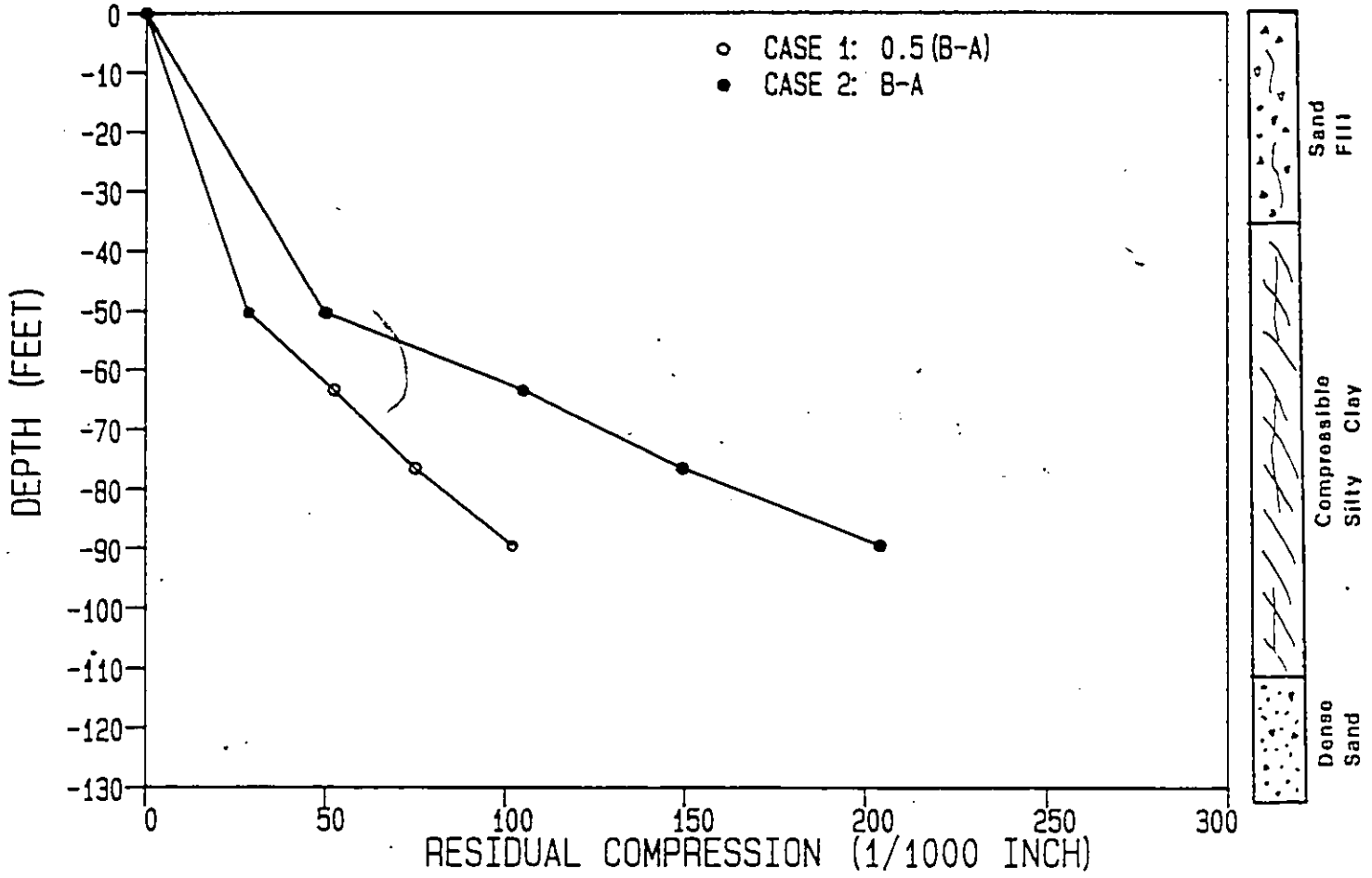

Fig. 5.3 Pile 1; H-Pile; Residual compression at telltale ends.

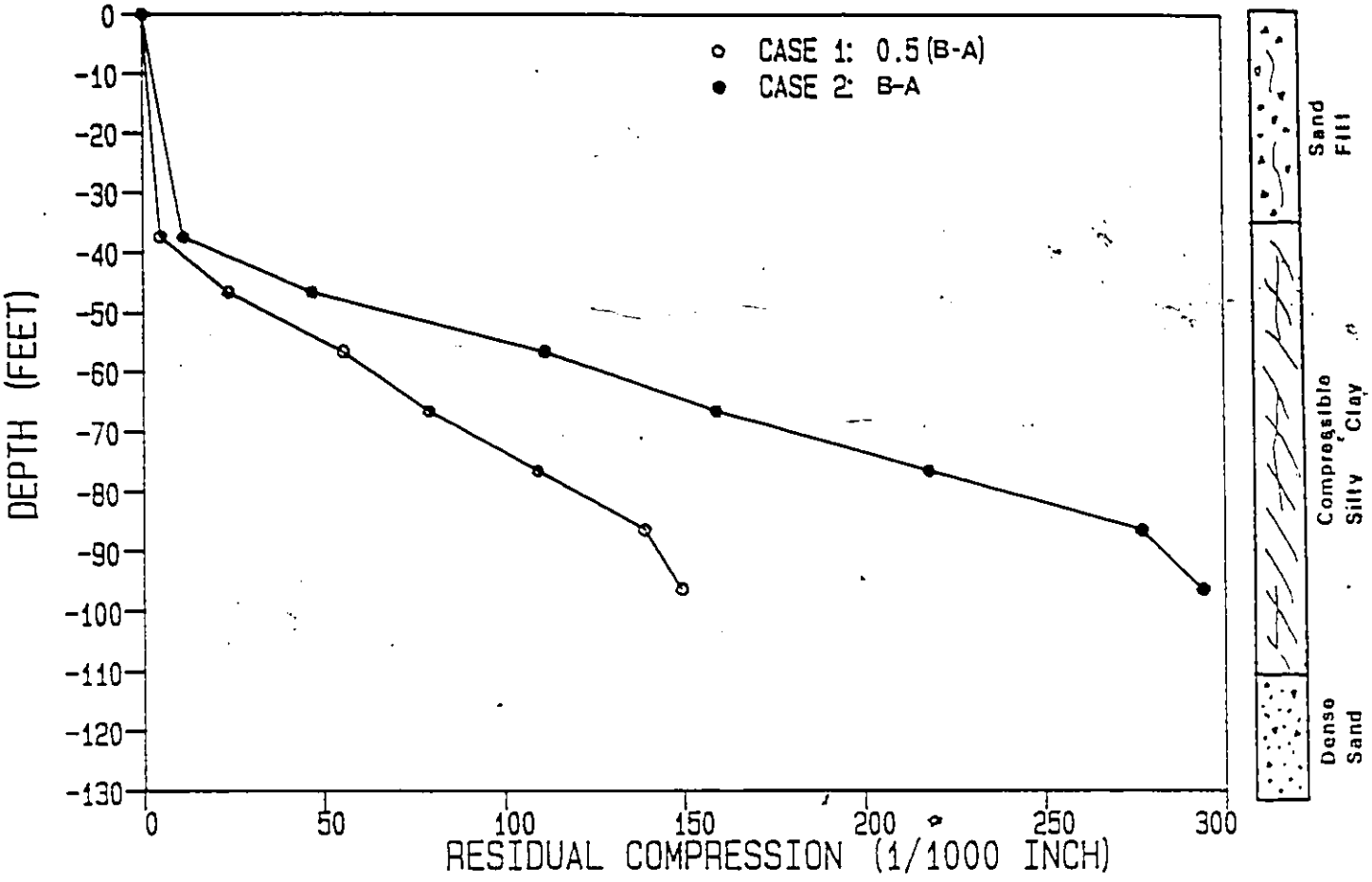

Fig. 5.4 Pile 3; Pipe pile; Residual compression at telltale ends.

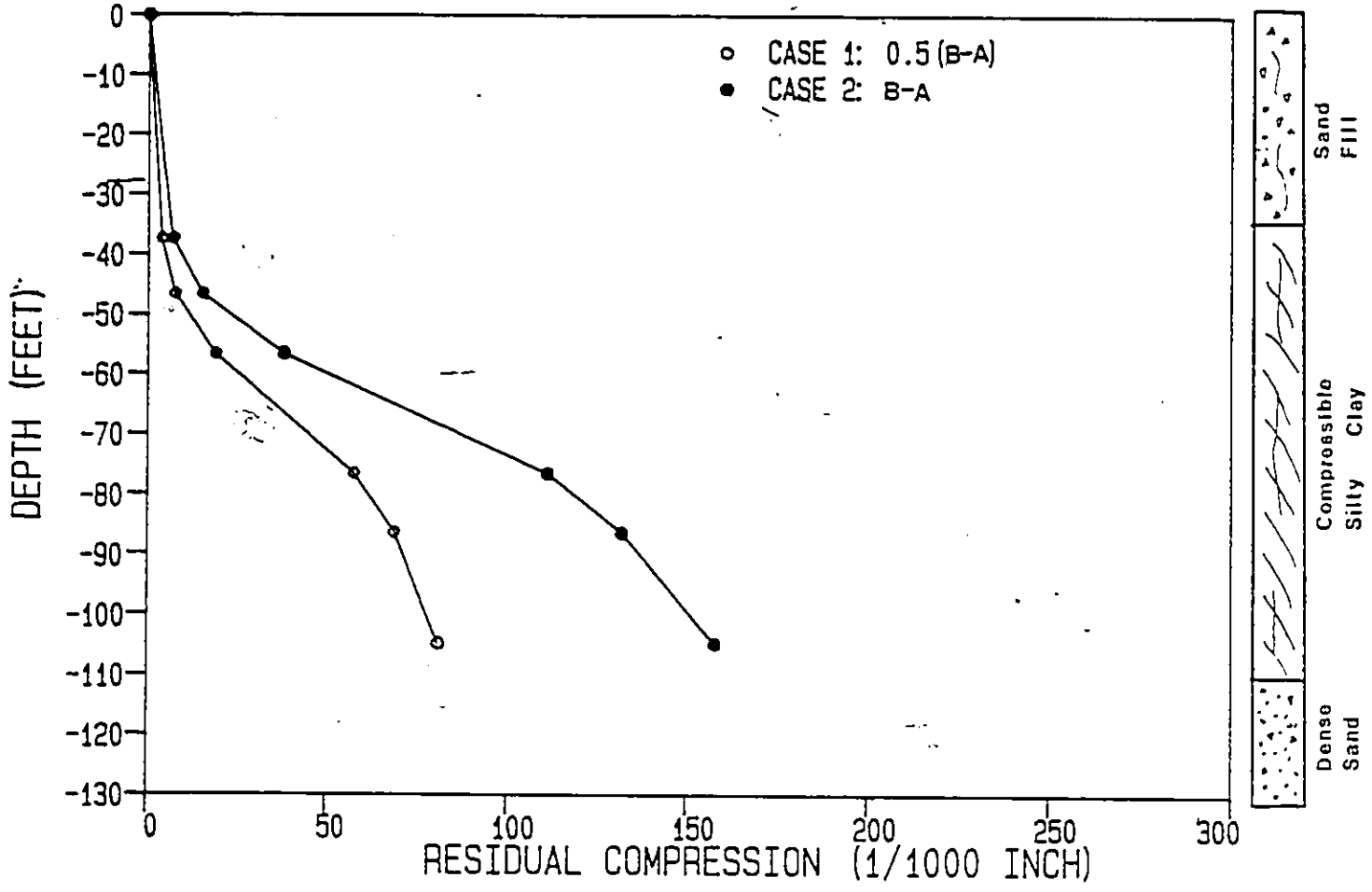

Fig. 5.5 Pile 4; H-Pile; Residual compression at telltale ends.

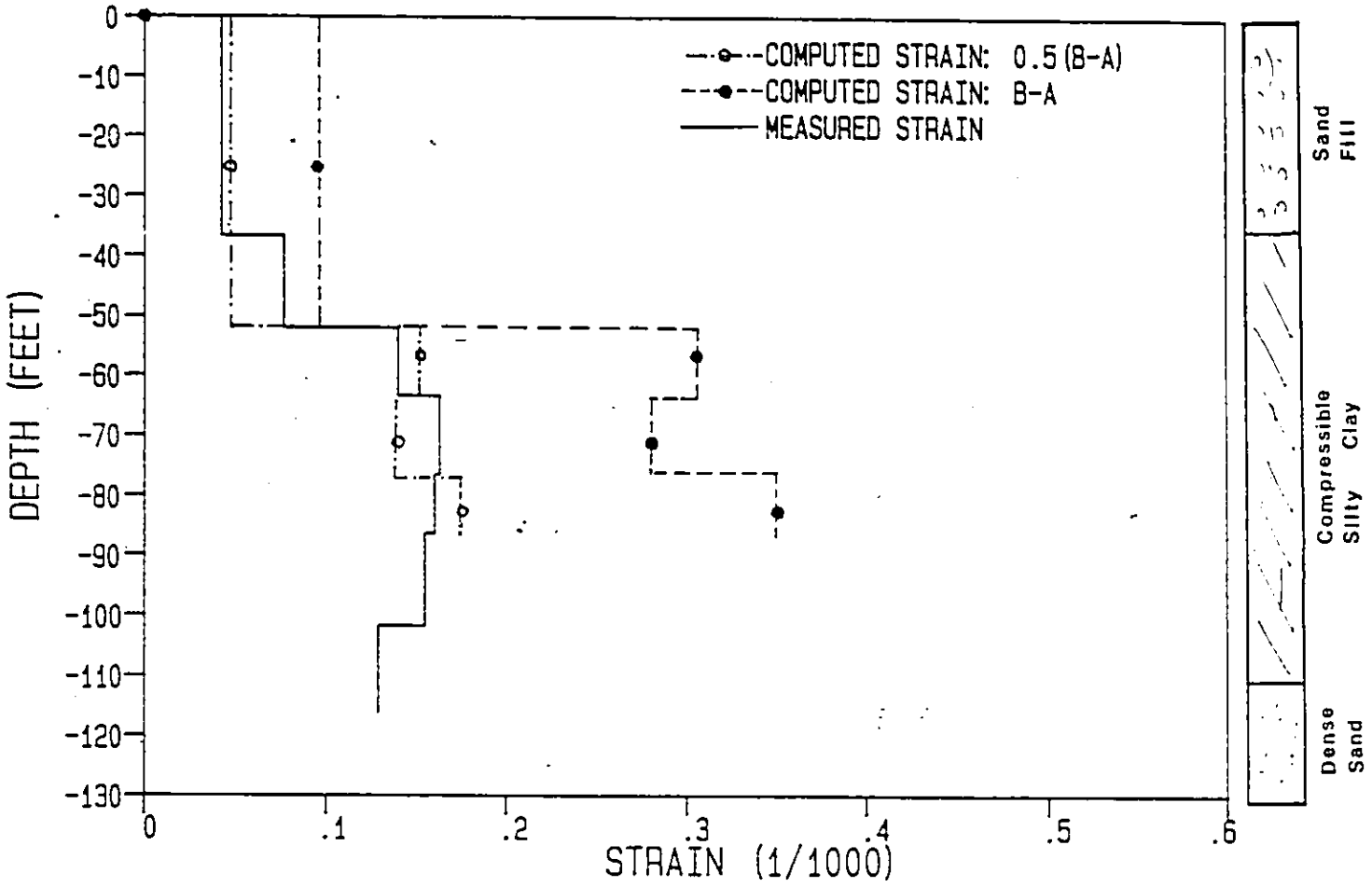

Fig. 5.6 Pile 1; H-Pile; Residual strain distribution

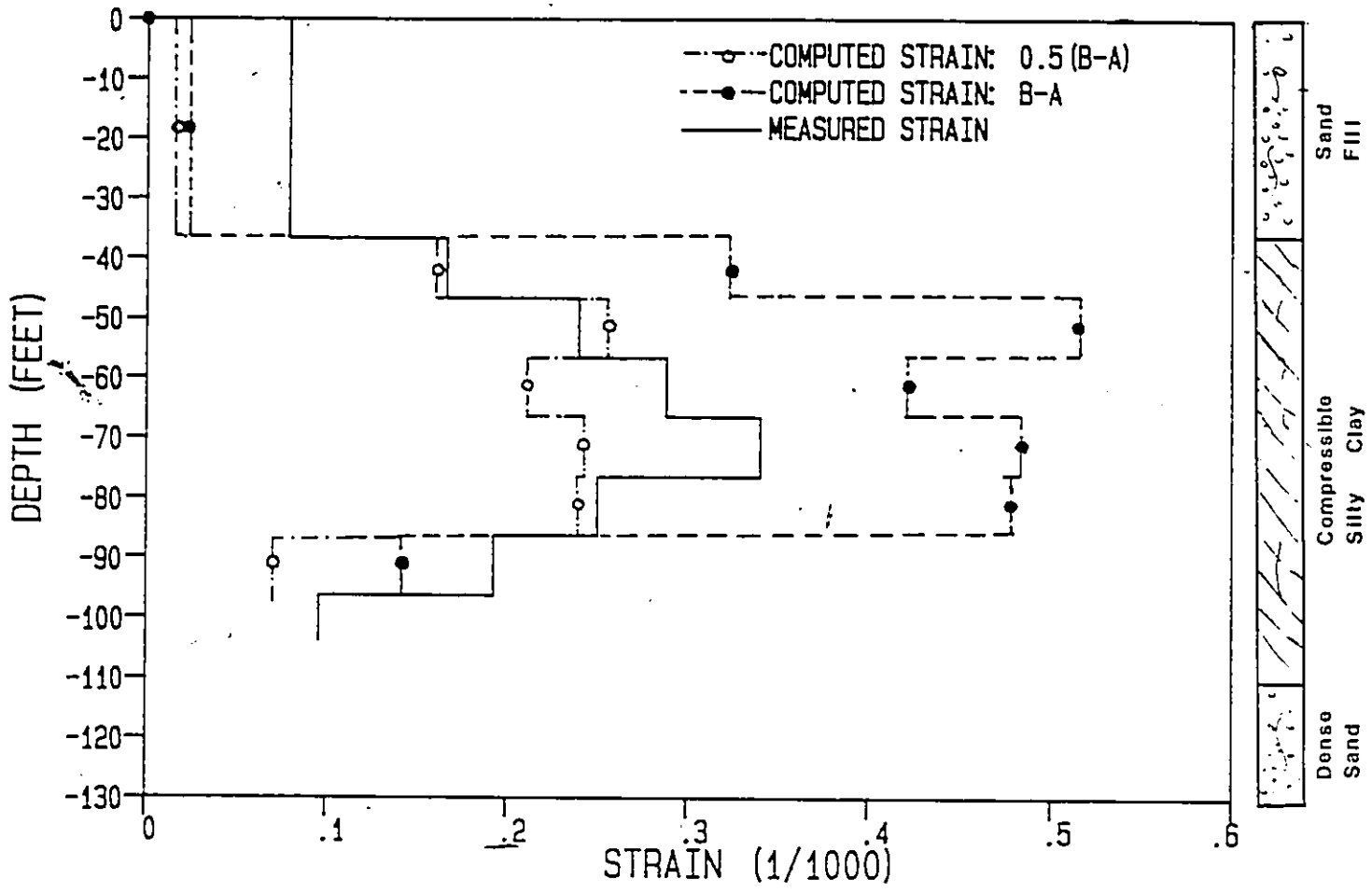

Fig. 5.7 Pile 3; Pipe pile; Residual strain distribution

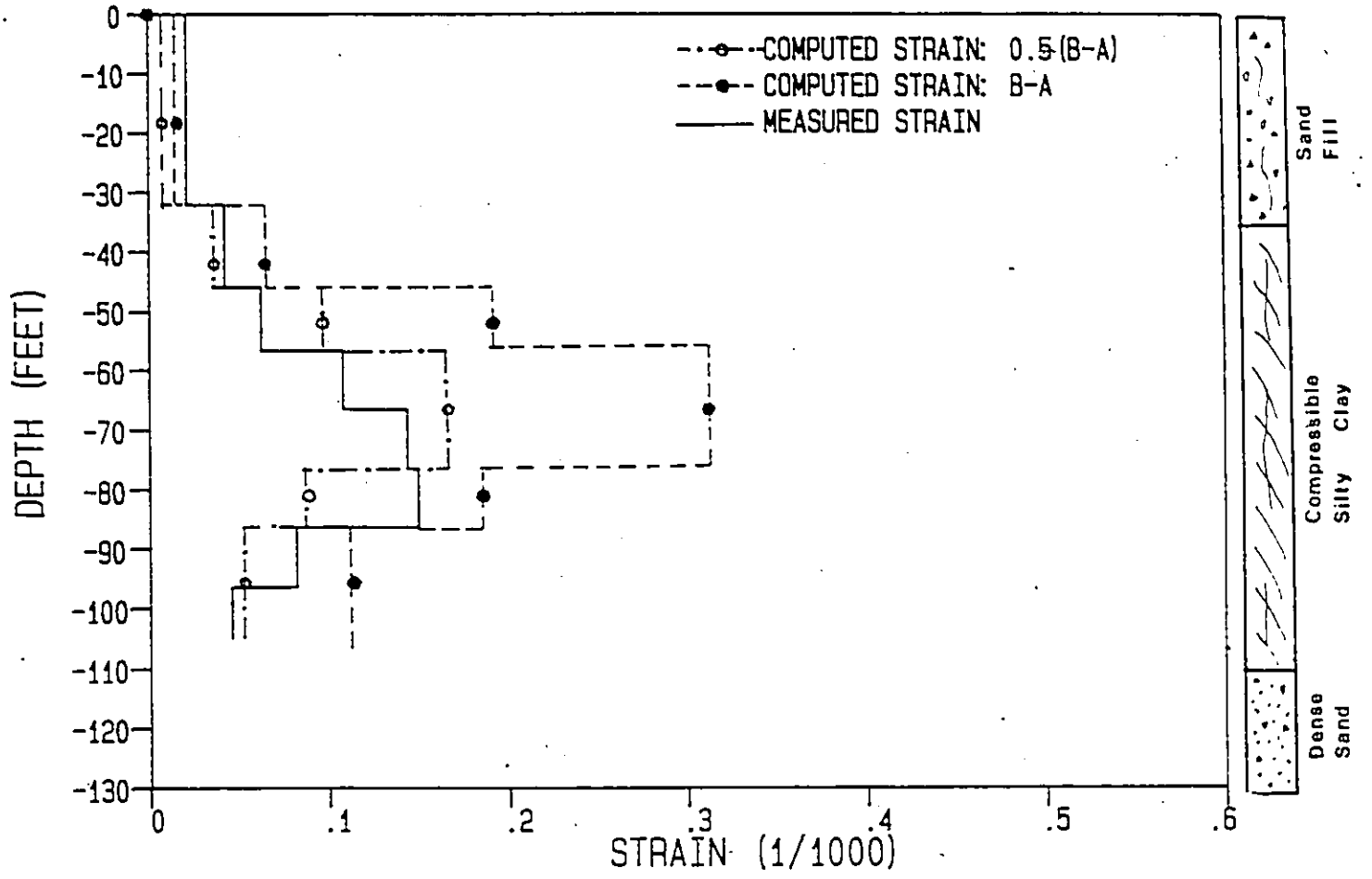

Fig. 5.8 Pile 4; H-Pile; Residual strain distribution

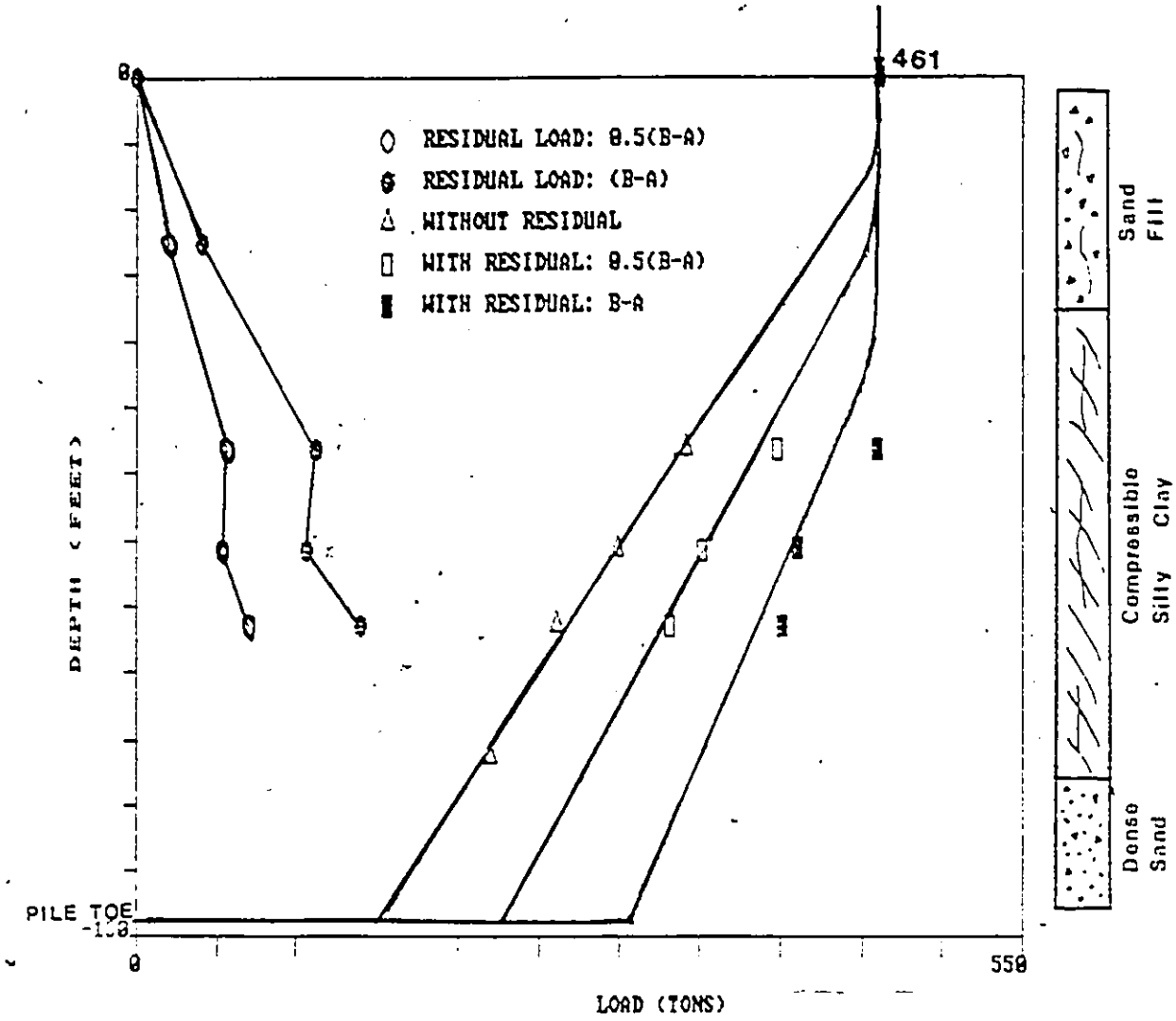

Fig. 5.9 Pile 1; H-Pile; Load distribution in push testing

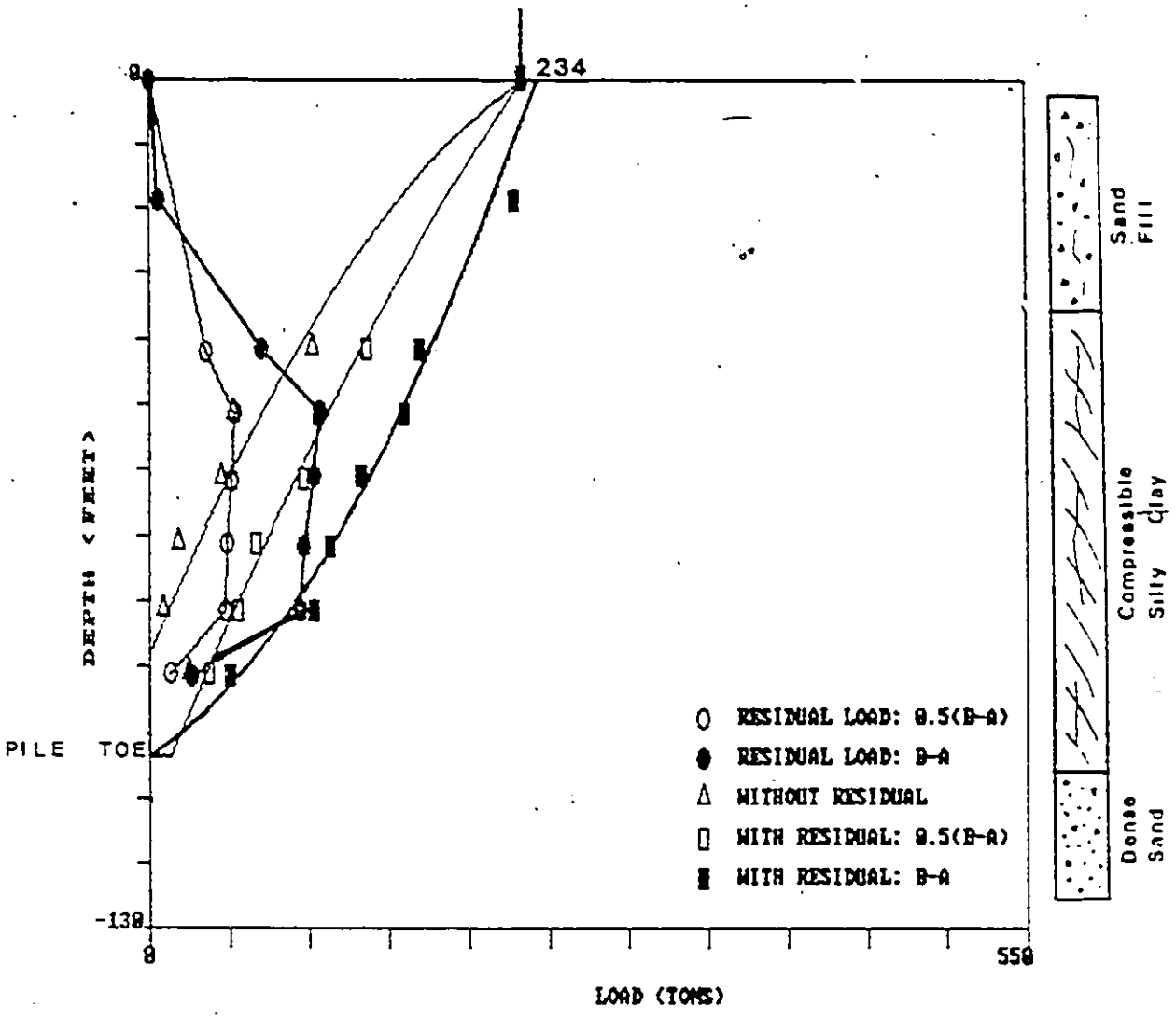

Fig. 5.10 Pile 3; Pipe pile; Load distribution in push testing.

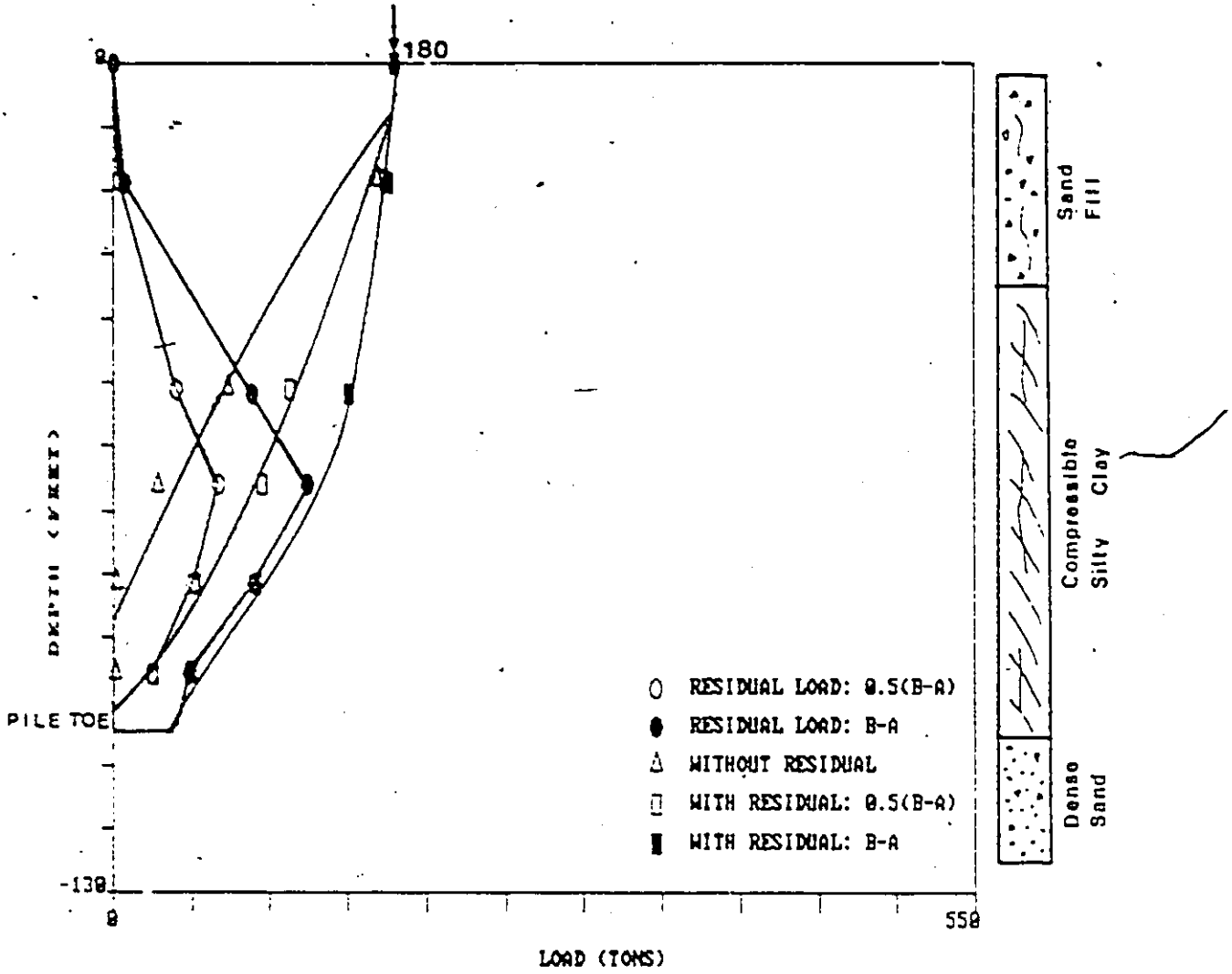

Fig. 5.11 Pile 4; H-Pile; Load distribution in push testing.

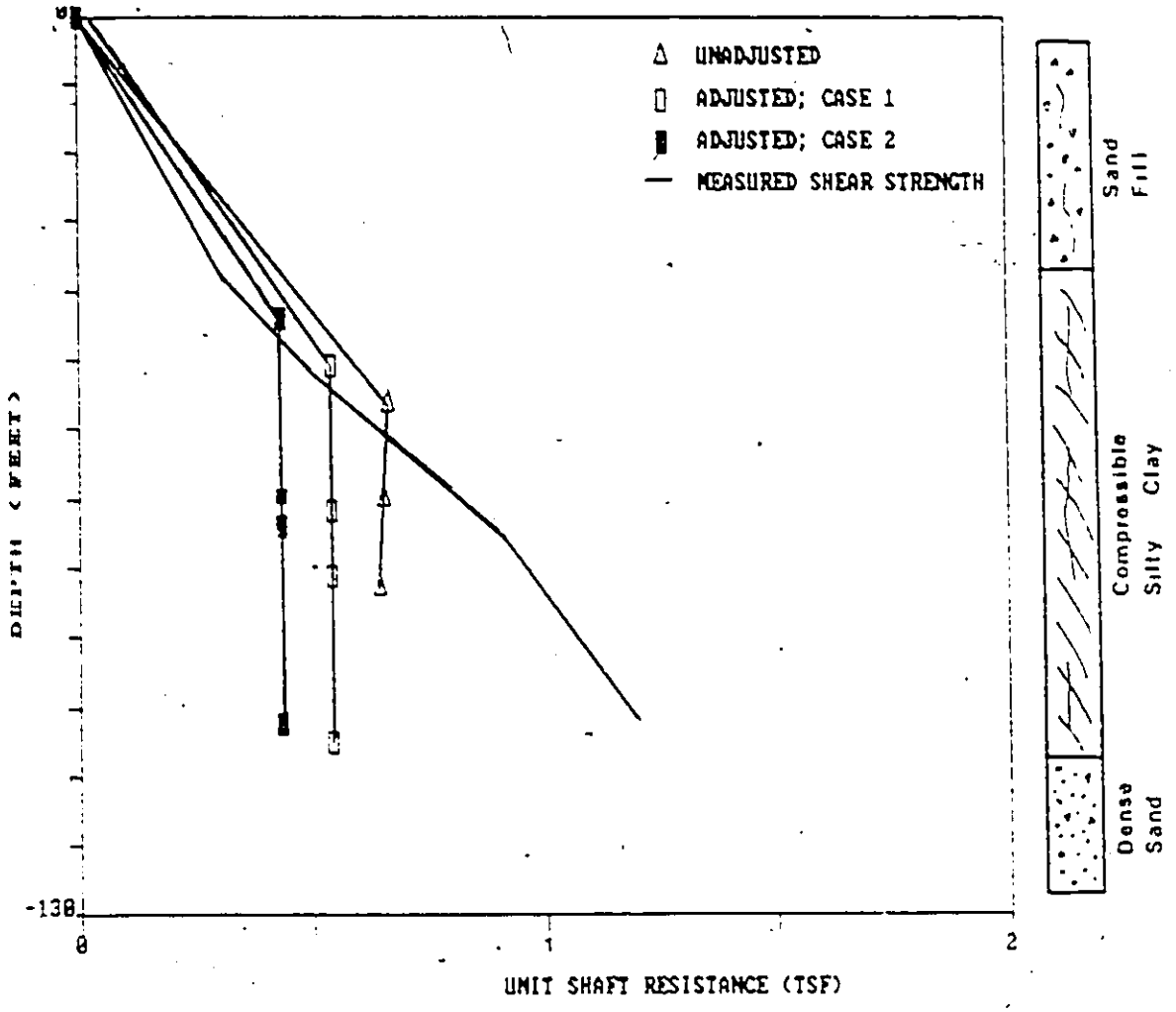

Fig. 5.12 Pile 1; H-Pile; Unit shaft resistance distribution in push testing.

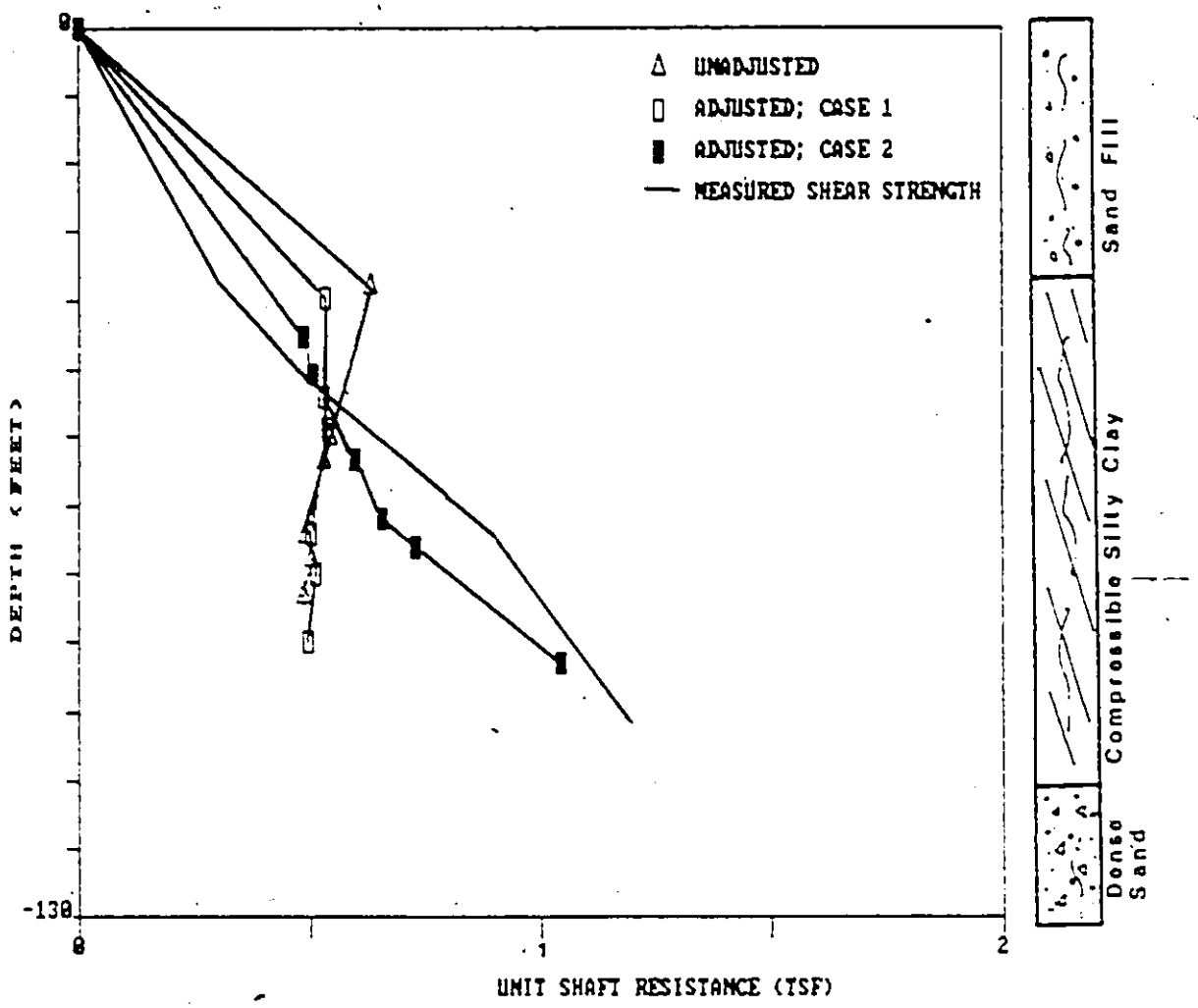

Fig. 5.13 Pile 3; Pipe pile; Unit shaft resistance distribution in push testing.

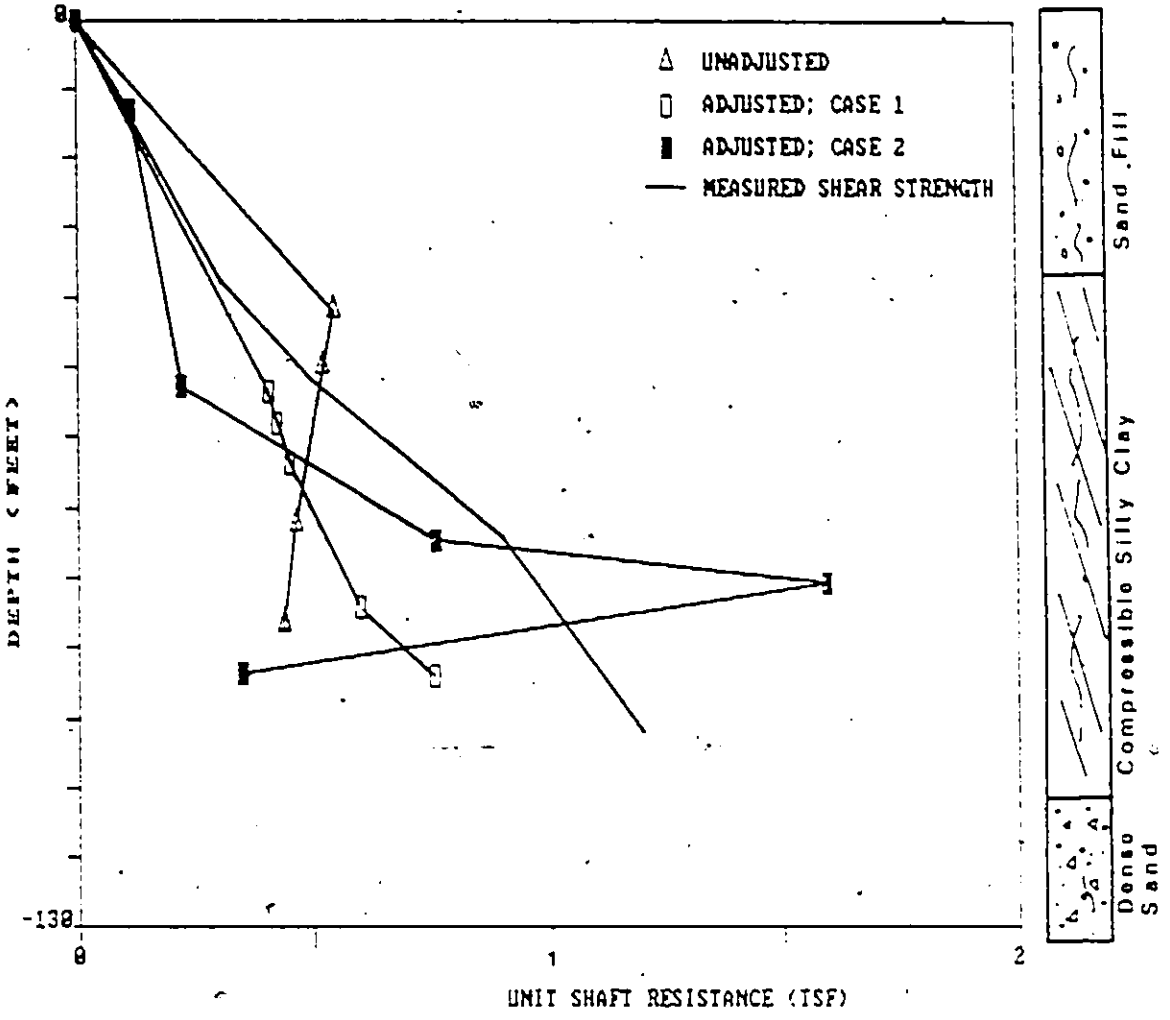

Fig. 5.14 Pile 4; H-Pile; Unit shaft resistance distribution in push testing.

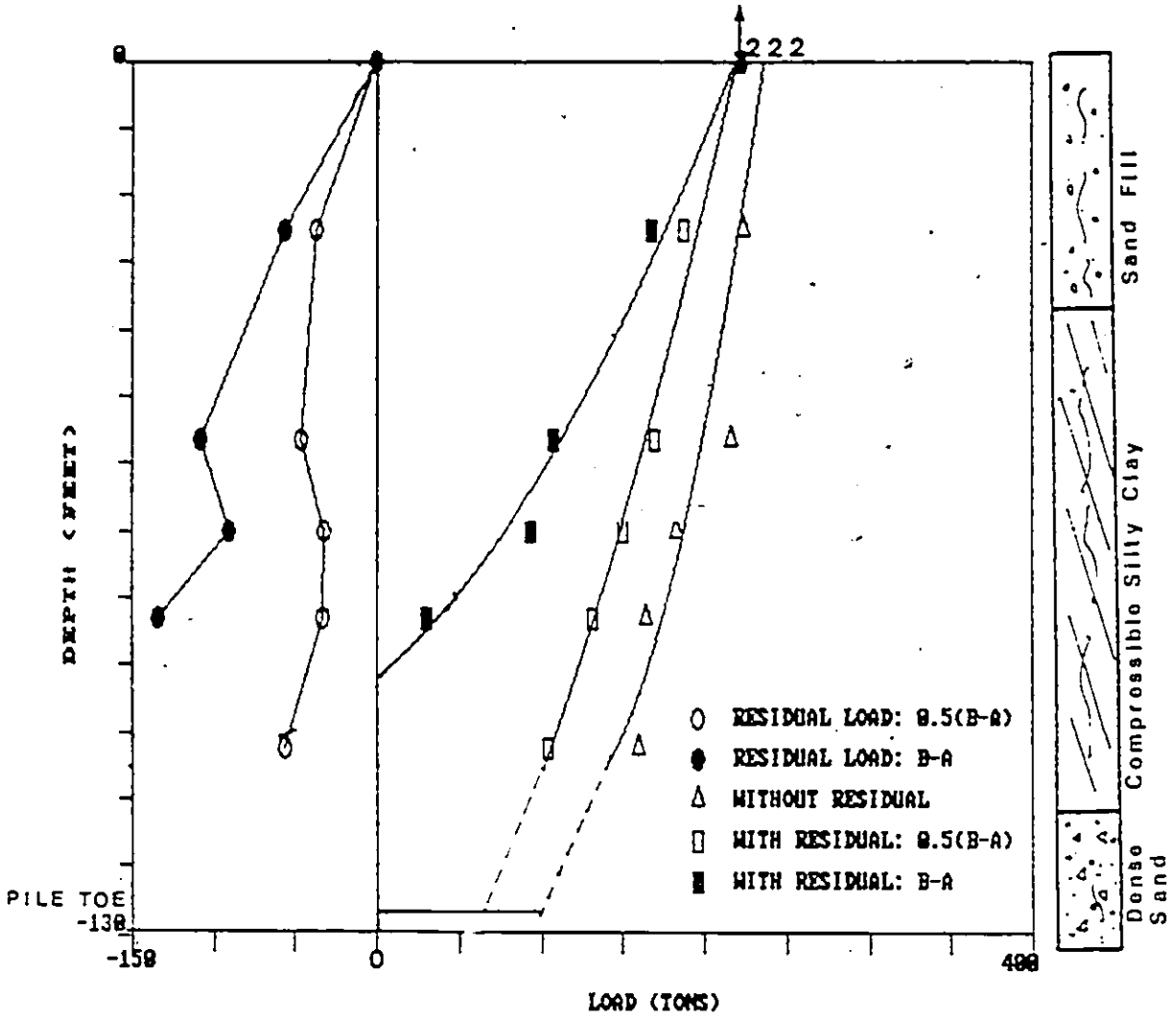

Fig. 5.15 Pile 1; H-Pile; Load distribution in pull testing.

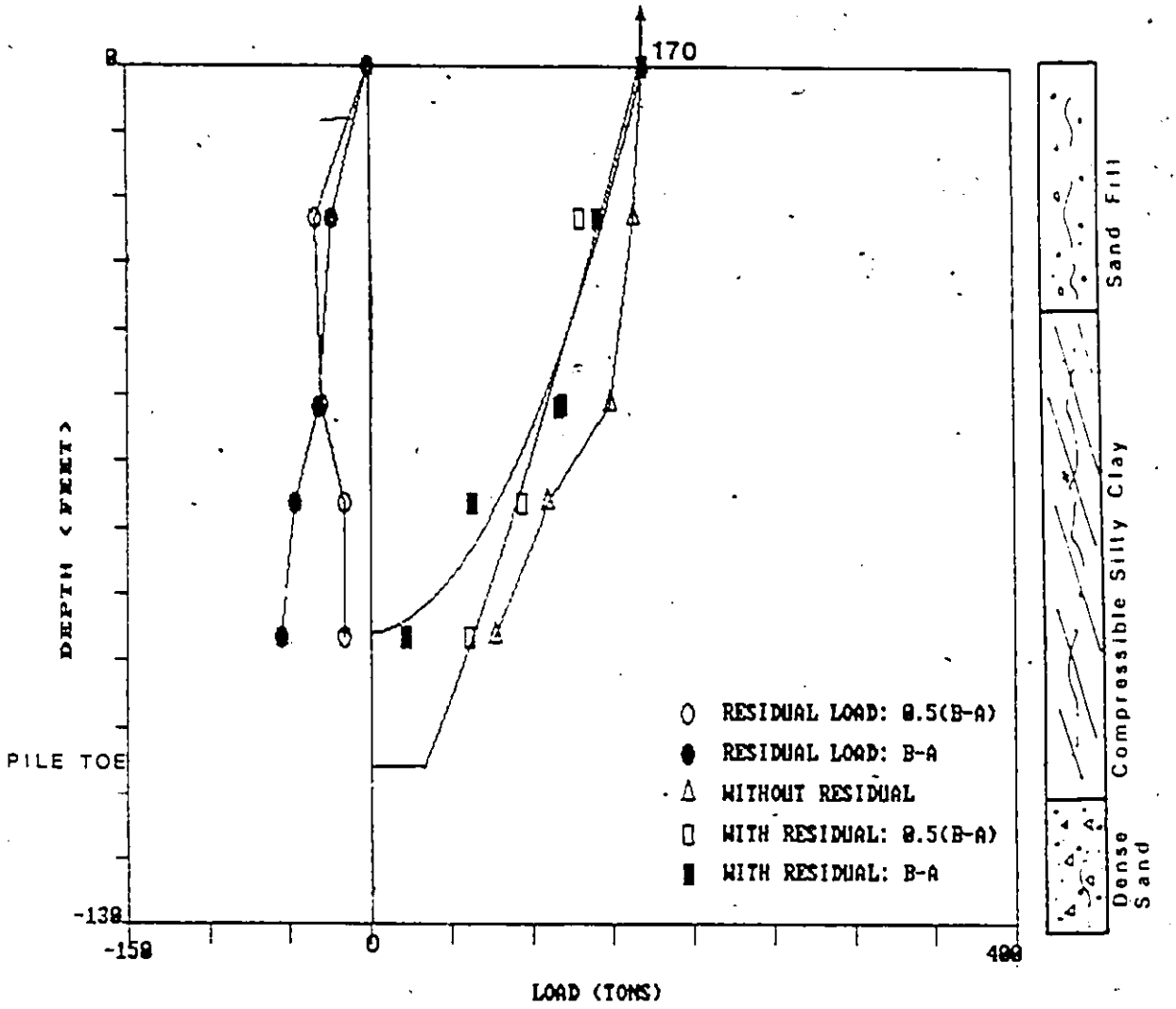

Fig. 5.16 Pile 3; Pipe pile; Load distribution in pull testing

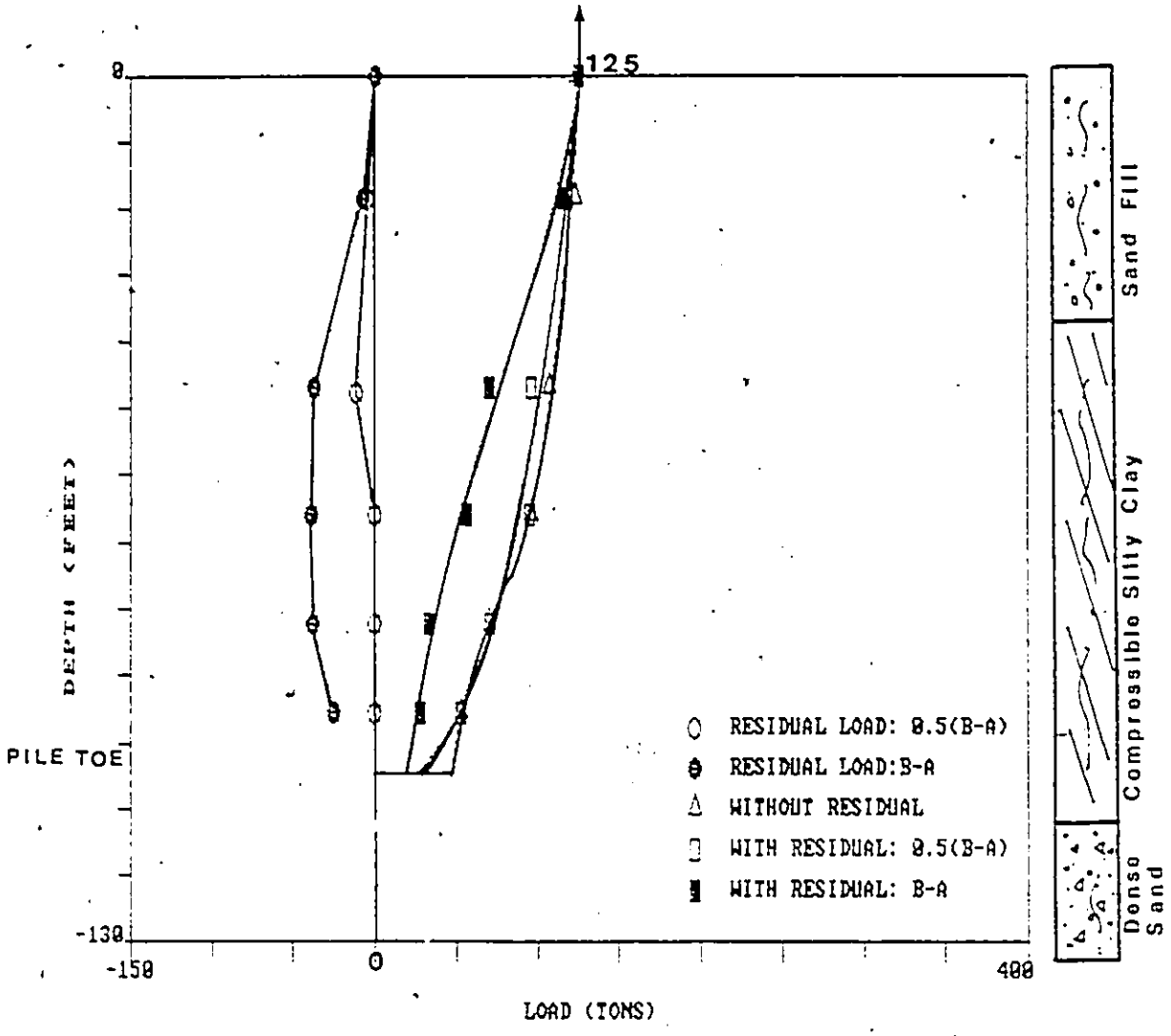

Fig. 5.17 Pile 4; H-Pile; Load distribution in pull testing.

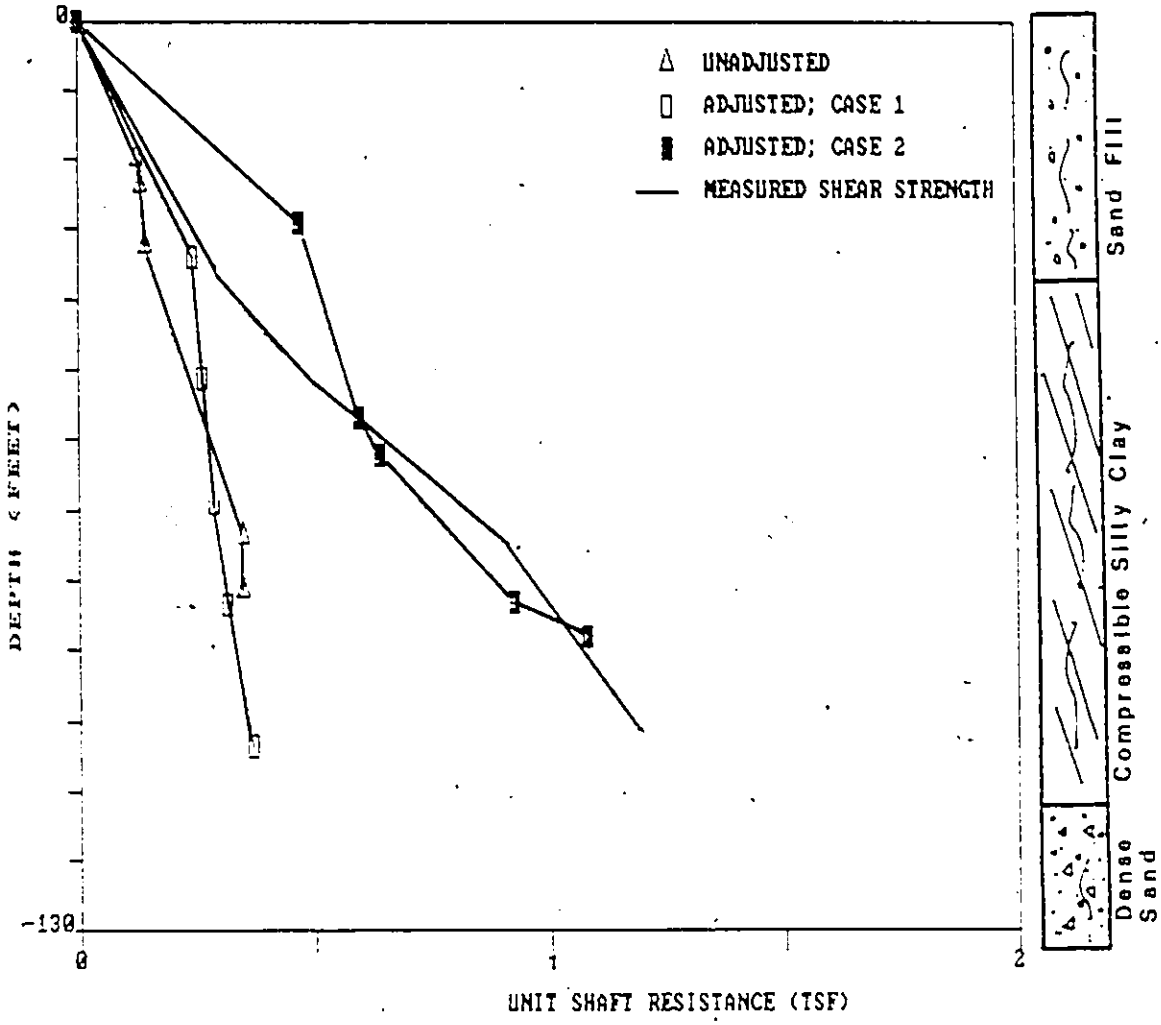

Fig. 5.18 Pile 1; H-Pile; Unit shaft resistance distribution in pull testing.

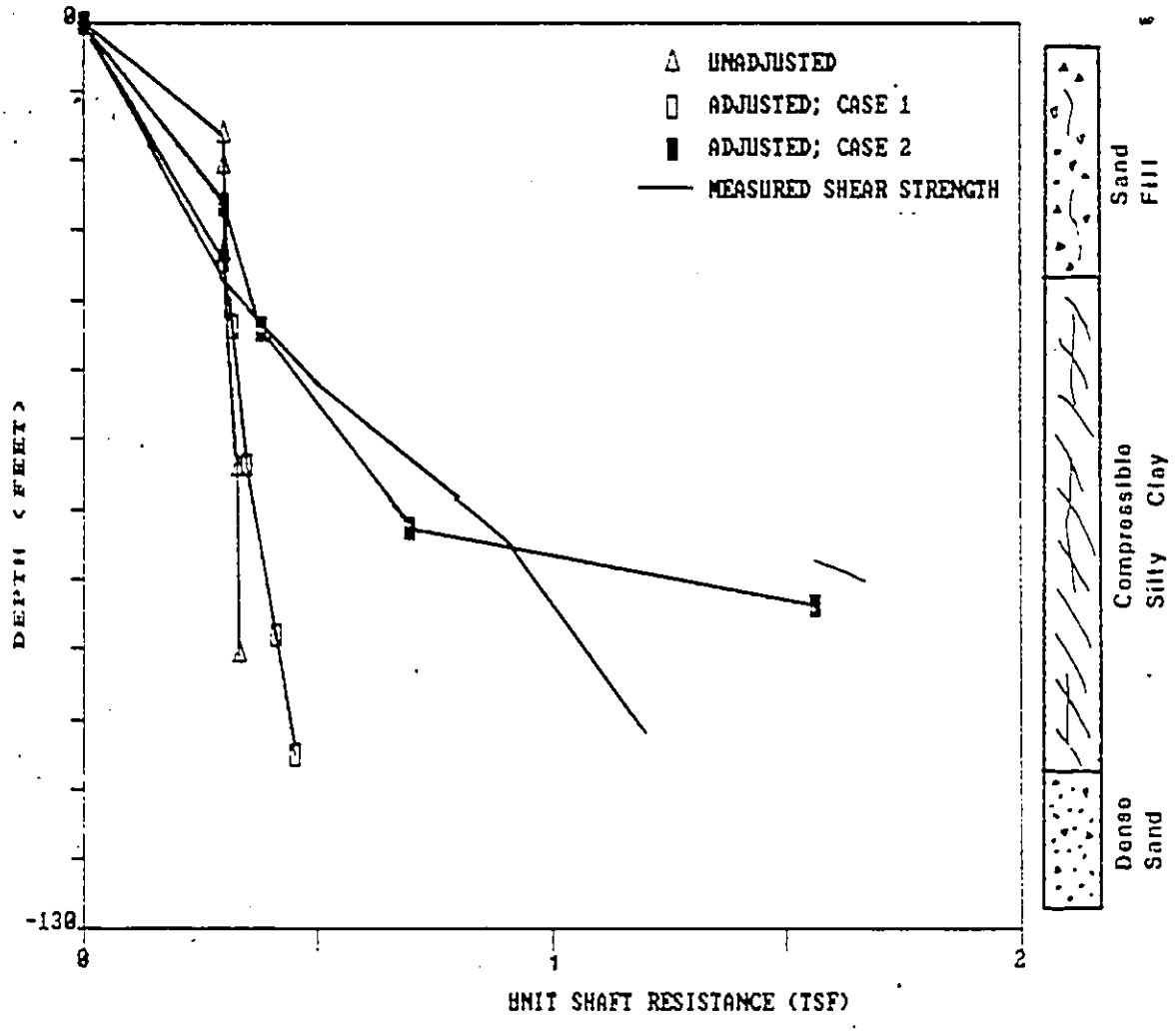

Fig. 5.19 Pile 3; Pipe pile; Unit shaft resistance distribution in pull testing.

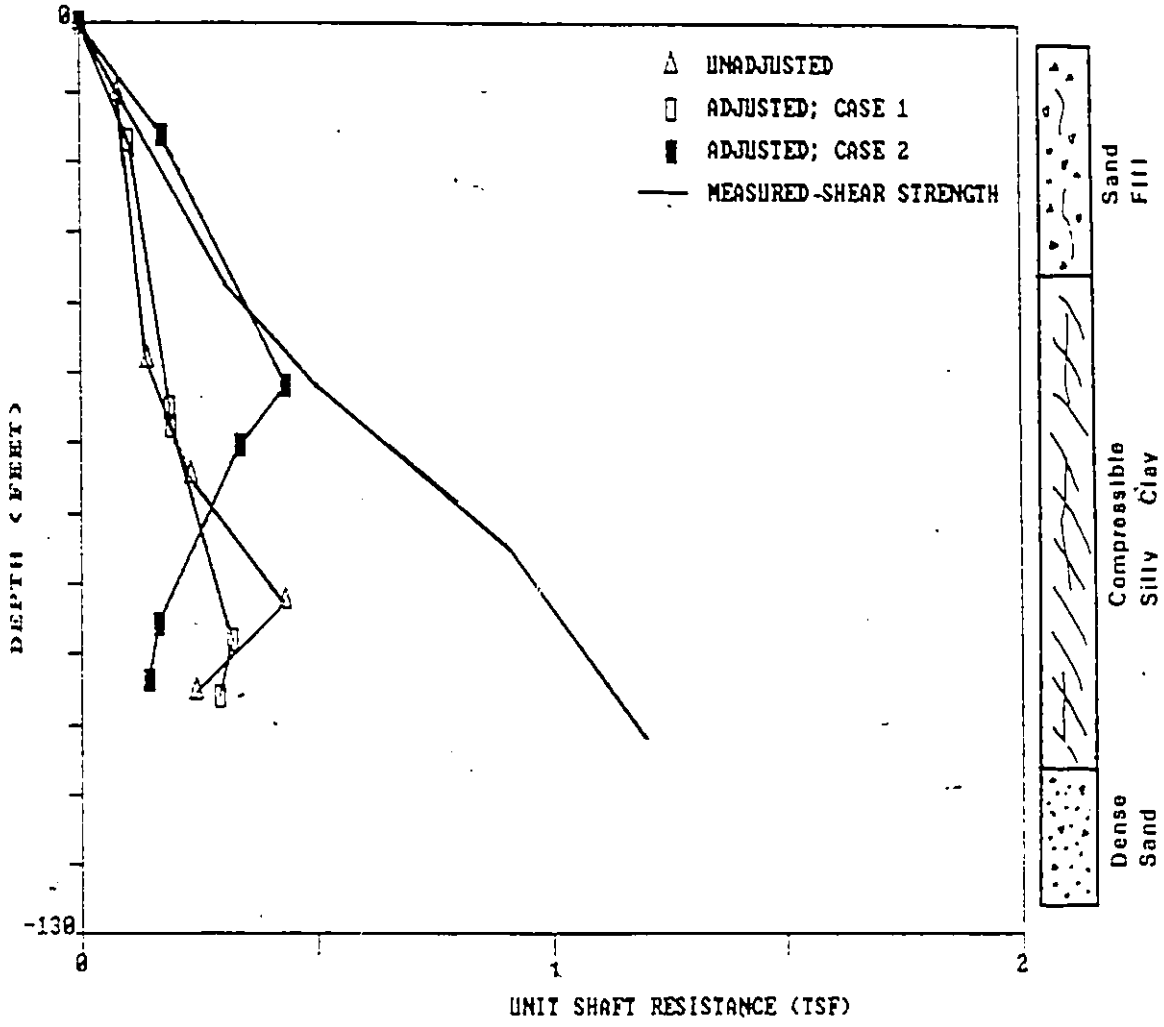

Fig. 5.20 Pile 4; H-Pile; Unit shaft resistance distribution in pull testing.

A P P E N D I C E S

APPENDIX A

Leonards and Lovell Theory

Telltale instrumented steel piles were used by Leonards and Lovell (1978), to analyse the load distribution of driven piles. Leonards and Lovell (1978) formulated that the measured elastic compression of a pile under a head load Q and resisting shaft and toe load R_s and R_t, respectively, is:

$$\Delta_m = C' \frac{QL}{AE} \qquad (1)$$

The pile compression as a free standing column is,

$$\Delta_c = \frac{QL}{AE} \qquad (2)$$

where C' denotes the ratio of the measured compression of the pile to the elastic compression of the pile considered as a free standing column.

Similarly, the elastic compression of the pile due to shaft load R_s is,

$$\Delta_s = C \frac{R_s L}{AE} \qquad (3)$$

The pile compression as a free standing column due to equivalent shaft load R_s is,

$$\Delta_{sm} = \frac{R_s L}{AE} \qquad (4)$$

where C denotes the ratio of the calculated compression of the pile due to a load R_s supported entirely by shaft resistance to the calculated compression if the pile was considered as a free standing column.

Elastic compression due to toe load is,

$$\Delta_t = \frac{R_t L}{AE} \qquad (5)$$

$$\Delta_m = \Delta_t + \Delta_s \qquad (6)$$

for static equlibrium of forces on the pile,

$$Q = R_t + R_s \qquad (7)$$

rearranging and substitution in Eq. 7

$$\frac{AE\Delta_M}{L} = C'Q \qquad (8)$$

$$\Delta_M = C\left(\frac{R_s L}{AE} + \frac{R_t L}{AE}\right) \qquad (9)$$

$$\frac{AE\Delta_M}{L} = C R_s + R_t \qquad (10)$$

$$R_t = (Q - R_s)$$

$$\frac{AE\Delta_M}{L} = C R_s + (Q - R)$$

$$C'Q = C R_s + (Q - R)$$

$$R_s - C R_s = Q - C'Q$$

$$R_s(1 - C) = Q(1 - C')$$

Let

$$R_t = \alpha Q \qquad (11)$$

$$R_s = Q(1 - \alpha)$$

$$\alpha = \frac{C' - C}{1 - C} \qquad (12)$$

$$C = \frac{C' - \alpha}{1 - \alpha} \qquad (13)$$

If the distribution of unit shaft friction is estimated then C may be determined without any knowledge of the shear resistance, or assigning any values to the distribution. The value α is then obtained from Eq. 12, consequently the toe and shaft loads are determined.

The shaft resistance of the pile was fully mobilized, when differentiating

Eq. 8 with respect to Q, then

$$\frac{AE}{L}\frac{d\Delta_m}{dQ} = C' + Q\frac{dC'}{dQ} = n \qquad (14)$$

similarly differentiating Eq.

$$\frac{AE}{L}\frac{d\Delta_m}{dQ} = \frac{dR_t}{dQ} + C\frac{dR_s}{dQ} + R_s\frac{dC}{dQ} = n \qquad (15)$$

n is a constant value when segments of the load deformation curve is linear. For n a constant value and rearranging and integrating Eq. 14, then

$$\frac{dC'}{dQ} = \frac{(n - C)}{Q} \qquad (16)$$

$$C' = \frac{(n - k)}{Q} \qquad (17)$$

For any range of Q over which n is constant a plot of C' versus 1/Q is a straight line with intercept n and slope k.

Similarly for the case when the shaft frictional resistance is fully moblized at a head load $Q = Q_m$ less than the pile failure load such that $Q > Q_m$. then R_s is constant and equal to the fully moblized value.

$$R_s = R_{sm} = K \qquad (18)$$

$$\frac{dR_s}{dQ} = 0 \qquad (19)$$

$$\frac{dR_t}{dQ} = 1 \qquad (20)$$

subsituting in Eq. 15 $\quad n = 1 + R_s\frac{dc}{dQ} \qquad (21)$

from the above equation n anf R_s are constants. The probability is very

low,that when R_s is constant that dC/dQ is constant, hence dC/dQ is taken to be zero. Then n is equal to 1.

A plot of Q versus measured will be parallel to a plot of Q versus (QL/AE) calculated. Then,

$$n = \frac{AE\, d\Delta m}{L\, dQ} \qquad (22)$$

Various values of n represent different stages of moblization of shaft resistance or load transfer. From Eq. 22, when

n > 1 the pile is yielding or buckling or a reduction of shaft resistance after full moblisation has accur.

n < 1 shaft resistance is not fully moblised, but may have reached a maximum constant value

n = 1 shaft resistance is fully moblized.

Using the above criteria, the head load at which the shaft resistance is fully mobilized is approximated.

APPENDIX B

Pile Driving Record

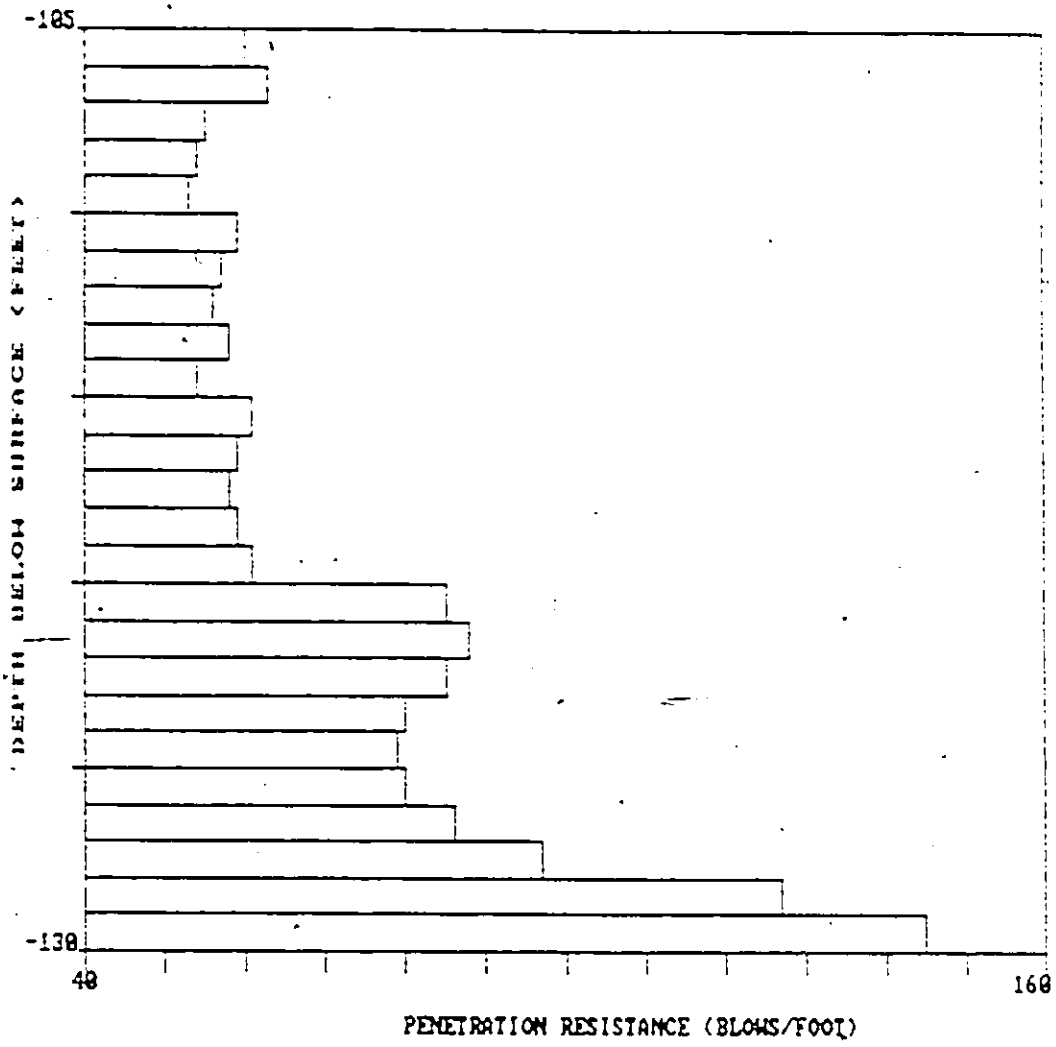

Fig. B3.1 Pile 1; H-pile; Driving diagram

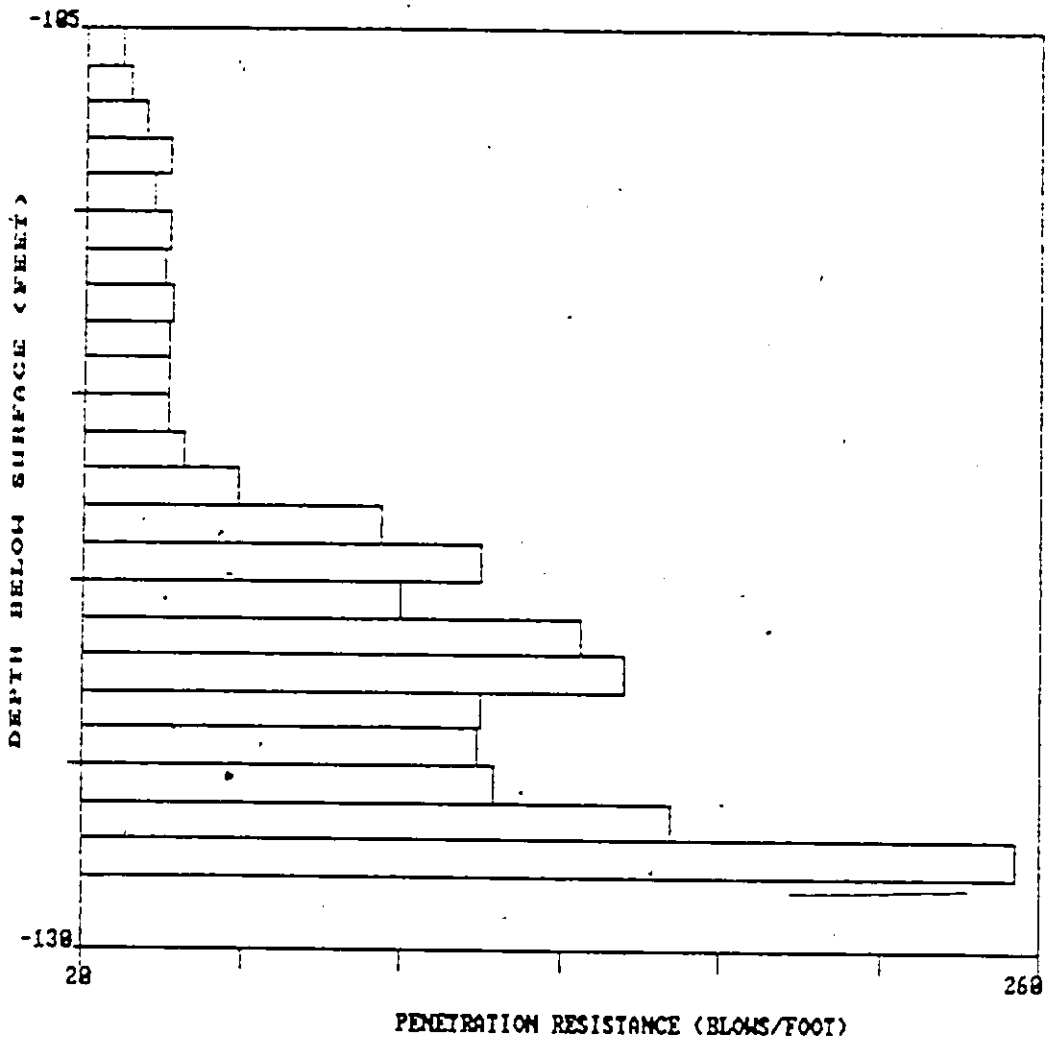

Fig. B3.2 Pile 2; Pipe Pile; Driving diagram

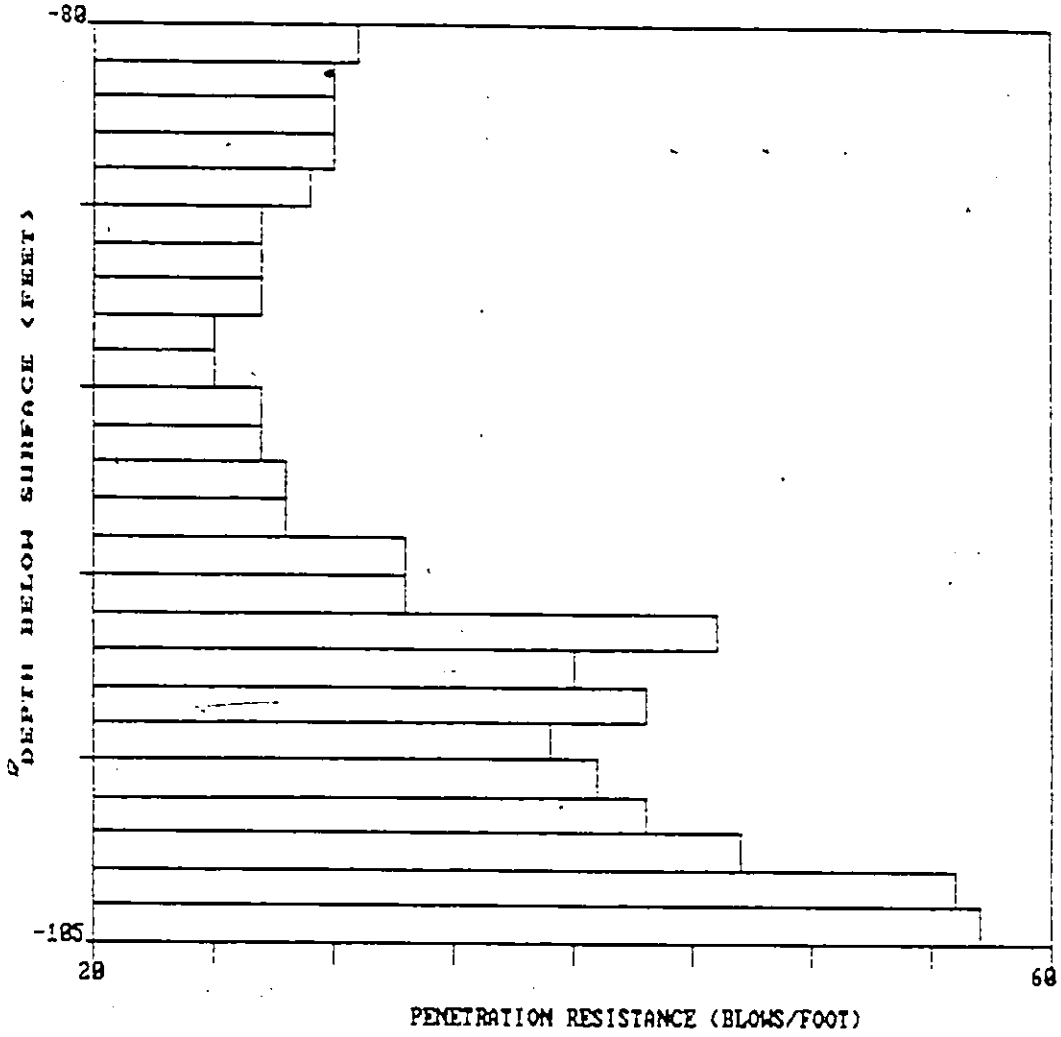

Fig. B3.3 Pile 3; Pipe pile; Driving diagram

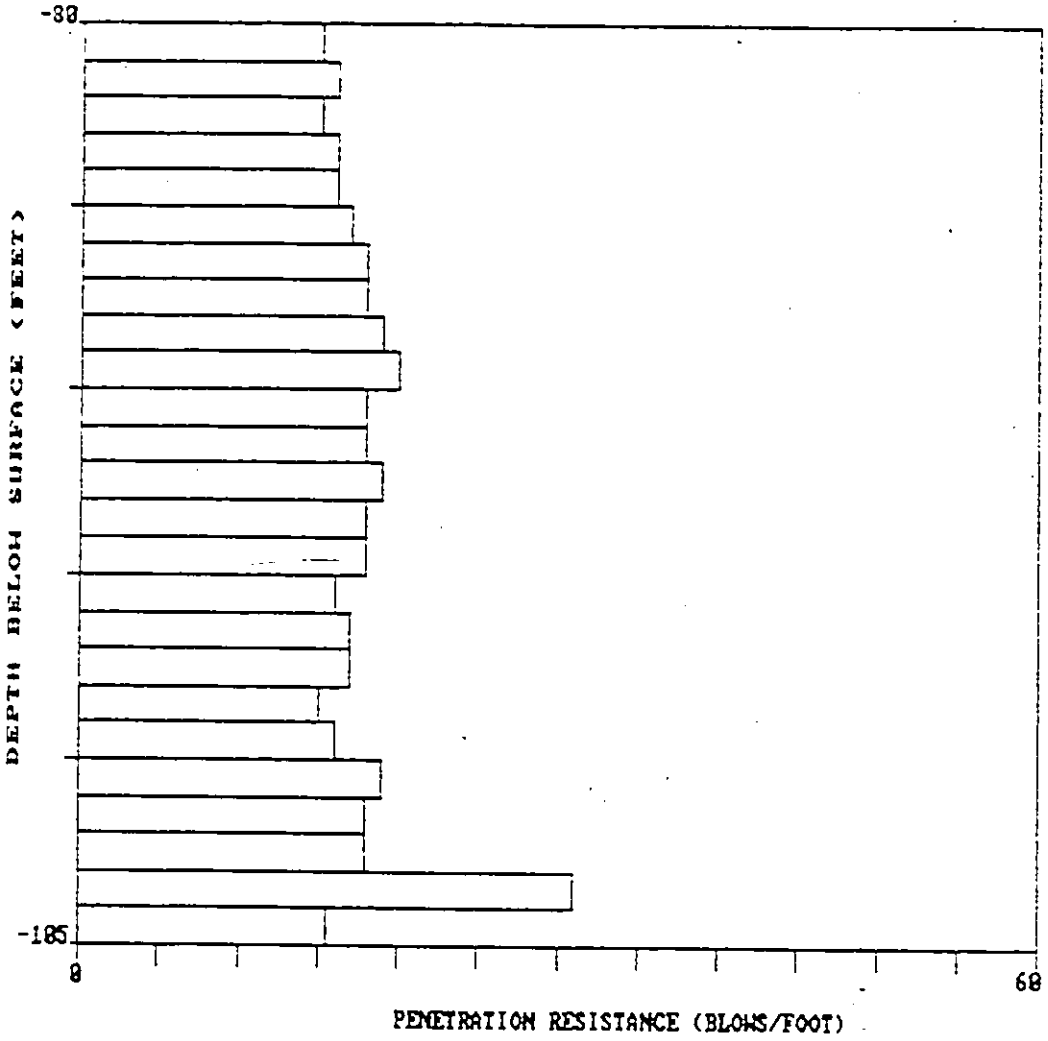

Fig. B 3.4 Pile 4; H-pile; Driving diagram

APPENDIX C

Reduced Static Test Data

FREDRICTON PILE TEST — PULL TEST — TABLE C4.1

PILE NO. 1
H-PILE

REDUCED READINGS

TELLTALE	5E	8H	4D	7G	3C	6F	2B
LENGTH (FEET)	115.8	102.7	89.54	76.42	63.3	50.2	37.08
X - AREA (SQ IN)	26.86	26.86	27.52	27.52	28.19	28.19	28.85

HEAD LOAD (SHORT TONS)	HEAD MOVEMENT	COMPRESSION (1/10000 INCH)						
0	0	0	0	0	0	0	0	0
53	1850	1546	1124	1290	1152	968	774	631
65	2250	1889	1355	1565	1391	1168	934	758
76	2650	2200	1564	1792	1604	1348	1079	873
87	3070	2540	1794	2095	1838	1548	1234	998
97	3560	2928	2055	2400	2103	1771	1413	1139
108	4010	3246	2269	2651	2323	1955	1560	1255
118	4430	3573	2494	2914	2550	2149	1715	1376
130	5000	3922	2732	3192	2765	2357	1880	1507
140	5350	4224	2911	3382	2990	2526	2033	1628
151	5820	4547	3134	3641	3214	2713	2185	1746
163	6360	4927	3395	3944	3480	2937	2365	1893
177	7000	5325	3667	4272	3755	3175	2553	2044
189	7630	5680	3917	4557	4009	3392	2728	2182
200	8370	6038	4173	4849	4264	3614	2909	2328
211	9420	6388	4430	5148	4527	3847	3096	2482
222	10890	6711	4687	5428	4776	4070	3230	2598
235	12740	7053	4951	5726	5048	4307	3407	2757
246	14900	7385	5210	6016	5313	4537	3616	2913
261	17570	7721	5490	6339	5595	4789	3817	3079
272	20350	7757	5753	6635	5863	5018	4008	3232
284	23800	----	6059	6957	6103	5274	4202	3396
295	27400	----	6343	7285	6439	5523	4419	3557
310	31100	----	6621	7610	6721	5771	4617	3715
320	36500	----	6919	7899	7023	6001	4834	3866
326	44100	----	7210	----	7321	6274	5040	4046
347	65800	----	7511	----	7618	6544	5268	4111
249	65200	----	6279	7134	6293	5361	4208	3323
129	62800	----	4256	5009	4263	3545	2687	2078
72	61200	----	3171	3852	3184	2604	1905	1373
0	58600	----	----	1980	1570	1223	803	564

FREDRICTON PILE TEST — PUSH TEST — TABLE C4.2

PILE NO.1
H-PILE

REDUCED READINGS

TELLTALE		5E	8H	4D	7G	3C	6F	2B
LENGTH (FEET)		115.8	102.7	89.54	76.42	63.3	50.2	37.08
X - AREA (SQ. IN)		26.86	26.86	27.52	27.52	28.19	28.19	28.85
HEAD LOAD (SHORT TONS)	HEAD MOVEMENT	COMPRESSION (1/10000 INCH)						
0	0	0	0	0	0	0	0	0
22	440	451	436	430	449	429	403	370
45	730	715	689	685	702	670	624	560
56	860	844	812	812	826	785	732	651
67	1030	996	953	954	970	918	853	753
79	1180	1169	1112	1122	1128	1066	983	863
90	1330	1341	1269	1280	1287	1208	1210	970
101	1520	1508	1418	1442	1436	1350	1237	1072
112	1770	1668	1577	1613	1579	1497	1368	1178
124	1910	1872	1740	1783	1780	1647	1495	1284
135	2150	2087	1923	1987	1949	1816	1639	1403
146	2370	2319	2114	2194	2145	1986	1790	1525
157	2660	2571	1831	2434	2362	2181	1952	1656
168	2900	2830	2541	2567	2579	2375	2114	1789
180	3190	3180	2745	2898	2883	2556	2268	1912
191	3480	3341	2955	3140	2994	2746	2427	2037
202	3780	3724	3179	3389	3224	2945	2598	2171
214	4090	3986	3382	3621	3435	3128	2755	2295
225	4430	4171	3600	3875	3654	3324	2916	2423
236	4900	4503	3848	4160	3907	3545	3098	2571
247	5360	4816	4077	4434	4137	3745	3267	2695
258	5860	5112	4286	4686	4352	3935	3413	2811
		32 HOURS MAINTAINED LOAD						
258	6500	5402	4469	4908	4519	4061	3503	2869
270	6690	5565	4603	5033	4676	4203	3633	2983
280	6940	5812	4797	5259	4874	4379	3782	3101
292	7310	6112	5014	5513	5094	4567	3937	3222
304	7830	6482	5370	5815	5349	4788	4114	3360

continued

continued

FREDRICTON PILE TEST — PUSH TEST — TABLE C4.2

PILE NO.1
H-PILE

REDUCED READINGS

TELLTALE		5E	8H	4D	7G	3C	6F	2B
LENGTH (FEET)		115.8	102.7	89.54	76.42	63.3	50.2	37.08
X - AREA (SQ. IN)		26.86	26.86	27.52	27.52	28.19	28.19	28.85
HEAD LOAD. (SHORT TONS)	HEAD MOVEMENT	COMPRESSION (1/10000 INCH)						
314	8470	6893	5555	6151	5644	5038	4320	3519
326	9060	7267	5803	6447	5899	5257	4498	3658
337	9670	7641	6058	6744	6164	5482	4681	3801
348	10360	8017	6311	7055	6416	5701	4859	3936
360	11040	8429	6589	7365	6709	5944	5060	4095
370	11710	8800	6855	7681	6980	6175	5242	4234
382	12400	9168	7103	7978	7230	6385	5416	4362
393	13940	9561	7366	8393	7499	6615	5600	4508
404	14760	9555	7535	8615	7776	6854	5793	4656
416	15600	10338	7893	8922	8040	7078	5974	4800
427	16430	10772	8155	9260	8342	7333	6184	4969
438	17350	11168	8455	9557	8621	7571	6381	5127
450	18320	11589	8742	9892	8913	7820	6585	5287
461	19480	12028	9041	10248	9219	8084	6794	5451
472	18750	12610	9460	10727	9644	8445	7078	5641
427	18850	12055	9022	10285	9133	7957	6627	5213
370	17770	11074	8107	9281	8199	7114	5886	4597
314	16100	9492	6971	8002	7055	6114	5081	3960
281	15400	8843	6396	7344	6449	5584	4633	3600
225	13720	7106	5234	5981	5259	4572	3802	2943
169	11910	5464	4012	4651	4115	3611	3007	2333
112	10000	3737	2970	3264	2947	2599	2203	1687
56	8060	2058	1824	1892	1781	1607	1495	1074
0	5230	-400	182	-61	82	177	237	191

FREDRICTON PILE TEST — PULL TEST — TABLE C4.3

PILE NO. 2
PIPE PILE

REDUCED READINGS

TELLTALE	1A	5E	8H	4D	3C	6F	2B
LENGTH (FEET)	127.9	117.8	102.7	89.56	63.8	50.2	37.1
X - AREA (SQ IN)	26.86	26.86	26.86	27.52	28.19	28.19	28.85

HEAD LOAD (SHORT TONS)	HEAD MOVEMENT	COMPRESSION (1/10000 INCH)						
0	0	0	0	0	0	0	0	0
53	2470	2340	2128	2320	1957	1484	1378	1115
61	3110	2809	2558	2725	2335	1867	1607	1297
72	3640	3438	3119	3299	2826	2230	1905	1539
83	4370	4106	3699	3886	3330	2599	2204	1779
93	5060	4742	4270	4456	3819	2954	2493	2012
103	5870	5500	4923	5101	4377	3361	2821	2277
113	6520	6109	5510	5683	4850	3705	3044	2497
123	7240	6717	6096	6168	5376	4042	3345	2707
134	8070	7546	6743	6913	5923	4449	3686	2980
145	8840	8271	7363	7519	6449	4831	3997	3230
158	9890	9266	8233	8398	7085	5316	4470	3614
170	10740	9979	8844	9004	7887	5808	4796	3881
182	11690	10894	9573	9721	8415	6281	5216	4216
194	12610	11710	10289	10436	9031	6758	5617	4548
206	13600	12573	11008	11158	9665	7242	6026	4886
216	14480	13310	11643	11833	10231	7666	6382	5158
229	15600	14229	12440	12625	10877	8170	6845	5544
244	16910	15286	13374	13546	11706	8816	7399	6007
255	18140	16104	14126	14302	12369	9334	7835	6367
268	19760	17049	14991	15174	13145	9947	8345	6797
282	22670	18009	15860	16076	13961	10575	8911	7296
295	27769	18804	16624	16866	14663	11151	9425	7728
207	27740	18432	16229	16514	14262	10921	9131	7538
147	25540	----	11501	14164	12047	8819	7137	5575
87	24000	----	9902	12473	10474	9904	5823	4571
0	16480	----	9082	11565	9850	7254	3564	2850

FREDRICTON PILE TEST — PUSH TEST — TABLE C4.4

PILE NO. 2
PIPE PILE

	REDUCED READINGS						
TELLTALE	1A	5E	8H	4D	3C	6F	2B
LENGTH (FEET)	127.9	117.4	102.7	89.56	63.83	50.2	37.08
X - AREA (SQ IN)	12.86	12.86	13.52	13.52	14.19	14.85	14.85

HEAD LOAD (SHORT TONS)	HEAD MOVEMENT	COMPRESSION (1/10000 INCH)						
0	0	0	0	0	0	0	0	0
28	600	735	573	636	560	572	564	659
56	1010	1034	986	1040	962	957	949	894
67	1210	1206	1165	1214	1135	1119	1113	1033
79	1430	1410	1375	1428	1344	1313	1307	1196
90	1610	1585	1555	1609	1520	1476	1468	1331
101	1800	1783	1755	1807	1712	1656	1645	1481
112	1990	1975	1952	1996	1904	1832	1814	1622
124	2200	2178	2163	2203	2110	2020	1990	1772
135	2410	2359	2347	2389	2290	2183	2145	1897
146	2620	2575	2567	2590	2500	2372	2329	2044
157	2850	2817	2804	2845	2737	2584	2525	2208
169	3100	3044	3041	3066	2956	2796	2704	2353
180	3330	3263	3258	3283	3164	2957	2870	2489
191	3540	3486	3479	3500	3376	3140	3041	2622
202	3790	3717	3715	3731	3596	3337	3226	2770
214	4030	3929	3925	3935	3797	3509	3377	2891
225	4280	4184	4173	4179	4034	3709	3559	3036
236	4540	4453	4437	4441	4284	3918	3745	3189
247	4700	4729	4700	4697	4530	4122	3925	3435
259	5360	5356	5226	5240	5033	4534	4214	3615
270	5550	5520	5389	5418	5190	4674	4366	3723
281	5800	5745	5614	5620	5404	4851	4494	3843
292	6100	6007	5866	5874	5643	5047	4665	3984
304	6410	6315	6148	6144	5904	5259	4854	4137

continued ....

CONTINUED

FREDRICTON PILE TEST — PUSH TEST — TABLE C4.4

PILE NO. 2
PIPE PILE

REDUCED READINGS

TELLTALE		1A	5E	8H	4D	3C	6F	2B
LENGTH (FEET)		127.9	117.4	102.7	89.56	63.83	50.2	37.08
X - AREA (SQ IN)		12.86	12.86	13.52	13.52	14.19	14.85	14.85
HEAD LOAD (SHORT TONS)	HEAD MOVEMENT	COMPRESSION (1/10000 INCH)						
315	6790	6668	6474	6463	6203	5503	5073	4315
326	7220	7027	6898	6781	6500	5744	5292	4485
337	7670	7389	7210	7106	6803	5991	5514	4680
349	8180	7808	7515	7476	7153	6266	5777	4901
360	8700	8262	7925	7882	7530	6599	6099	5154
371	9320	8784	8405	8352	7976	6984	6453	5469
382	10140	9454	9027	8959	8562	7507	6949	5930
394	11080	10261	9895	9690	9303	8209	7605	6539
405	12560	11519	11059	10938	10500	9338	8734	7585
416	15330	14003	13578	13418	12947	11705	11091	9847
427	18090	16683	-----	16170	15671	14366	14366	12289
360	17580	14187	-----	12537	13149	11884	9751	9821
304	16870	13018	11741	11362	11961	10814	8734	8891
250	-----	12726	11476	11085	9854	10569	8488	8608
225	15690	11703	10412	10081	8819	9655	7631	7877
169	13880	10179	8911	8579	7403	8442	6497	6905
112	12150	8736	7334	7050	5947	7190	5333	5916
56	10290	6987	5617	5381	5362	5835	4045	4883
0	6980	6447	5322	5041	4172	3446	2038	3062

FREDRICTON PILE TEST — PULL TEST — TABLE C4.5

PILE NO. 3
PIPE PILE

REDUCED READINGS

TELLTALE	1A	5E	8H	4D	7G	3C	6F	2B
LENGTH (FEET)	104.9	96.1	86.2	76.4	66.2	56.9	46.5	37.2
X - AREA (SQ IN)	12.86	12.86	12.86	13.52	14.19	14.19	14.19	14.85

HEAD LOAD (SHORT TONS)	HEAD MOVEMENT	COMPRESSIONS (1/10000 INCH)							
0	0	0	0	0	0	0	0	0	0
30	1020	927	857	930	801	822	699	643	574
53	2140	2038	1919	1952	1732	1637	1428	1228	1076
61	2530	2426	2293	2301	2052	1919	1684	1431	1252
72	3060	2910	2748	2732	2457	2270	2003	1682	1475
83	3660	3424	3232	3205	2860	2648	2342	1961	1711
93	4250	3903	3791	3627	3251	2956	2612	2204	1924
103	4890	4431	4192	4101	3686	3333	2957	2478	2162
113	5470	4880	4629	4509	4060	3660	3255	2717	2319
123	6110	5355	5056	4911	4427	3978	3546	2947	2572
134	6940	5906	5610	5550	4886	4379	3914	3241	2807
145	7900	6487	6157	5974	5390	4799	4195	3549	3083
158	9300	7201	6827	6604	5963	5309	4763	3931	3428
170	11040	7804	7388	7125	6457	5745	5173	4267	3735
122	14860	6860	6429	6279	5666	5060	4521	3726	3213
65	12400	5948	5458	5250	4639	4137	3587	2727	2388
0	9810	3176	2889	2742	2329	1898	1560	1072	792

FREDRICTON PILE TEST — PUSH TEST — TABLE C4.5

PILE NO. 3
PIPE PILE

REDUCED READINGS

TELLTALE	1A	5E	8H	4D	7G	3C	6F	2B
LENGTH (FEET)	104.7	96.1	86.2	76.4	66.2	56.9	46.5	37.2
X - AREA (SQ IN.)	12.86	12.86	12.86	13.52	13.52	14.19	14.19	14.85

HEAD LOAD (SHORT TONS)	HEAD MOVEMENT	COMPRESSION (1/10000 INCH)							
0	0	0	0	0	0	0	0	0	0
50	830	847	847	855	831	850	807	800	746
63	1190	1205	1216	1217	1195	1204	1156	1131	1051
71	1360	1379	1397	1397	1374	1378	1321	1289	1194
79	1540	1580	1616	1596	1570	1572	1507	1463	1351
89	1790	1820	1834	1840	1804	1803	1726	1667	1534
100	2047	2205	2218	2222	2193	2177	2095	1991	1816
110	2610	2327	2374	2358	2333	2328	2213	2143	1913
122	2810	2518	2570	2546	2525	2511	2390	2307	2161
133	3140	2810	2864	2832	2808	2776	2644	2537	2427
147	3720	3191	3210	3211	3180	3149	3023	2866	2578
156	3960	3396	3419	3414	3382	3340	3203	3032	2724
167	4330	3703	3727	3713	3667	3611	3454	3263	2922
178	4830	4043	4021	4042	3986	3912	3741	3525	3146
190	5520	4411	4426	4386	4334	4237	4059	4013	3404
210	6350	4761	4785	4743	4684	4581	4386	4122	3680
212	7520	5147	5260	5111	5063	4944	4753	4466	3992
223	9060	5509	5579	5467	5423	5301	5111	4809	4307
234	11370	5880	5993	5842	5792	5677	5481	5170	4637
246	16820	6283	6411	6277	6198	6101	5871	5544	4970
151	15350	4584	4563	4586	4492	4491	4329	4076	3620
103	14150	3346	3216	3366	3282	3338	3220	3048	2718
55	12690	1952	1916	1981	1992	2064	2029	1967	1821
19	1063	56	-42	43	206	364	492	637	717
0	0	-15	-46	-23	150	312	445	599	687

FREDRICTON PILE TEST — PULL TEST — TABLE C4.7

PILE NO. 4
H-PILE

REDUCED READINGS

TELLTALE		1A	5E	8H	4D	3C	6F	2B
LENGTH (FEET)		104.9	96.07	86.22	76.38	56.71	46.71	37.07
X - AREA (SQ IN)		26.86	26.86	27.52	27.52	28.19	28.85	28.85
HEAD LOAD (SHORT TONS)	HEAD MOVEMENT	COMPRESSION (1/10000 INCH)						
0	0	0	0	0	0	0	0	0
29	890	799	775	728	691	531	428	363
53	1530	1334	1279	1206	1119	863	696	590
61	1800	1537	1468	1388	1286	994	801	681
72	2700	1777	1593	1600	1484	1148	927	784
83	2940	2028	1930	1824	1690	1303	1055	892
94	3130	2291	2178	2060	1909	1477	1195	1010
104	3720	2535	2408	2275	2108	1631	1319	1113
114	4320	2765	2632	2493	2298	1779	1439	1213
125	5030	2990	2847	2698	2489	1929	1560	1315
136	8370	3208	3027	2871	2664	2087	1685	1436
148	14450	3387	3218	3079	2851	2276	1863	1578
106	13890	2831	2684	2553	2344	1815	1445	1202
53	12960	1998	1881	1762	1581	1150	864	693
0	11380	772	705	635	524	293	139	82

FREDRICTON PILE TEST — PUSH TEST — TABLE C4.8

PILE NO. 4
H-PILE

REDUCED READINGS

TELLTALE		1A	5E	8H	4D	3C	6F	2B
LENGTH (FEET)		104.9	96.07	86.22	76.38	56.71	46.91	37.07
X - AREA (SQ IN)		26.86	26.86	26.86	27.52	28.19	28.19	28.85
HEAD LOAD (SHORT TONS)	HEAD MOVEMENT	COMPRESSION (1/10000 INCH)						
0	0	0	0	0	0	0	0	0
17	280	262	206	268	234	232	225	209
34	560	519	446	519	480	455	432	392
56	820	763	688	757	715	673	630	567
67	980	892	812	883	842	792	739	661
79	1160	1050	1073	1039	995	933	864	771
90	1390	1202	1121	1190	1148	1075	992	881
101	1630	1355	1289	1345	1294	1212	1114	987
112	1930	1522	1457	1508	1459	1364	1251	1106
124	2290	1702	1633	1680	1633	1524	1394	1231
135	2750	1858	1801	1839	1784	1663	1518	1338
146	3310	2020	1975	1898	1943	1807	1645	1448
157	4050	2202	2159	2180	2126	1975	1796	1578
168	4960	2372	2325	2346	2293	2133	1935	1682
180	6140	2519	2468	2489	2438	2271	2061	1806
191	7760	2673	2614	2637	2693	2423	2200	1926
202	10140	2834	2782	2807	2747	2489	2347	2038
214	14160	2986	2922	2944	2894	2718	2460	2148
224	18570	3174	3098	3137	3082	2880	2605	2273
168	18090	2475	2438	2463	2425	2282	2060	1751
112	17240	1623	1604	1634	1629	1590	1446	1260
56	16110	653	617	698	729	844	805	730
0	14230	-807	-673	-689	-583	-85	-9	9

APPENDIX D

Failure Load Analysis

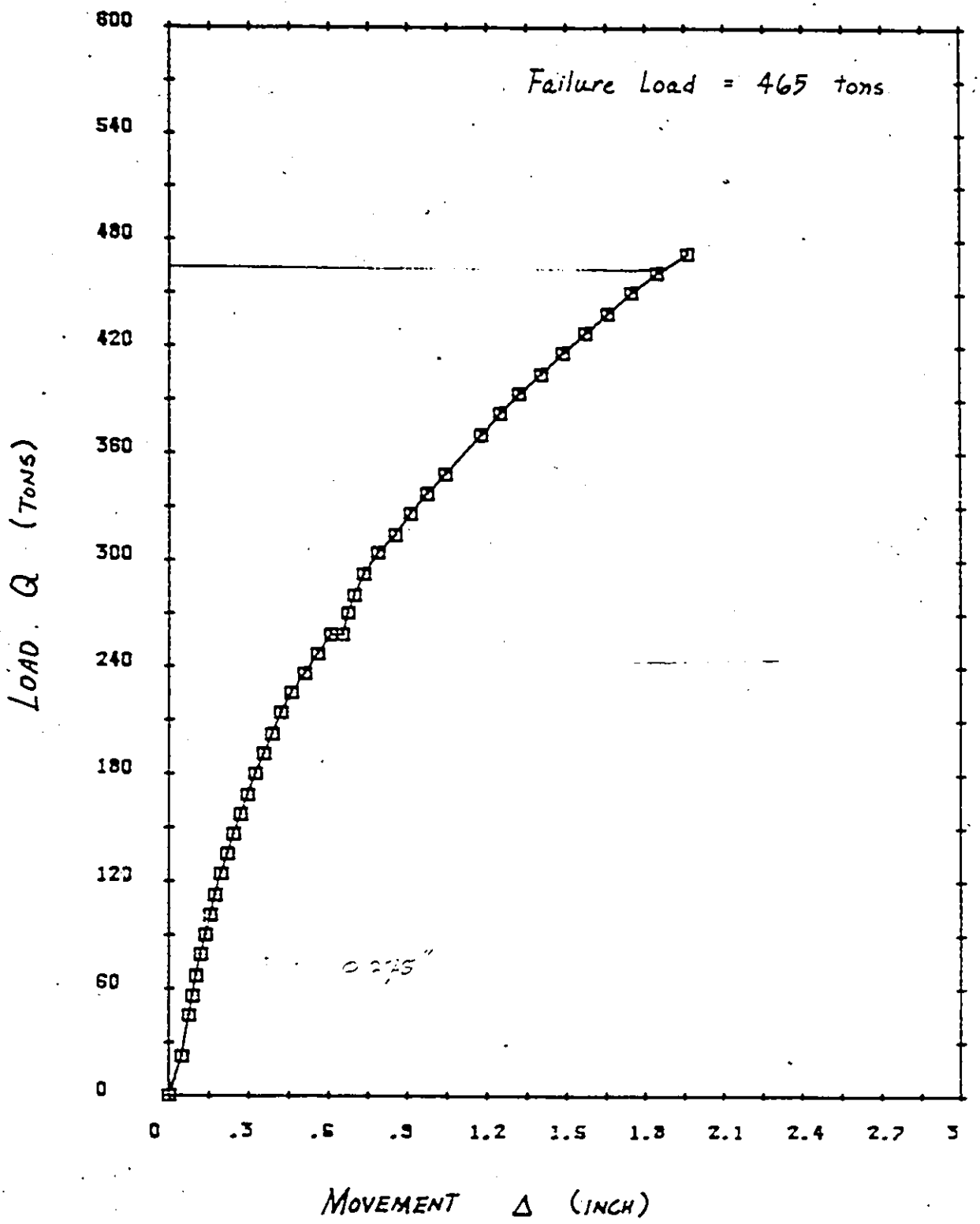

FIG D4.1 PILE 1 ; PUSH TEST ; DAVISSON OFFSET CRITERION

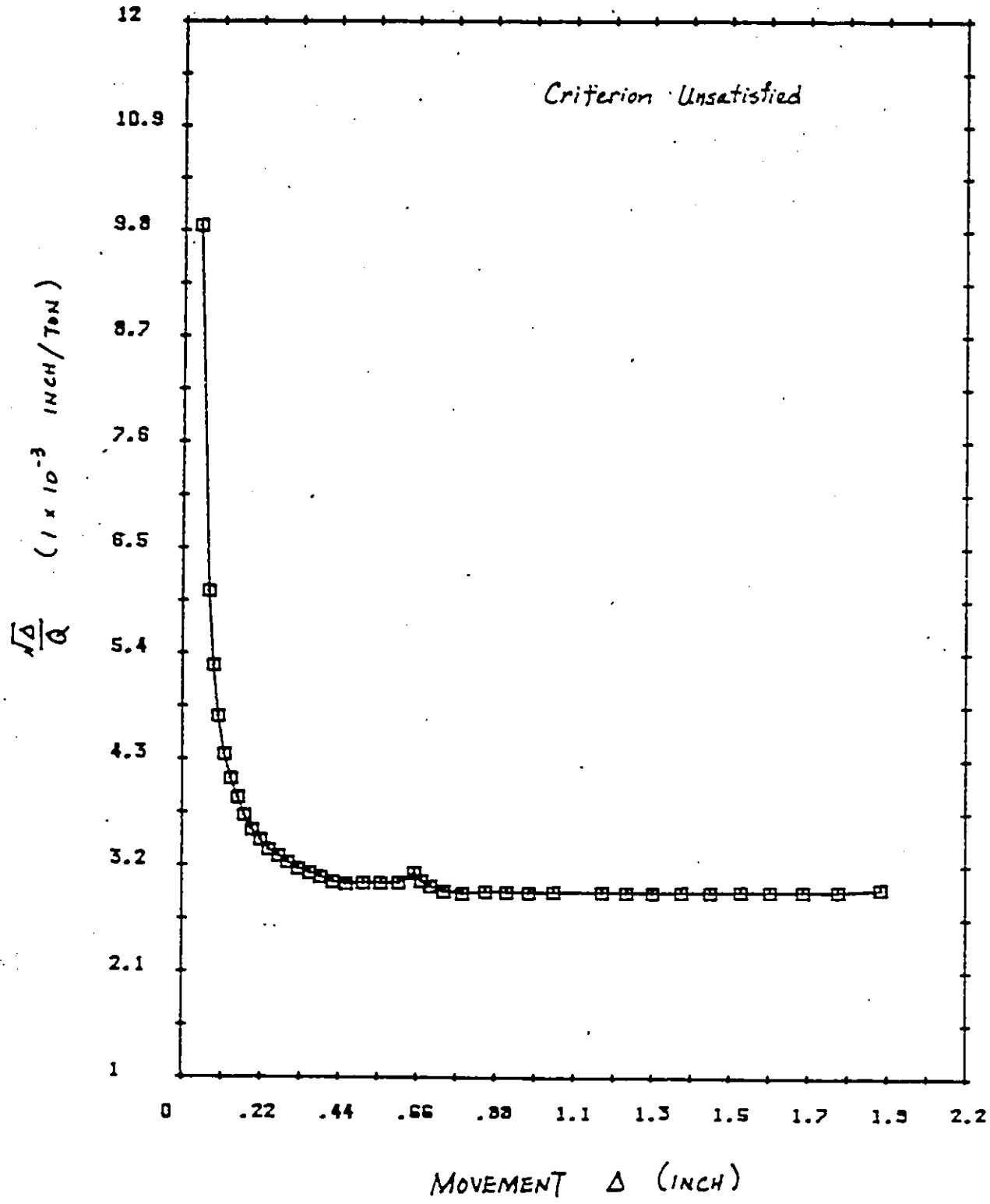

FIG. 24.2 PILE 1; PUSH TEST; BRINCH HANSEN 80% CRITERION

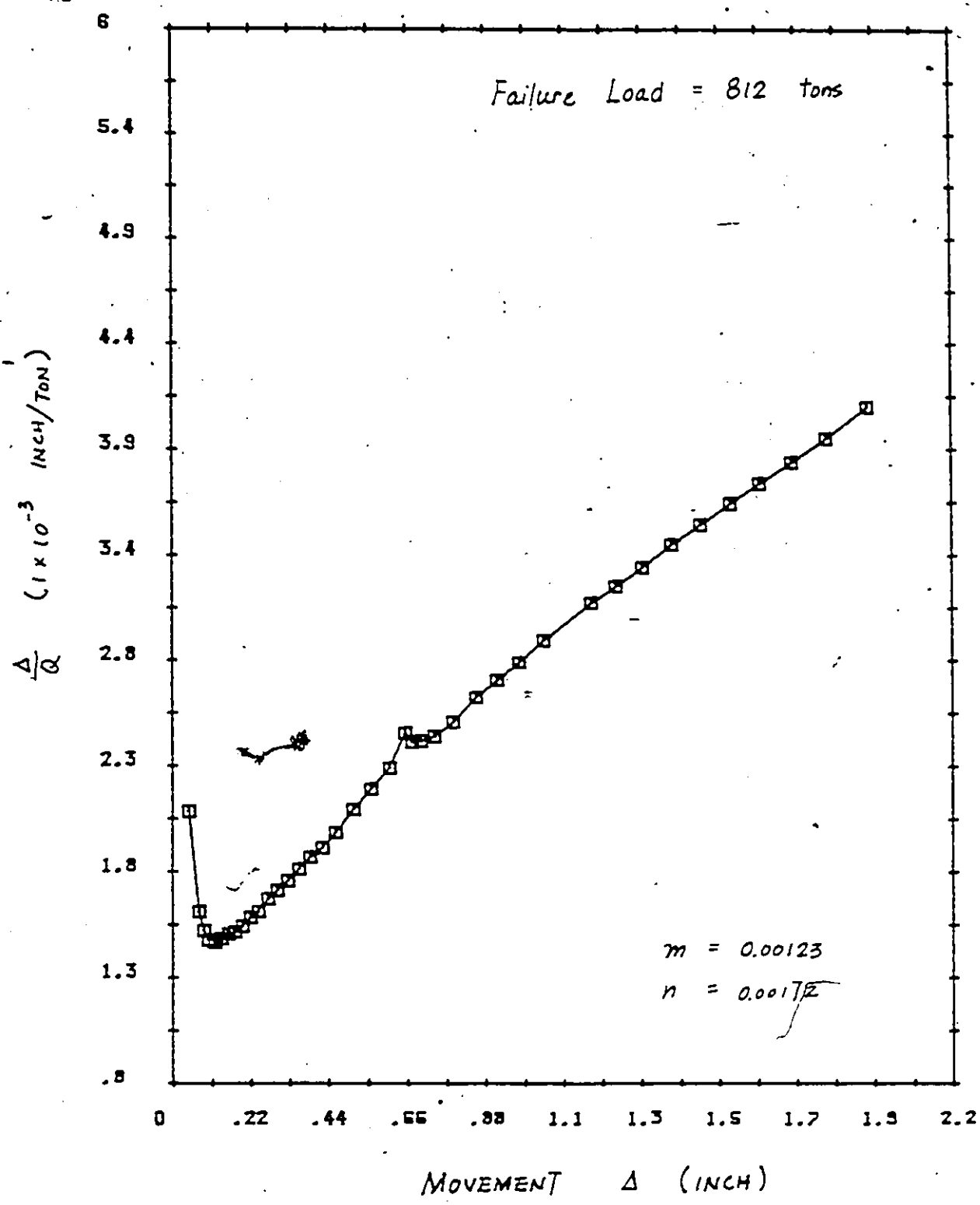

FIG. D4.3 PILE 1; PUSH TEST; CHIN CRITERION

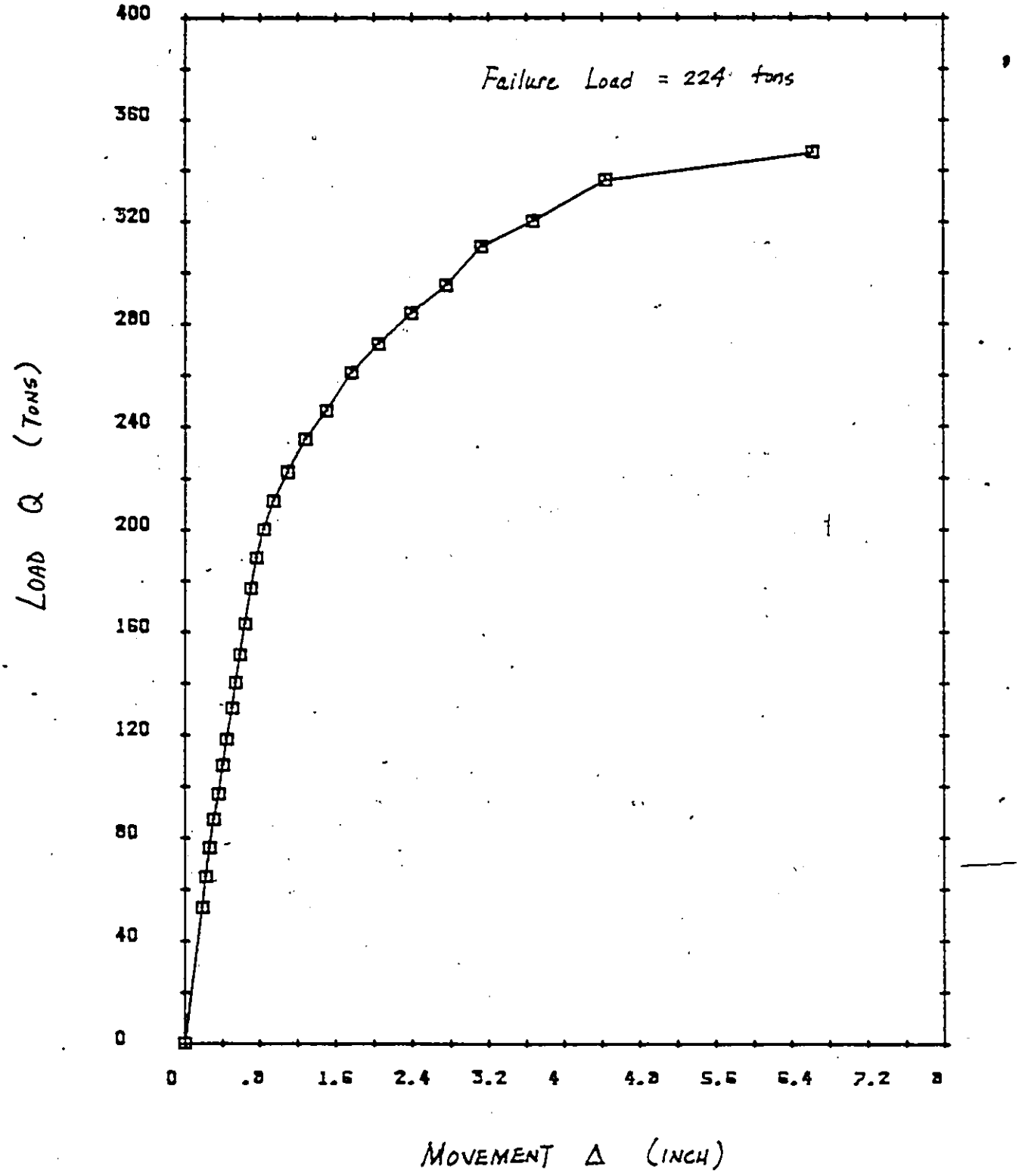

FIG. D.44 PILE 1; PULL TEST; DAVISSON OFFSET CRITERION

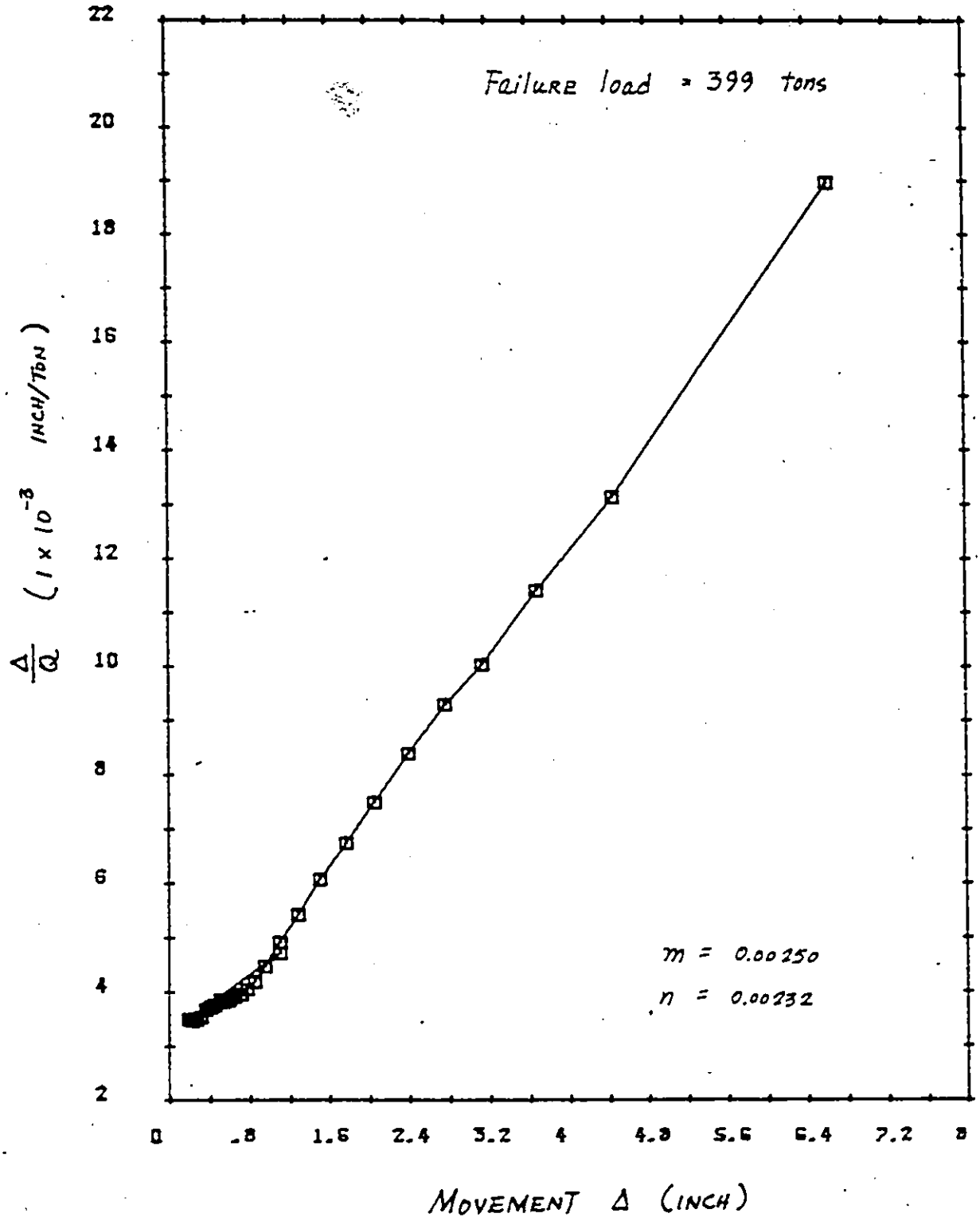

FIG D-4-5 PILE 1 ; PULL TEST ; CHIN CRITERION

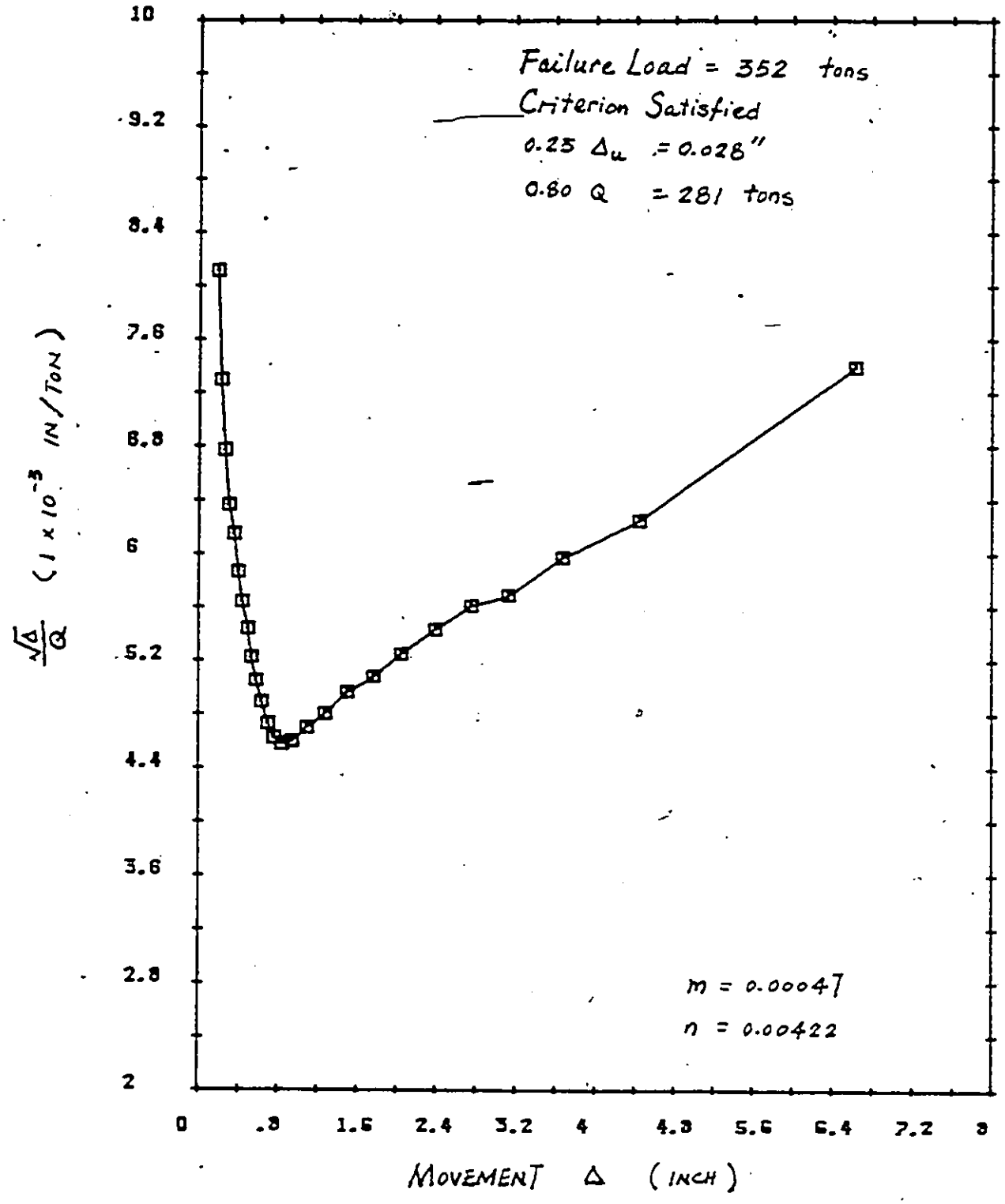

FIG. 24.6 PILE 1; PULL TEST; BRINCH HANSEN 80% CRITERION

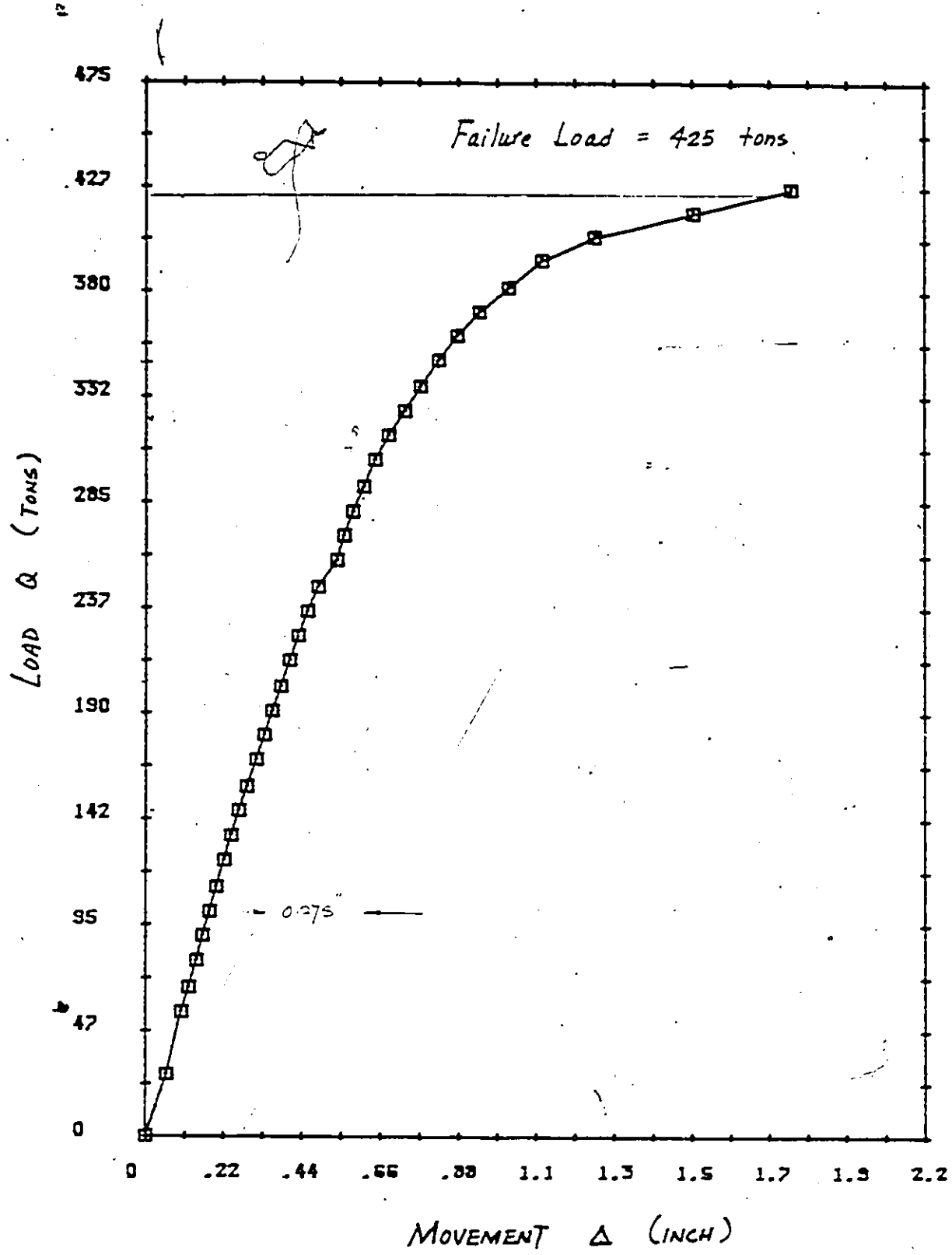

FIG 47 PILE 2; PUSH TEST; DAVISSON CRITERION

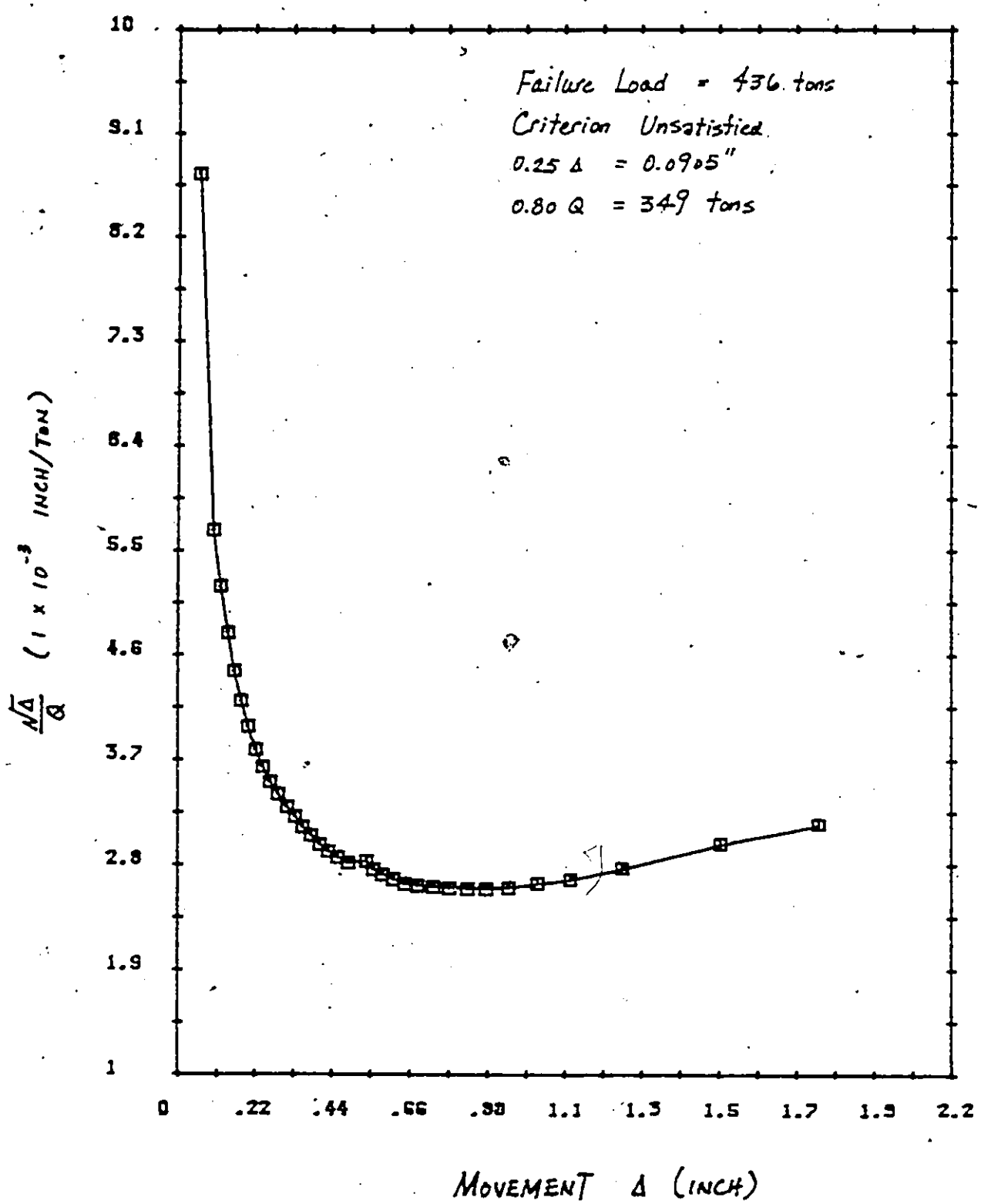

FIG D 4.8 PILE 2; PUSH TEST; BRINCH HANSEN 80% CRITERION

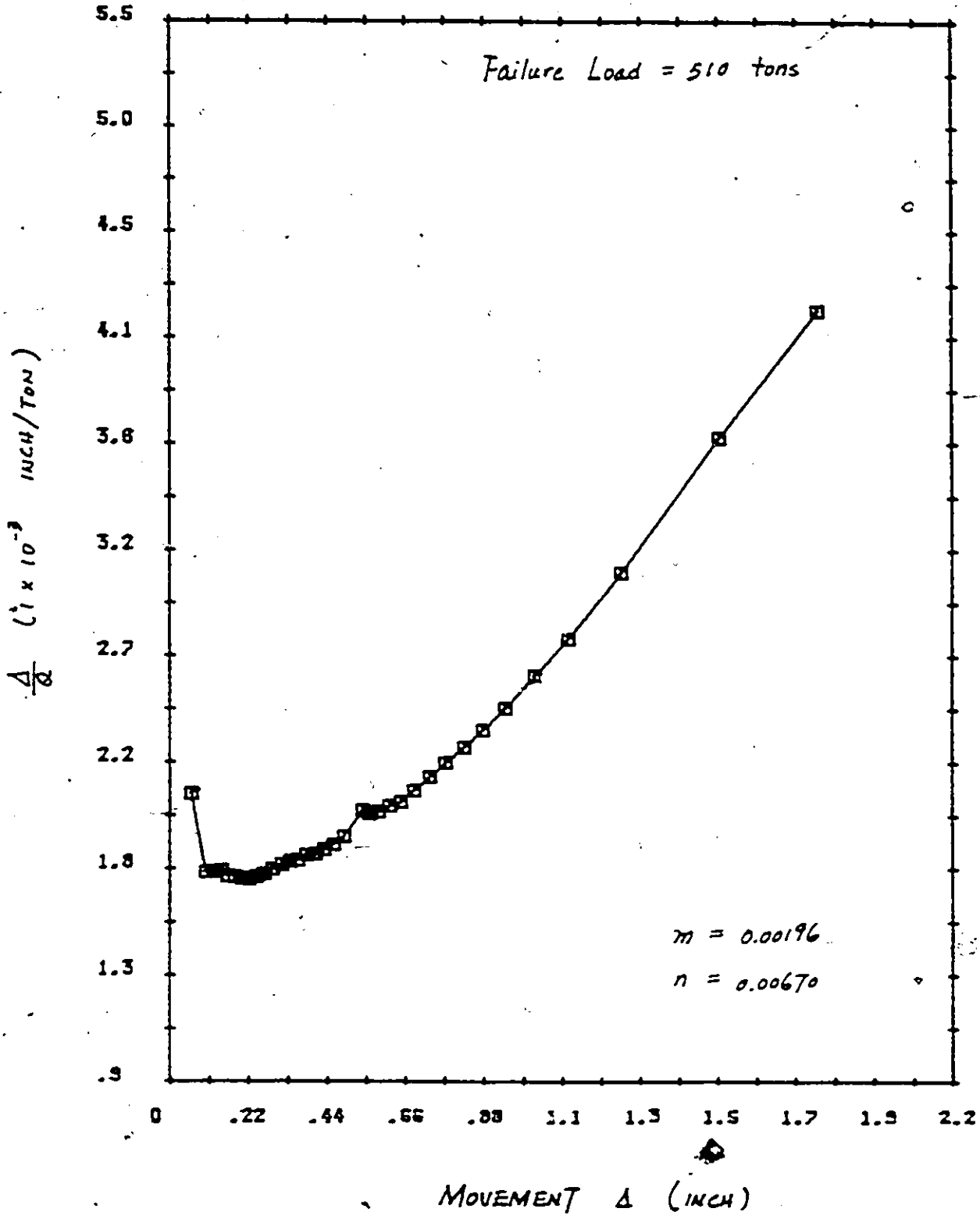

FIG 2.4.9 PILE 2 ; PUSH TEST ; CHIN CRITERION

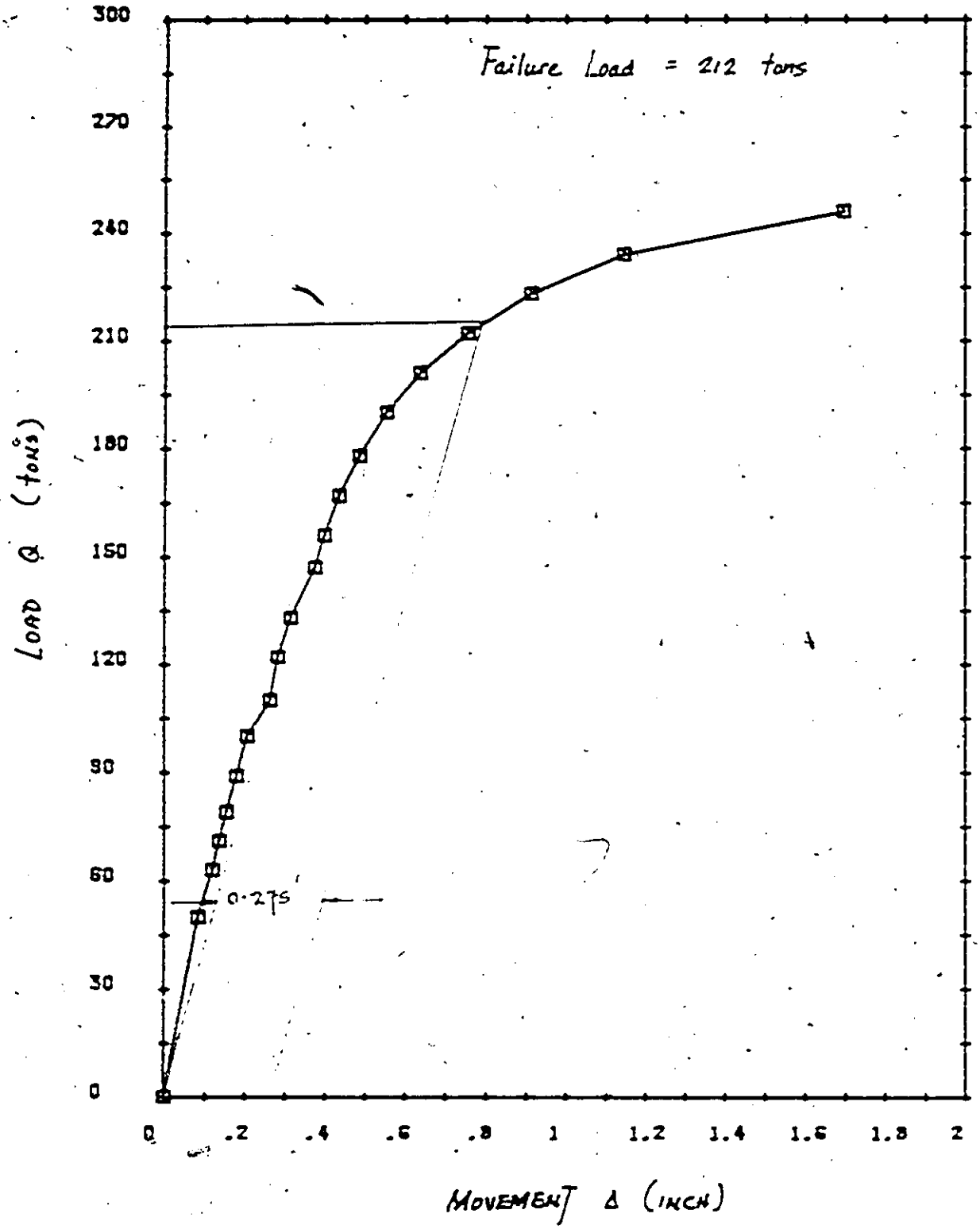

FIG. D4-10 PILE 3; PUSH TEST; DAVISSON OFFSET CRITERION

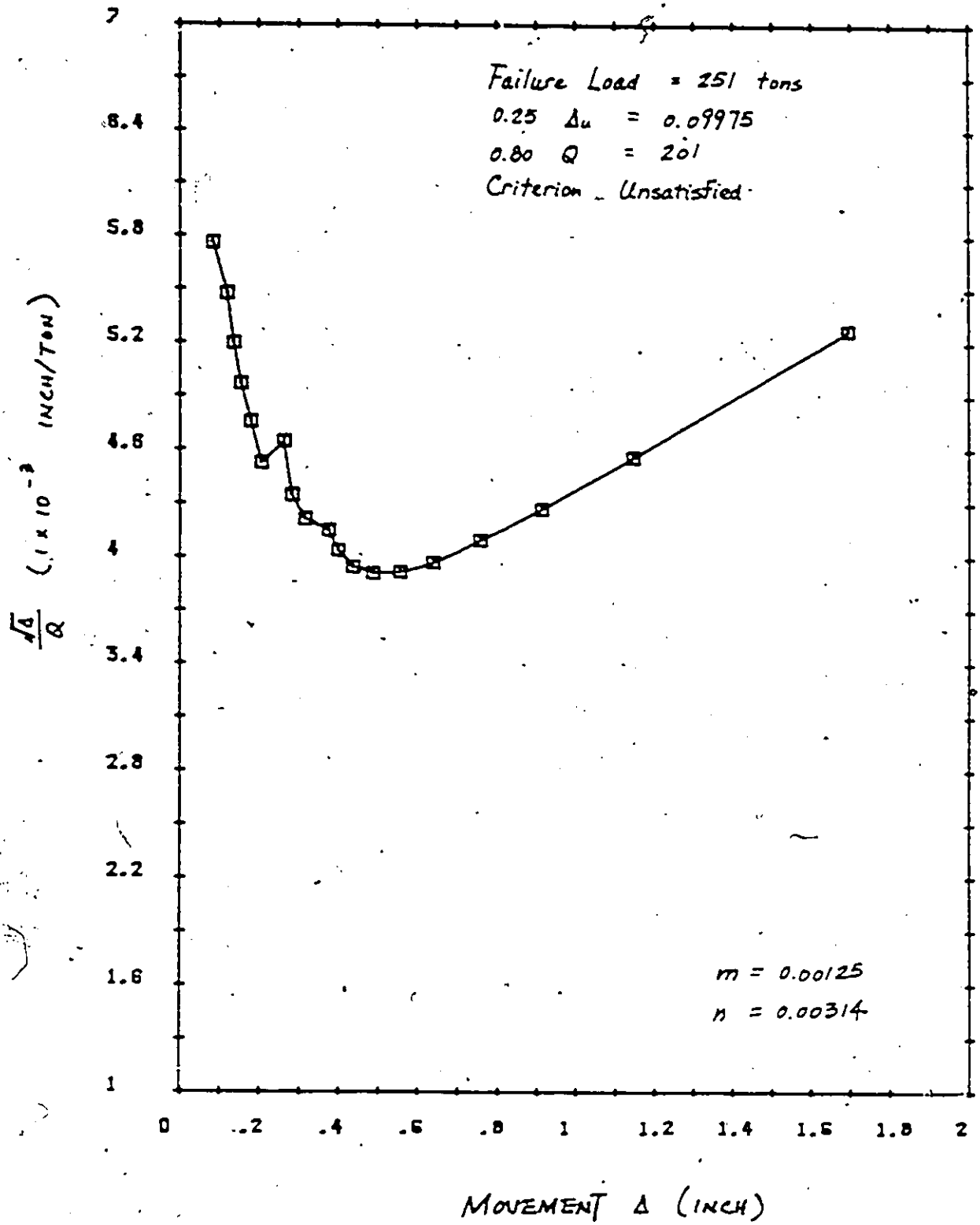

FIG D-411 PILE 3; PUSH TEST; BRINCH HANSEN 80% CRITERION

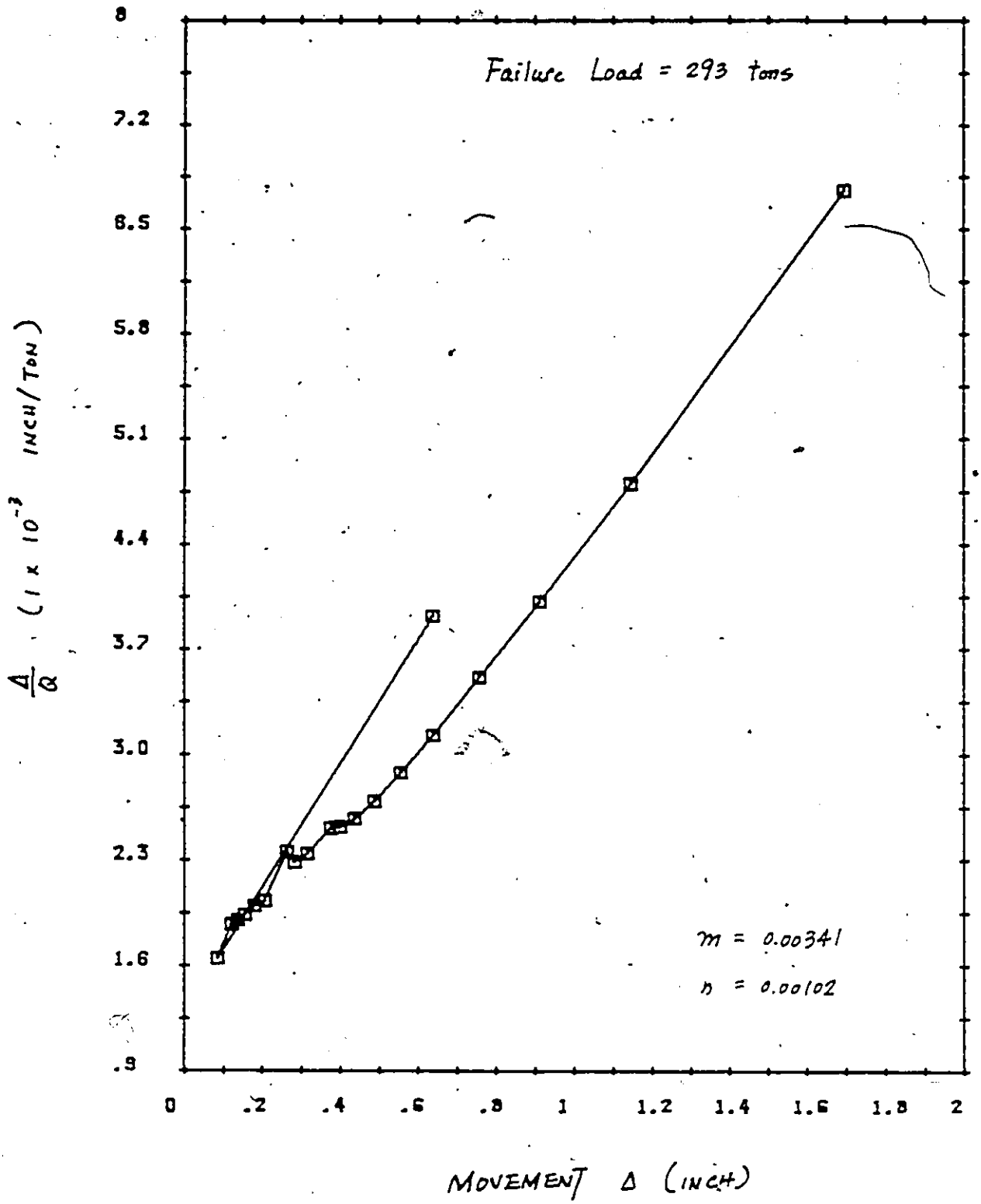

FIG. 2.4.12 PILE 3; PUSH TEST; CHIN CRITERION

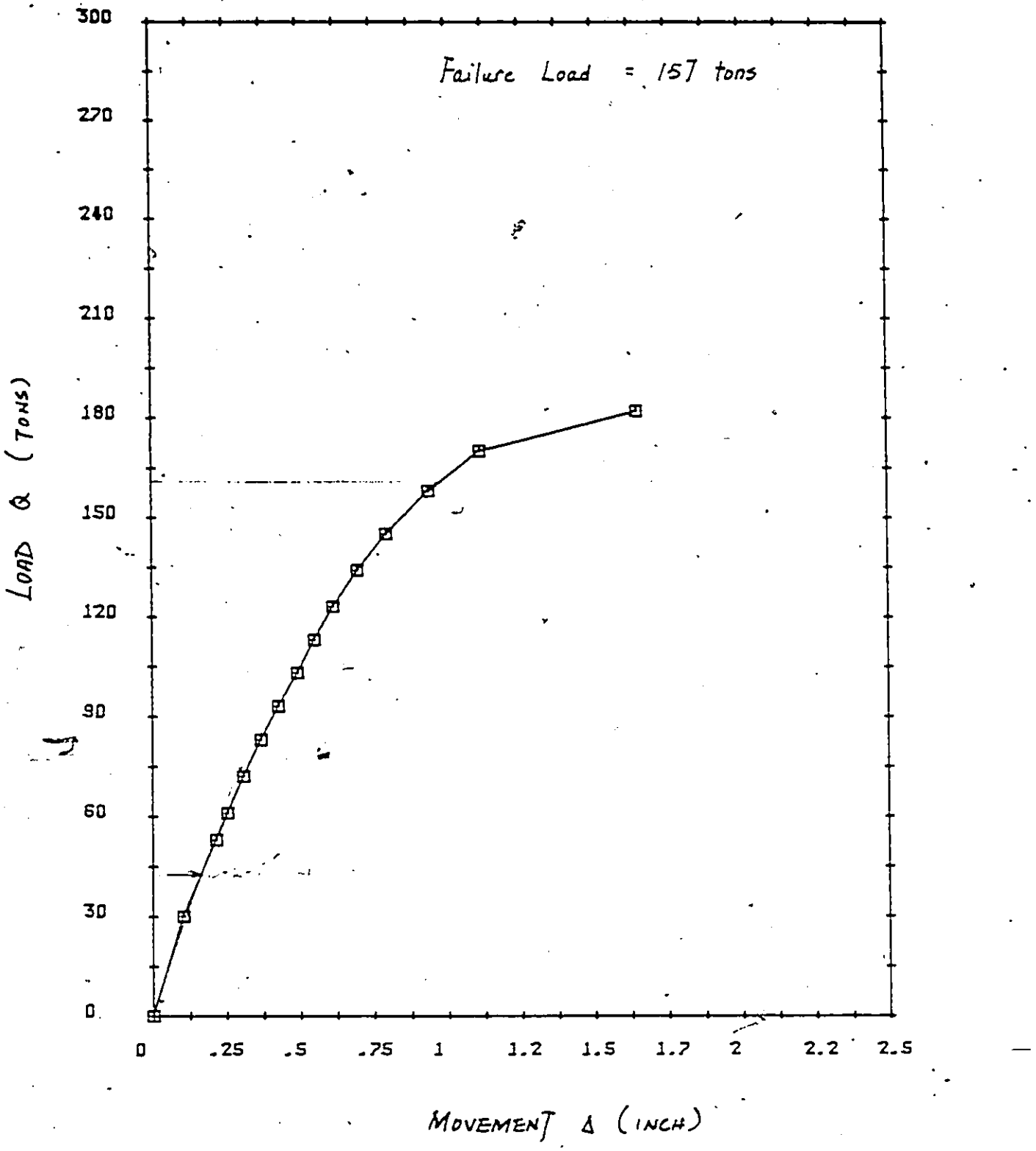

FIG. D.4.13 PILE 3; PULL TEST; DAVISSION CRITERION

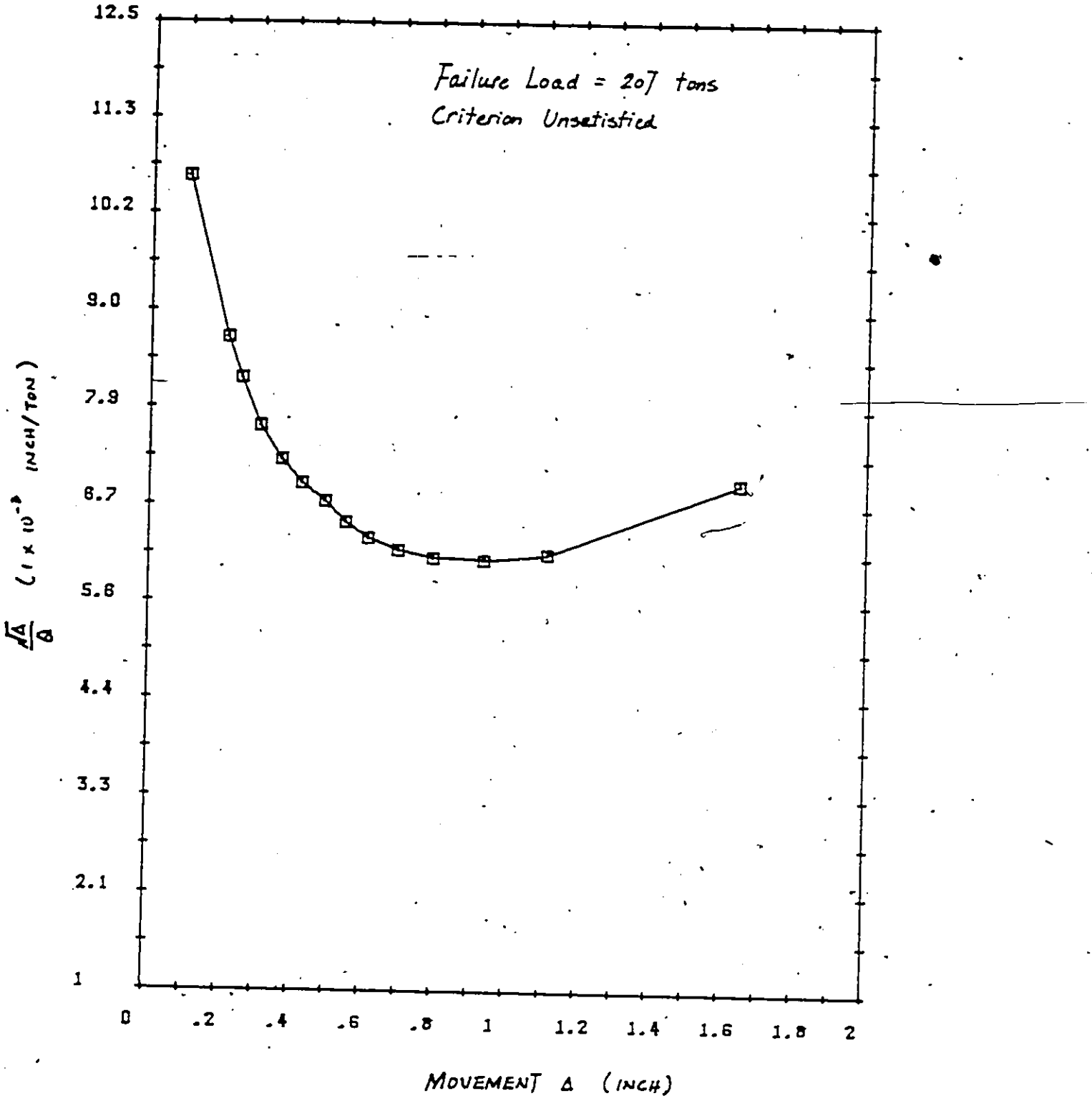

FIG. D4.14 PILE 3; PULL TEST; BRINCH HANSEN 80% CRITERION

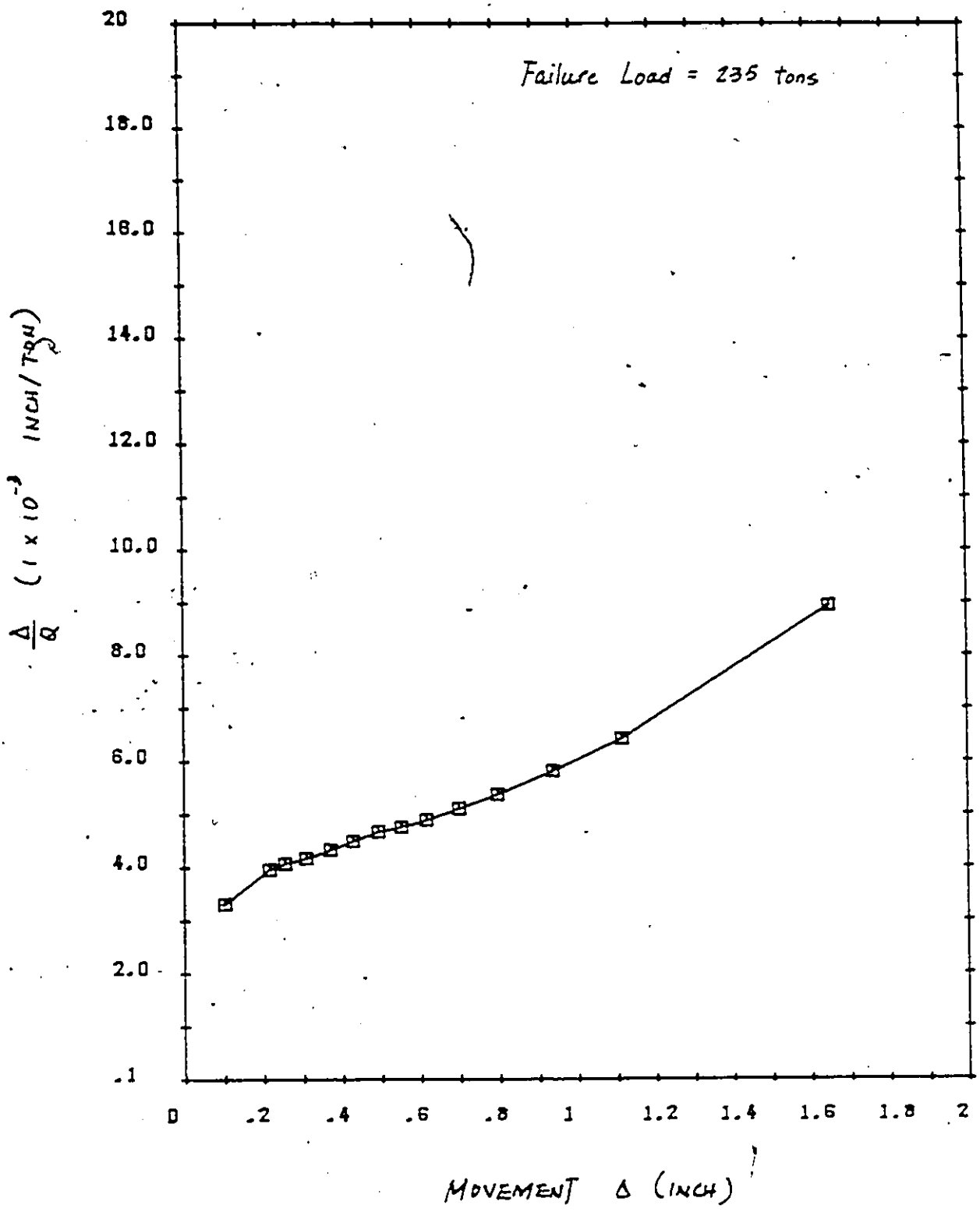

FIG. D4.15 PILE 3 ; PULL TEST ; CHIN CRITERION

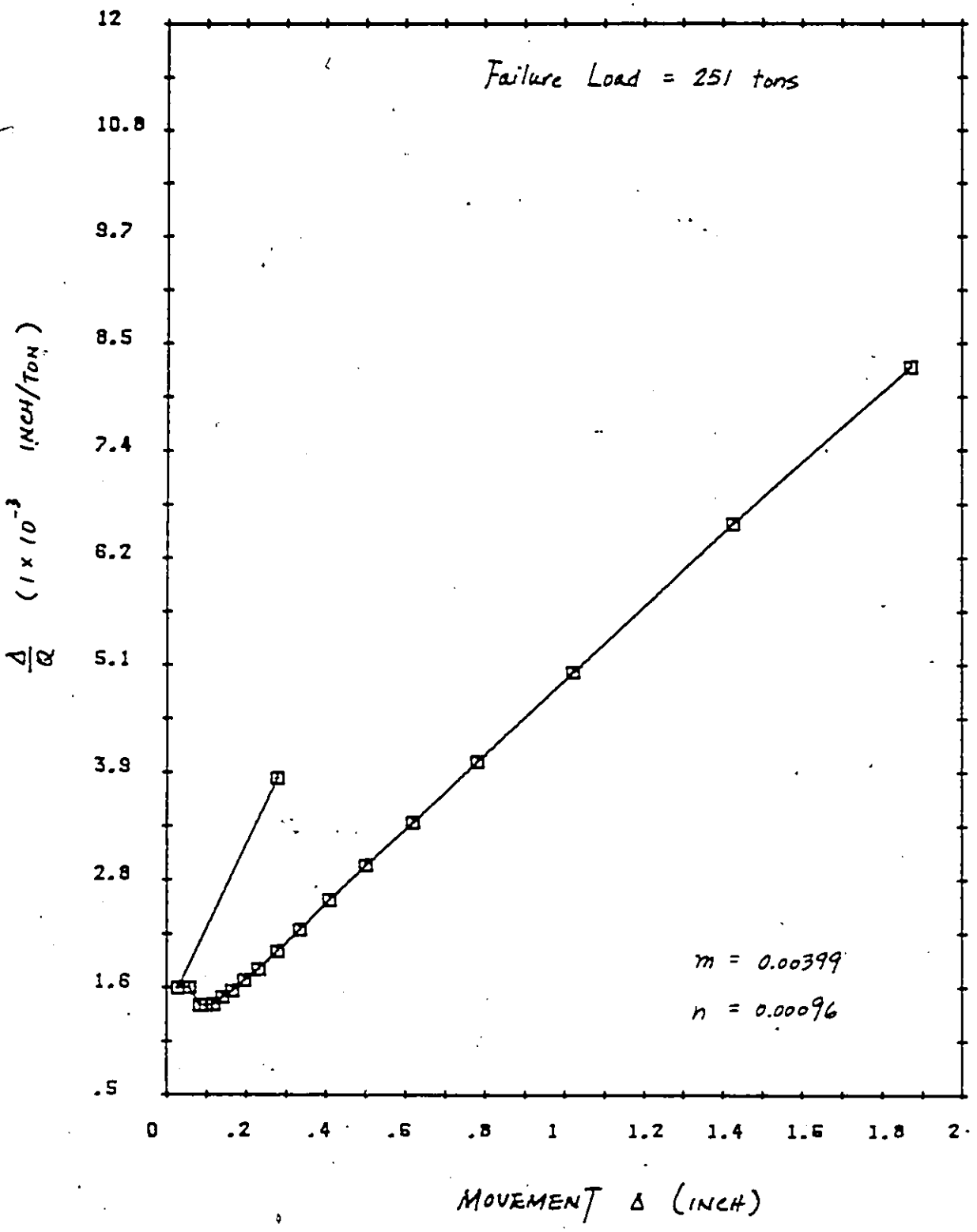

FIG-D 4.16 PILE 4; PUSH TEST; CHIN CRITERION

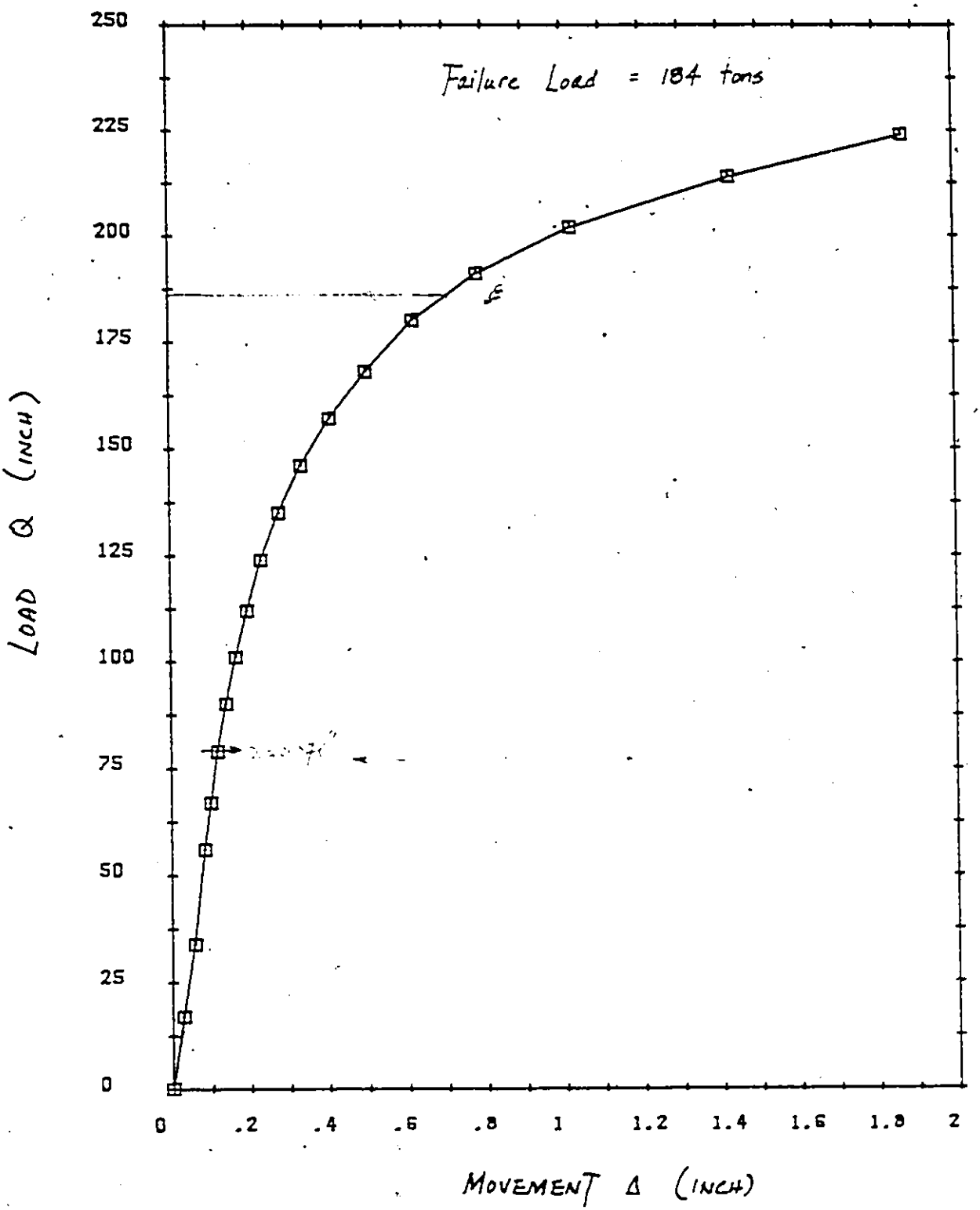

FIG. D4.7 PILE 4; PUSH TEST; DAVISSON OFFSET CRITERION

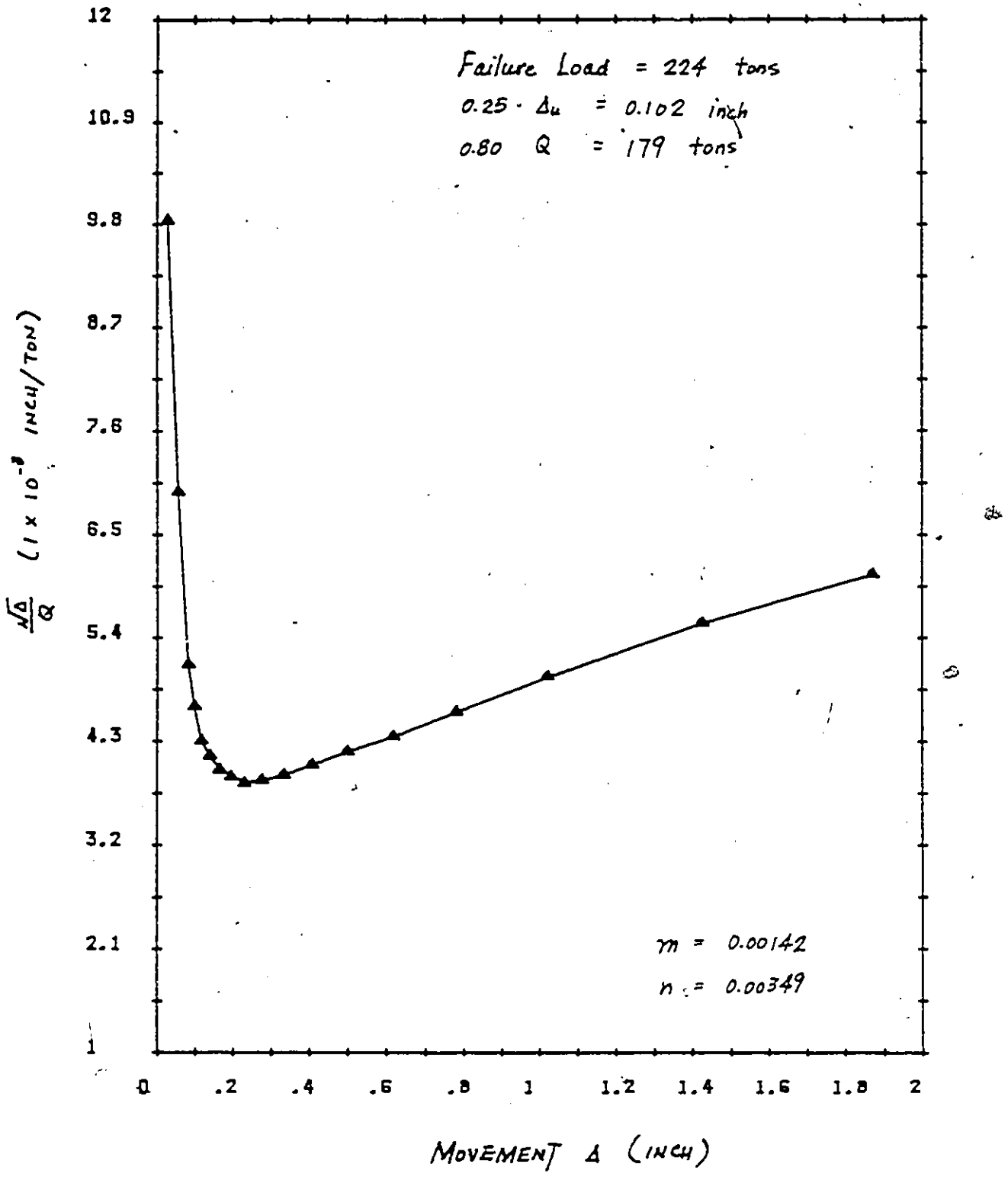

FIG. D 4.18 PILE 4; PUSH TEST; BRINCH HANSEN 80% CRITERION

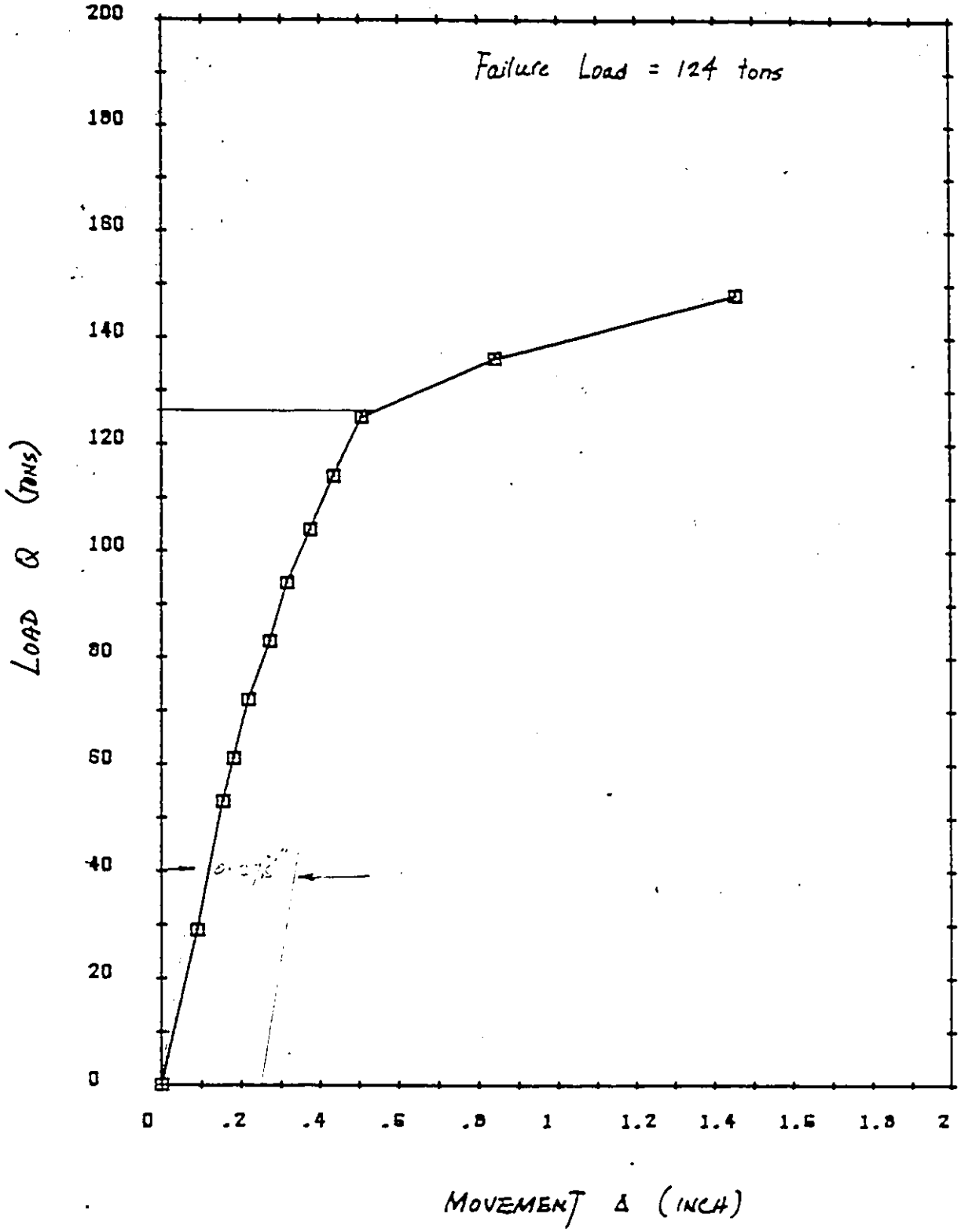

FIG D 4.18 PILE 4; PULL TEST; DAVISSON OFFSET CRITERION

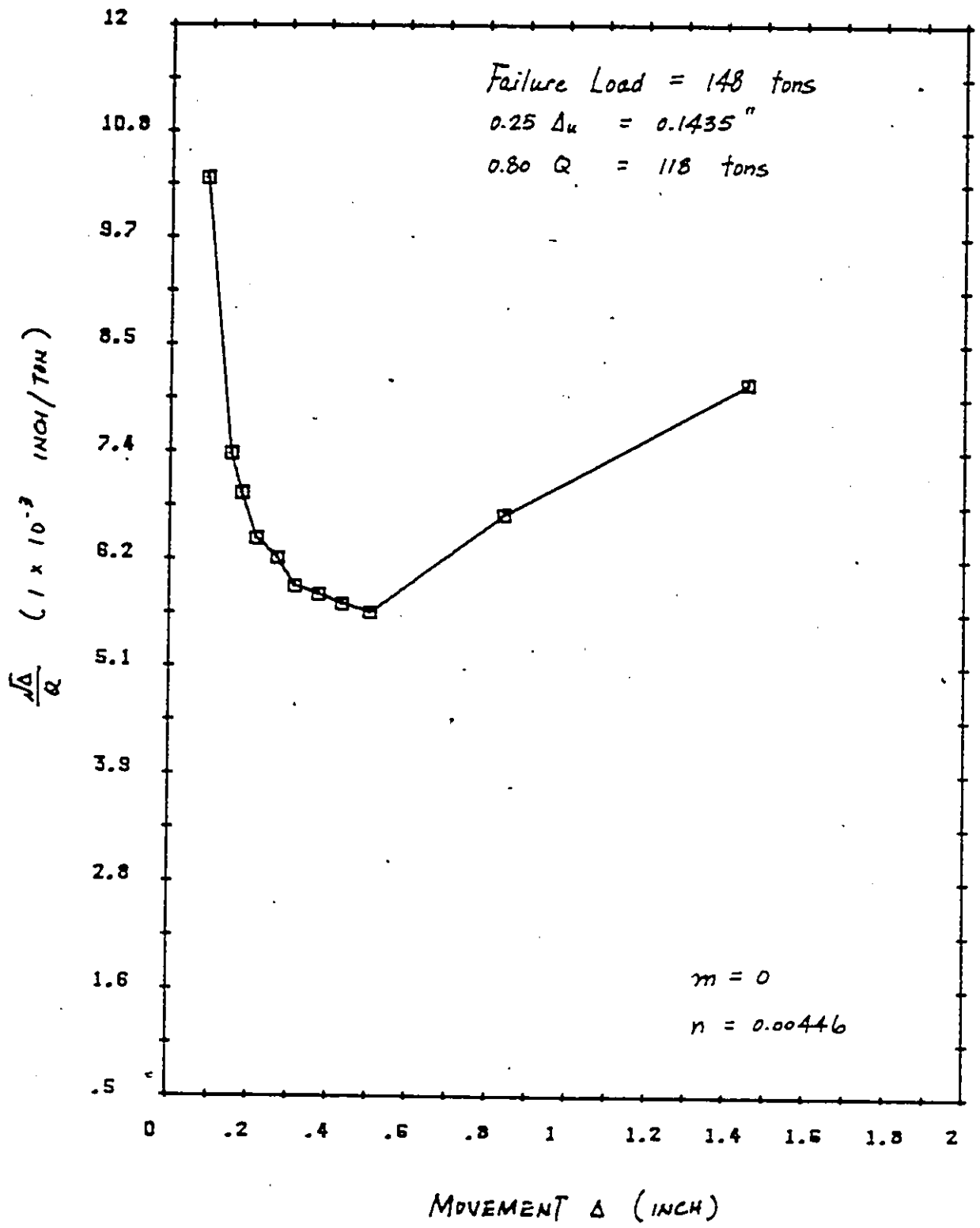

FIG D-419 PILE 4; PULL TEST; BRINCH HANSEN 80% CRITERION

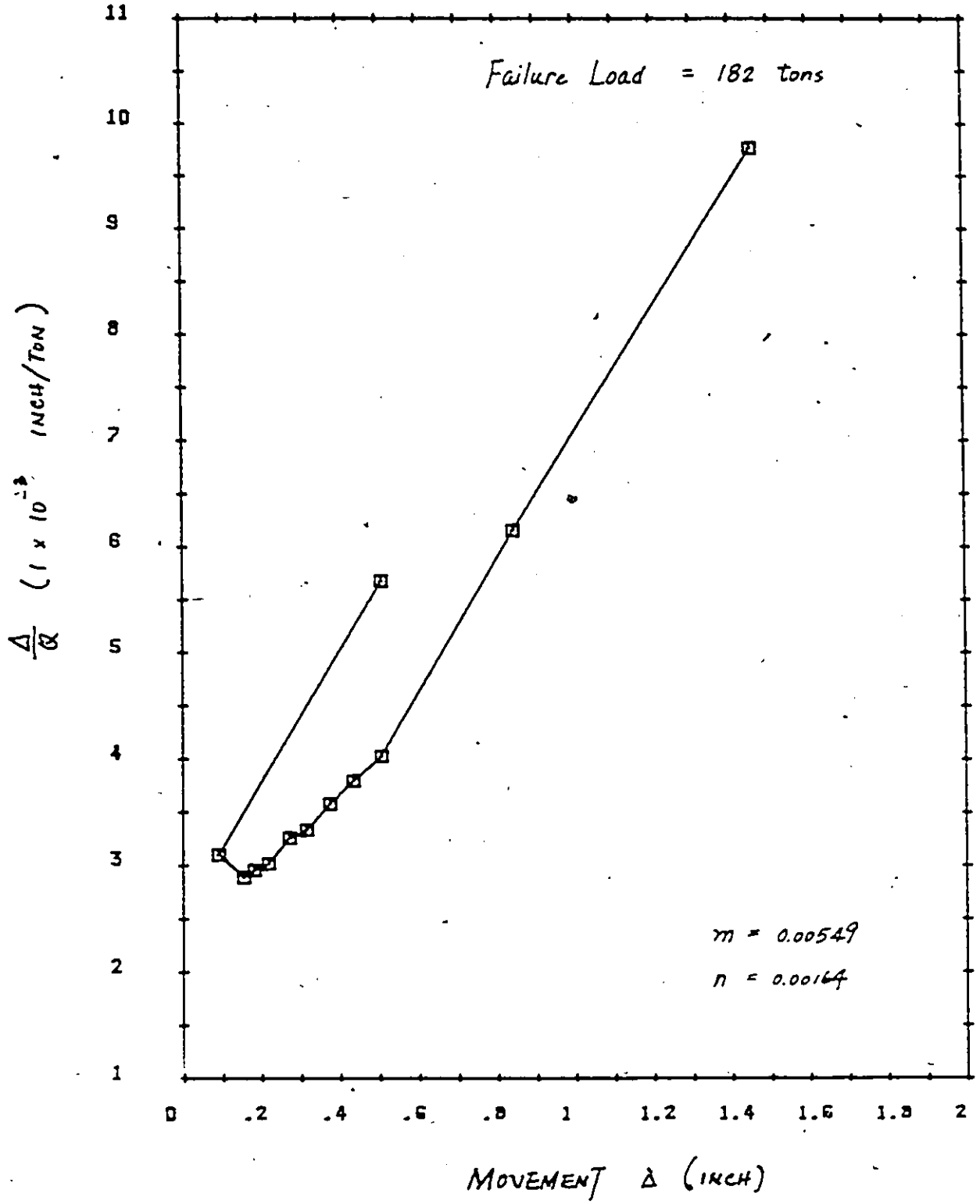

Fig D.4.20 PILE 4 ; PULL TEST ; CHIN CRITERION

APPENDIX E

Spread sheet Calculations From Eq. 2.11

PILE NO. 1 PULL TEST
COMPUTED N VALUES

LOAD	TELLTALE NO. 5E	8H	4D	7G	3C	6F	2B
0	0	0	0	0	0	0	0
53	.8162	.7168	.9371	.9838	1.001	1.014	1.118
65	.7998	.6507	.8823	.9014	.9133	.9260	.9938
76	.7911	.6422	.7945	.8764	.8967	.9155	.9817
87	.8648	.7067	1.060	.9628	.9964	.9786	1.067
97	1.086	.8822	1.174	1.199	1.222	1.243	1.324
108	.8089	.6576	.8785	.9052	.9167	.9281	.9902
118	.9149	.7605	1.013	1.027	1.063	1.076	1.136
130	.8138	.6704	.8919	.8109	.9499	.9549	1.025
140	.8450	.6050	.7315	1.018	.9261	1.063	1.136
151	.8216	.6852	.9065	.9217	.9316	.9597	1.007
163	.8860	.7352	.9721	1.003	1.023	1.042	1.150
177	.7954	.6567	.9020	.8890	.9316	.9326	1.013
189	.8277	.7042	.9144	.9580	.9910	1.013	1.080
200	.9106	.7866	1.022	1.049	1.106	1.143	1.246
211	.8903	.7897	1.046	1.082	1.161	1.181	1.315
222	.9216	.7897	.9800	1.025	1.111	.8460	.9902
234	.7974	.7436	.9561	1.026	1.082	1.024	1.244
247	.7146	.6734	.8588	.9226	.9695	1.117	1.127
260	.7232	.7280	.9566	.9818	1.062	1.074	1.199
272	.0839	.7408	.9497	1.011	1.046	1.105	1.197
284	-18.1	.8619	1.033	.9052	1.169	1.123	1.283
295	0	.8727	1.148	1.382	1.240	1.370	1.374
310	0	.6264	.8342	.8509	.9060	.9167	.9891
320	0	1.007	1.113	1.367	1.260	1.507	1.418
326	0	1.639	-50.7	2.248	2.493	2.384	2.817
347	0	.4845	0	.6401	.7046	.7540	.2906

PILE NO. 2 PULL TEST
COMPUTED N VALUES

LOAD	TELLTALE NO. 1A	5E	8H	4D	3C	6F	2B
0							
53	.5678	.5661	.7135	.6979	.7532	.897	.9825
61	.7539	.7579	.8252	.8930	1.288	.9876	1.062
72	.7354	.7191	.8506	.8436	.8877	.9346	1.027
83	.7810	.7435	.8698	.8660	.9024	.9378	1.019
93	.8179	.8051	.9291	.9242	.9550	.9971	1.088
103	.9748	.9207	1.051	1.055	1.095	1.132	1.238
113	.7852	.8277	.9487	.8940	.9254	.7694	1.027
123	.7819	.8263	.7906	.9941	.9065	1.038	.9807
134	.9692	.8293	1.104	.9398	.9953	1.070	1.159
145	.8476	.7947	.8980	.9038	.9342	.9754	1.061
158	.9843	.9436	1.102	.9246	1.004	1.255	1.379
170	.7641	.7179	.9232	1.253	1.107	.9372	-2.85
182	.9906	.8566	.9739	.8716	1.060	1.208	5.195
194	.8745	.8413	.9712	.9702	1.069	1.153	1.292
206	.9248	.8448	.9807	.9985	1.085	1.176	1.318
218	.9478	.8954	1.100	1.070	1.141	1.228	1.270
229	.9091	.8644	.9930	.9392	1.043	1.229	1.387
244	.9062	.8780	1.001	1.045	1.158	1.274	1.441
255	.9563	.9039	1.120	1.139	1.267	1.367	1.538
268	.9548	.9082	1.093	1.148	1.268	1.353	1.545
282	.8818	.8752	1.050	1.102	1.207	1.295	1.465
295	.7864	.8188	.9865	1.021	1.192	1.364	1.552
307	.0544	.0633	.0652	.0861	.0707	.1153	.1008

PILE NO.3 PULL TEST
COMPUTED N VALUES

LOAD	TELLTALE NO. 1A	5E	8H	4D	7G	3C	6F	2B
0								
30	.5802	.5904	.7233	.7061	.8433	.8362	.9502	1.063
53	.8163	.8588	.9331	.9634	.9815	1.024	1.015	1.091
61	.8197	.8696	.9161	.952	.9764	1.034	1.012	1.101
72	.7436	.7694	.8228	.8763	.8839	.9367	.9104	1.014
83	.7897	.8184	.903	.8719	.9519	.9954	1.012	1.073
93	.8095	1.040	.8862	.9306	.8532	.8721	.9696	1.065
103	.8112	.8471	.9049	.9412	.9494	1.013	.9939	1.082
113	.8431	.9031	.9520	.9890	1.006	1.069	1.060	.8722
123	.8028	.7942	.8442	.8735	.8809	.9399	.9177	1.265
134	.8465	.9368	1.220	.9931	1.010	1.081	1.066	1.068
145	.8926	.9249	.8095	1.090	1.058	.8251	1.117	1.255
158	.9282	.9586	1.018	1.049	1.087	1.411	1.172	1.327
170	.8492	.8696	.9117	.9798	1.006	1.104	1.117	1.279
182	-10.4	-10.6	-11.5	-11.8	-12.2	-12.9	-13.1	0

PILE NO. 4 PULL TEST
COMPUTED N VALUES

LOAD	TELLTALE NO. 1A	5E	8H	4D	3C	6F	2B
0	0						
29	.7043	.7473	.7869	.8434	.8849	.8662	.9287
53	.8534	.8794	.9349	.9453	1.001	.9814	1.051
61	.8500	.8657	.9344	.9682	1.037	1.009	1.106
72	.8932	.5089	.9675	1.020	1.084	1.077	1.113
83	.8408	1.235	.9200	.9554	.9816	.9844	1.050
94	.9788	1.010	1.677	1.129	1.224	1.196	1.275
104	.8173	.8428	.8831	.9230	.9752	.9536	1.001
114	.8560	.9120	.9949	.9791	1.041	1.025	1.080
125	.8374	.8753	.9355	.9843	1.055	1.034	1.102
136	.7302	.6595	.7106	.8116	1.001	.9613	1.176
148	.5996	.6999	.8543	.8673	1.197	1.369	1.380

PILE NO. 4 PUSH TEST
COMPUTED N VALUES

TELLTALE NO.

LOAD	1A	5E	8H	4D	3C	6F	2B
0							
17	.4808	.4144	.6306	.6346	.8461	.9993	1.158
34	.4717	.4828	.5906	.6671	.8133	.9193	1.014
56	.3460	.3762	.4327	.4924	.6144	.6795	.7493
67	.3659	.3855	.4582	.5322	.6707	.7481	.8050
79	.4108	.7439	.52	.5878	.7285	.7865	.8635
90	.4311	.1492	.5491	.6412	.8004	.8785	.942
101	.4340	.5223	.5636	.6119	.7722	.837	.9077
112	.4737	.5223	.5927	.6915	.8567	.9403	1.019
124	.468	.5016	.5733	.6685	.8267	.8997	.9812
135	.4425	.5223	.5782	.6328	.7835	.8511	.9163
146	.4595	.5410	.2145	.6664	.8116	.8717	.942
157	.5162	.5721	1.025	.7669	.9469	1.036	1.113
168	.4822	.5161	.6036	.6999	.8905	.9540	.8906
180	.3822	.4075	.4767	.5570	.713	.7928	.9734
191	.4368	.4539	.5382	1.069	.8567	.9540	1.028
202	.4567	.5223	.6182	.2263	.372	1.009	.9591
214	.3952	.3990	.4567	.5647	1.183	.7110	.8635
224	.5866	46.50		.8667	1.004	1.095	1.178

APPENDIX F

Calculation of Shaft Resistance Distribution

Pile 1:

Pull Testing: Unadjusted load (without residual load)

Equation of load distribution curve: $y = -0.015x^2 + 4.792x - 300$

$dy/dx = -0.03x + 4.792$

$$r_s = \frac{1/(dy/dx)}{A_s}$$

x (tons)	y (feet)	1/(dy/dx) (tons/ft)	A_s (ft^2/ft)	r_s (tsf)
224	19.79	0.519	4.1	0.131
222	23.59	0.535	4.1	0.126
217	32.56	0.582	4.1	0.142
183	73.67	1.432	4.1	0.349
165	81.39	6.329	4.1	1.540

Pile 1:

Pull Testing: Adjusted load (with residual load, Case 1)

Equation of load distribution curve: $y = 0.001980x^2 + 0.2496x - 150.9$

$dy/dx = 0.00396x + 0.2496$

$$r_s = \frac{1/(dy/dx)}{A_s}$$

x (tons)	y (feet)	1/(dy/dx) (tons/ft)	A_s (ft^2/ft)	r_s (tsf)
222	9.09	0.887	4.1	0.216
188	33.99	1.006	4.1	0.245
170	51.25	1.084	4.1	0.264
150	68.90	1.186	4.1	0.289
132	83.45	1.294	4.1	0.316
104	103.50	1.513	4.1	0.369

Pile 1:

Pull Testing: Adjusted load (with residual load, Case 2)

Equation of load distribution curve: $y = 0.000933x^2 + 0.2067x - 90.1$

$$dy/dx = 0.00187x + 0.2067$$

$$r_s = \frac{1/(dy/dx)}{A_s}$$

x (tons)	y (feet)	1/(dy/dx) (tons/ft)	A_s (ft^2/ft)	r_s (tsf)
222	1.680	1.603	4.1	0.392
168	29.10	1.923	4.1	0.469
108	56.90	2.455	4.1	0.596
94	62.50	2.618	4.1	0.638
31	82.9	3.788	4.1	0.923
10	88.0	4.444	4.1	1.084

Pile 1:

Push Testing: Unadjusted load (without residual load)

Equation of load distribution curve: $y = 0.00008x^2 + 0.424x - 191$

$$dy/dx = 0.000167x + 0.424$$

$$r_s = \frac{1/(dy/dx)}{A_s}$$

x (tons)	y (feet)	1/(dy/dx) (tons/ft)	A_s (ft^2/ft)	r_s (tsf)
472	9.36	2.898	4.1	0.707
342	55.70	2.726	4.1	0.664
299	71.64	2.674	4.1	0.652
261	86.50	2.630	4.1	0.642

Pile 1:

Push Testing: Adjusted load (with residual load, Case 1)

Equation of load distribution curve: $y = 0.4500x - 230$

$$dy/dx = 0.4500$$

$$r_s = \frac{1/(dy/dx)}{A_s}$$

x (tons)	y (feet)	1/(dy/dx) (tons/ft)	A_s (ft^2/ft)	r_s (tsf)
492	8.60	2.220	4.1	0.542
398	50.90	2.220	4.1	0.542
352	71.60	2.220	4.1	0.542
331	81.10	2.220	4.1	0.542
278	105.00	2.220	4.1	0.542

Pile 1:

Push Testing: Adjusted load (with residual load, Case 2)

Equation of load distribution curve: $y = 0.564x - 300$

$$dy/dx = 0.564$$

$$r_s = \frac{1/(dy/dx)}{A_s}$$

x (tons)	y (feet)	1/(dy/dx) (tons/ft)	A_s (ft^2/ft)	r_s (tsf)
511	11.79	1.773	4.1	0.433
454	44.00	1.773	4.1	0.433
410	68.76	1.773	4.1	0.433
401	73.80	1.773	4.1	0.433
350	102.6	1.773	4.1	0.433

Pile 3:

Pull Testing: Unadjusted load (without residual load)

Equation of load distribution curve: $y = -0.8037x + 153$

$dy/dx = -0.8037$

$$r_s = \frac{1/(dy/dx)}{A_s}$$

x (tons)	y (feet)	1/(dy/dx) (tons/ft)	A_s (ft^2/ft)	r_s (tsf)
170	16.37	1.243	4.12	0.302
164	21.20	1.243	4.12	0.302
149	33.25	1.243	4.12	0.302
110	64.59	1.243	3.75	0.331
77	91.10	1.243	3.61	0.334

Pile 3:

Pull Testing: Adjusted load (with residual load, Case 1)

Equation of load distribution curve: $y = 0.00122x^2 + 0.543x - 125.6$

$dy/dx = 0.00242x + 0.543$

$$r_s = \frac{1/(dy/dx)}{A_s}$$

x (tons)	y (feet)	1/(dy/dx) (tons/ft)	A_s (ft^2/ft)	r_s (tsf)
170	1.97	1.048	4.12	0.256
130	34.30	1.168	3.90	0.300
119	43.70	1.204	3.76	0.320
94	63.78	1.297	3.70	0.351
61	87.90	1.447	3.50	0.414
35	104.90	1.592	3.50	0.455

Pile 3:

Pull Testing: Adjusted load (with residual load, Case 2)

Equation of load distribution curve: $y = 0.00269x^2 + 0.0433x - 85.7$

$$dy/dx = 0.00539x + 0.0433$$

$$r_s = \frac{1/(dy/dx)}{A_s}$$

x (tons)	y (feet)	1/(dy/dx) (tons/ft)	A_s (ft^2/ft)	r_s (tsf)
170	0.740	1.042	4.12	0.253
141	26.30	1.245	4.12	0.302
117	43.90	1.484	3.90	0.380
63	72.40	2.611	3.75	0.696
22	83.6	6.173	3.60	1.506
10	88.0	4.444	4.1	1.084

Pile 3:

Push Testing: Unadjusted load (without residual load)

Equation of load distribution curve: $y = -0.00088x^2 + 0.582x - 88.1$

$$dy/dx = 0.00176x + 0.582$$

$$r_s = \frac{1/(dy/dx)}{A_s}$$

x (tons)	y (feet)	1/(dy/dx) (tons/ft)	A_s (ft^2/ft)	r_s (tsf)
234	0.09	5.876	4.12	1.430
224	1.88	5.326	4.12	1.290
101	38.29	2.474	3.90	0.634
52	60.21	2.040	3.75	0.544
45	63.69	1.988	3.75	0.530
24	74.64	1.853	3.75	0.494
18	77.91	1.817	3.71	0.503
8	83.50	1.761	3.61	0.483

Pile 3:

Push Testing: Adjusted load (with residual load, Case 1)

Equation of load distribution curve: $y = -0.000502x^2 + 0.5920x - 111$

$$dy/dx = -0.001x + 0.592$$

$$r_s = \frac{1/(dy/dx)}{A_s}$$

x (tons)	y (feet)	1/(dy/dx) (tons/ft)	A_s (ft^2/ft)	r_s (tsf)
234	0.04	2.800	4.12	0.680
136	39.77	2.195	3.90	0.536
105	54.37	2.055	3.75	0.530
96	58.79	2.020	3.75	0.538
66	74.11	1.902	3.61	0.507
55	79.45	1.863	3.61	0.516
37	89.78	1.802	3.61	0.499

Pile 3:

Push Testing: Adjusted load (with residual load, Case 2)

Equation of load distribution curve: $y = 0.0011x^2 + 0.155x - 103$

$$dy/dx = 0.0022x + 0.155$$

$$r_s = \frac{1/(dy/dx)}{A_s}$$

x (tons)	y (feet)	1/(dy/dx) (tons/ft)	A_s (ft^2/ft)	r_s (tsf)
234	6.70	1.493	4.12	0.362
229	10.10	1.517	4.12	0.368
169	45.60	1.898	3.90	0.486
159	50.80	1.980	3.90	0.508
132	63.60	2.247	3.75	0.599
113	71.70	2.475	3.75	0.660
102	76.00	2.639	3.61	0.731
50	92.80	3.773	3.61	1.045

Pile 4:

Pull Testing: Unadjusted load (without residual load)

Equation of load distribution curve: $y = -0.00035x^3 + 0.078x^2 - 6.35x + 264$

$$dy/dx = -0.00105x^2 + 0.156x - 6.35$$

$$r_s = \frac{1/(dy/dx)}{A_s}$$

x (tons)	y (feet)	1/(dy/dx) (tons/ft)	A_s (ft^2/ft)	r_s (tsf)
125	7.18	0.308	4.10	0.075
124	10.40	0.318	4.10	0.078
108	48.70	0.572	4.10	0.139
96	65.10	0.945	4.10	0.231
71	82.40	1.763	4.10	0.430
53	95.70	0.991	4.10	0.241

Pile 4:

Pull Testing: Adjusted load (with residual load, Case 1)

Equationof load distribution curve: $y = 0.00019x^3 - 0.037x^2 + 3.185x - 188$

$$dy/dx = 0.00057x^2 - 0.0745x + 3.185$$

$$r_s = \frac{1/(dy/dx)}{A_s}$$

x (tons)	y (feet)	1/(dy/dx) (tons/ft)	A_s (ft^2/ft)	r_s (tsf)
125	1.27	0.359	4.10	0.090
119	16.70	0.418	4.10	0.102
97	55.00	0.757	4.10	0.185
71	87.98	1.300	4.10	0.317
53	95.87	1.194	4.10	0.291

Pile 4:

Pull Testing: Adjusted load (with residual load, Case 2)

Equation of load distribution curve: $y = -0.00017x^3 + 0.039x^2 - 3.488x + 164$

$$dy/dx = -0.000516x^2 + 0.0778x - 3.488$$

$$r_s = \frac{1/(dy/dx)}{A_s}$$

x (tons)	y (feet)	1/(dy/dx) (tons/ft)	A_s (ft^2/ft)	r_s (tsf)
125	1.630	0.547	4.10	0.133
116	15.95	0.711	4.10	0.173
71	51.86	1.169	4.10	0.432
57	60.57	1.379	4.10	0.334
33[9]	85.80	0.675	4.10	0.164
28	93.80	0.584	4.10	0.142

Pile 4:

Push Testing: Unadjusted load (without residual load)

Equation of load distribution curve: $y = -0.000625x^2 + 0.560x - 87.5$

$$dy/dx = -0.00125x + 0.560$$

$$r_s = \frac{1/(dy/dx)}{A_s}$$

x (tons)	y (feet)	1/(dy/dx) (tons/ft)	A_s (ft^2/ft)	r_s (tsf)
180	6.90	2.983	4.10	0.728
169	10.71	2.863	4.10	0.698
90	42.16	2.237	4.10	0.546
73	49.90	2.130	4.10	0.520
28	72.30	1.904	4.10	0.465
2	86.38	1.795	4.10	0.438
1	86.91	1.790	4.10	0.438

Pile 4:

Push Testing: Adjusted load (with residual load, Case 1)

Equation of load distribution curve: $y = 0.00157x^2 + 0.245x - 101$

$$dy/dx = 0.00314x + 0.245$$

$$r_s = \frac{1/(dy/dx)}{A_s}$$

x (tons)	y (feet)	1/(dy/dx) (tons/ft)	A_s (ft^2/ft)	r_s (tsf)
180	6.32	1.234	4.10	0.301
173	11.83	1.269	4.10	0.310
113	53.45	1.669	4.10	0.407
105	58.16	1.739	4.10	0.424
95	63.75	1.841	4.10	0.449
52	84.21	2.451	4.10	0.598
25	94.19	3.091	4.10	0.753

Pile 4:

Push Testing: Adjusted load (with residual load, Case 2)

Equation of load distribution curve: $y = 0.000096x^3 - 0.0266x^2 + 2.62x - 171$

$$dy/dx = 0.000287x^2 - 0.0532x + 2.62$$

$$r_s = \frac{1/(dy/dx)}{A_s}$$

x (tons)	y (feet)	1/(dy/dx) (tons/ft)	A_s (ft^2/ft)	r_s (tsf)
180	3.70	0.428	4.10	0.104
176	12.65	0.467	4.10	0.114
151	52.70	0.888	4.10	0.217
117	74.50	3.105	4.10	0.758
91	80.80	6.547	4.10	1.594
49	95.30	1.426	4.10	0.348